Hydrogel Composite Adhesives Inspired by Algae and Mussels

by

Aleksander Cholewinski

A thesis

presented to the University of Waterloo

in fulfillment of the

thesis requirement for the degree of

Doctor of Philosophy

in

Chemical Engineering (Nanotechnology)

Waterloo, Ontario, Canada, 2019

Examining Committee Membership

The following served on the Examining Committee for this thesis. The decision of the Examining Committee is by majority vote.

External Examiner	**Prof. Noshir Pesika** Associate Professor, Department of Chemical & Biomolecular Engineering, Tulane University, USA
Supervisor	**Prof. Boxin Zhao** Professor, Department of Chemical Engineering
Internal Member	**Prof. William Anderson** Professor, Department of Chemical Engineering
Internal Member	**Prof. Michael Pope** Assistant Professor, Department of Chemical Engineering
Internal-external Member	**Prof. Juewen Liu** Professor, Department of Chemistry

Author's Declaration

This thesis consists of material all of which I authored or co-authored: see Statement of Contributions included in the thesis. This is a true copy of the thesis, including any required final revisions, as accepted by my examiners.

I understand that my thesis may be made electronically available to the public.

Statement of Contributions

The research work described in Chapter 3 has been published in:

- Cholewinski, A., Yang, F. K. & Zhao, B. Underwater Contact Behavior of Alginate and Catechol-Conjugated Alginate Hydrogel Beads. Langmuir 33, 8353–8361 (2017).

The research work described in Chapter 4 has been published in:

- Cholewinski, A., Yang, F. K. & Zhao, B. Algae–mussel-inspired hydrogel composite glue for underwater bonding. Mater. Horizons 6, 285–293 (2019).

I am the first author of all these journal publications.

Abstract

The ocean is a vast source of a multitude of materials used in daily life, but has also provided numerous sources of inspiration for creating novel bio-inspired materials. Marine mussels are one of the best-known marine organisms that have inspired numerous underwater adhesives. These materials have found applications in a broad variety of fields; their usage in biomedical applications is the most prevalent, due to the abundance of wet environments within the body. However, many organisms that adhere to rocks and the sea floor have their own unique strategies for achieving adhesion in wet conditions. Many synthetic bio-inspired adhesives look purely to the chemistry of mussel adhesion for inspiration, while other facets of mussel adhesive strategies (such as process control) offer their own improvements. The objective of this dissertation is to develop and fabricate underwater adhesives that take inspiration from the adhesive chemistry and processes of both marine mussels and benthic algae.

Algae and mussel systems were firstly combined by covalently modifying alginate polymer chains (extracted from brown algae) with catechol functionality (inspired by mussel chemistry). After ionic crosslinking, the resulting hydrogels were adhesive to soft and organic materials, showing promise adhesion to animal tissue samples. The effects of catechol functionalization on the mechanical properties of the gels were also investigated, and differences in adhesion between soft and rigid substrates was observed. Secondly, alginate and dopamine were combined together through noncovalent interactions; the ionic crosslinking of alginate and coordinate bonding of dopamine were exploited by using ferric ions to link the adhesive and cohesive components. By mimicking the processes of mussel and algae adhesion, a sequential application method was developed to improve adhesion of the algae-mussel-inspired glue, leading to adhesive strengths

over 100 times that of pure alginate and over 5 times that of a non-sequential method. Finally, the stability and workability of the algae-mussel glue was improved by controlling dissolution and dispersion of the components. This was used to formulate both one-part and two-part adhesives that could be used hours or days after preparation, respectively, with the ability to be applied directly to objects underwater to bond them together.

Acknowledgements

Firstly, I would like to thank my research supervisor, Professor Boxin Zhao, for his guidance and support throughout my PhD studies. His encouragement and suggestions have helped me to gain experience and develop ideas for research. His enthusiasm and passion for research has provided me inspiration for my own work, and his offering of time and advice has helped me to stay productive and motivated. Special thanks go to my examining committee, who have helped to shape my PhD work.

I would also like to thank my lab mates for their friendship and help in my studies. I would like to especially thank Fut (Kuo) Yang, who helped me when I was starting in the lab, and with whom I had many fruitful discussions.

Finally, I would like to thank my family and friends for giving me love and laughter, and for supporting me in times of stress.

Dedication

I dedicate this dissertation to my parents, without whose love and guidance I would not be half the person I am today. Their bountiful love has been the foundation for all I have achieved.

Table of Contents

List of Figures

List of Tables

List of Abbreviations

AAm	Acrylamide
AFM	Atomic force microscope
BSE	Backscattered electrons
DA	Dopamine
DEAP	Diethoxyacetophenone
DI H_2O	Deionized water
DMSO	Dimethyl sulfoxide
Dopa	3,4-dihydroxyphenylalanine
DSC	Differential scanning calorimetry
EDC	1-ethyl-3-(3-dimethylaminopropyl) carbodiimide
EDX	Energy-dispersive X-ray spectroscopy
ESEM	Environmental scanning electron microscope
FID	Free induction decay
FTIR	Fourier transform infrared spectroscopy
IPN	Interpenetrating network
Lys	Lysine
MBAA	N,N'-methylenebisacrylamide
Mfp	Mussel foot protein
NHS	N-hydroxysuccinimide
NMR	Nuclear magnetic resonance
PAAm	Polyacrylamide
PDA	Polydopamine
PDMS	Polydimethylsiloxane
PTFE	Polytetrafluoroethylene
SE	Secondary electrons
SEM	Scanning electron microscope
Sulfo-NHS	N-hydroxysulfosuccinimide
Tris	Tris(hydroxymethyl)aminomethane

Tyr	Tyrosine
UV-Vis	Ultraviolet-Visible
WDX	Wavelength-dispersive X-ray spectroscopy
XPS	X-ray photoelectron spectroscopy

Chapter 1 Introduction

1.1 Blue Economy and Algae

The ocean has always been a rich source of natural resources to enrich lives and promote economic opportunities. In recent years, many countries have been moving toward maximizing the use of ocean space in their territories, which has been combined with a distinct emphasis on sustainability. This is particularly important for many small island states, which possess large quantities of ocean resources compared with those based on land. These countries stand to benefit greatly from proper usage of their marine territory, but also have the most to lose from improper management of these resources. As such, there has been a push to temper exploitation of these maritime resources with consideration on the current and future health of the environment. This combination of developing an ocean economy with proper preservation of the marine environment has been termed the ‘Blue Economy’.

While a large emphasis of the blue economy is on better-known sources of ocean resources, such as the shipping, fishing, and offshore oil and gas industries, other categories exist that can provide economic benefit to countries with marine territory. One of these is aquaculture of less common species, including various seaweeds. This can be combined with traditional aquaculture of fish to counterbalance the excess nutrients into the environment, helping to prevent eutrophication. Seaweeds themselves have a variety of uses; they are commonly harvested as food sources, and are useful sources of hydrocolloids like agar, alginate, and carrageenans, which find applications in the food, pharmaceutical, and biotech industries. Sodium alginate, as a specific example, has a variety of applications. It is used as a stabilizer and thickener in the food industry, while its gelation and swelling properties lead to its use for encapsulation of cells or drugs, as well

as for absorbent wound dressings. Finding ways to increase the applications of materials like sodium alginate, such as by incorporating adhesion, would further incentivize aquaculture of algae to sustainably and fully benefit from marine territory.

1.2 Bioinspired Adhesion

Along with material resources, the ocean also provides inspiration for a variety of adhesive strategies. Many sessile marine organisms have developed their own unique strategies for adhering to surfaces underwater. Two specific examples are marine mussels and brown algae, which have different goals and methods in adhering to solid surfaces. Marine mussels attach to stiff surfaces using byssal threads with adhesive plaques. These rely on adhesive proteins in the plaque, with the pH and chemistry carefully controlled at the surface until bonding has been achieved. While multiple mussel foot proteins are involved in the formation of the thread and plaque, a small number are localized at the interface between the plaque and the surface the mussel is trying to adhere to. These proteins were found be rich in 3,4-dihydroxyphenylalanine (Dopa) (20-30 mol%), a catecholic amino acid.

Brown algae, particularly fucoids (of the order Fucales), secrete an adhesive mixture as zygotes to attach to surfaces. The attachment is similar to the secretion of cell wall components, with the primary adhesive consisting primarily of calcium alginate (alginates are also the main components of the cell walls in brown algae), polyphenols, and sulfated fucans[1]. This results in a sticky coating that can engage in initial adhesion to a surface. The secondary adhesive is formed through a transformation of the primary adhesive, chiefly through the formation of covalent bonds to link together the components. This crosslinking comes from oxidase reactions catalyzed by haloperoxidases, which lead to activation of phenoxy radicals on polyphenols and their subsequent crosslinking.

1.3 Incorporating Mussel Adhesion

Catechol has been determined to be a major component responsible for mussel adhesion. As such, most attempts at mimicking mussel adhesion have involved incorporating catechol into a system. One of the most common methods for doing so is through chemical conjugation to a polymer. This can involve adding catechol to an existing polymer on end groups or side chains, or by polymerizing a monomer incorporating catechol, but the goal has been to develop polymers with adhesive properties.

One molecule of particular interest in relation to mussel chemistry is dopamine. While better known as a neurotransmitter, dopamine is also an effective small-molecule mimic of mussel adhesive proteins, as it contains both a catechol and an amine group – mussel adhesive proteins typically exhibit Dopa groups (with catechol) close to lysine groups (with amine). In basic aqueous conditions, dopamine can self-polymerize through auto-oxidation to form polydopamine. During its formation, polydopamine can coat almost any surface, including metals, plastics, and even Teflon. As such, dopamine and polydopamine have been widely investigated for coating applications, though less so for more general adhesive purposes.

1.4 Thesis Outline

This dissertation is arranged into six chapters. The current chapter, *Chapter 1,* provides an overall introduction to this dissertation. The following chapter, *Chapter 2,* introduces core concepts in hydrogels and adhesion, as well as detailing work in the field involving alginate, hydrogel adhesion, and mussel-inspired adhesion. *Chapter 3* describes the results of chemically modifying alginate chains with catechol groups, including effects on adhesion and the stiffness of gelled alginate beads. In *Chapter 4*, the dual inspirations of algae and mussels are combined to create a novel algae-mussel glue. This material exploits interactions between the adhesive and

cohesive components, and this chapter shows how sequential application helped to maximize adhesive strength. *Chapter 5* covers direct mixing of algae-mussel glue components, with a goal of making a more stable pre-glue material that is easier to use. Components are dispersed in glycerol, and both two-part and one-part variations of this glue are detailed. Finally, *Chapter 6* provides concluding remarks and an overall summary of the dissertation.

Chapter 2 Literature Review

The following chapter discusses relevant literature to a number of topics related to this dissertation. A large focus of this chapter is on the properties, structure, and applications of hydrogels, which are important to developing new gels like those found in this dissertation. Additionally, the adhesive strategies of both brown algae and marine mussels are covered in detail, as they serve as the primary inspirations for the adhesives developed herein. This is followed by a review of recent literature on the topics of bioinspired adhesion, with particular emphasis on adhesive materials inspired by either algae or mussels. Finally, this chapter also covers a number of techniques commonly used to characterize hydrogels and their adhesion

2.1 Hydrogels

2.1.1 Hydrogels Definition and Categorization

Hydrogels are crosslinked hydrophilic polymers that can absorb large quantities of water, anywhere from ~10% to thousands of times their own dry weight. Hydrogels can be categorized in several different ways: synthetic or biological; physically- or chemically-crosslinked; and homopolymers, copolymers, or interpenetrating networks; along with other methods of classification. Hydrogels fabricated from natural polymers (e.g., chitosan, alginate, and gelatin) have advantages for biomedical applications in that many of them are non-toxic, can avoid triggering inflammatory or immunological responses, and can often be broken down by enzymes in the body[2]. Advantages of synthetic polymer-based hydrogels (e.g., polyacrylamide, polyethylene glycol, and poly(N-isopropylacrylamide)) are that they tend to have well-defined structures, higher strength and water absorption, and greater ability to tailor their properties[3].

One of the primary classifications of hydrogels is based on the nature of their crosslinks: chemical or physical (with examples of each shown in **Figure 2-1**). Chemical hydrogels consist of macromolecules that are linked together by covalent bonds, which provides them with strength and resistance to environmental changes. Physical hydrogels can be linked together by a variety of non-covalent forces, including van der Waals, electrostatic, hydrogen bonding, or hydrophobic forces, as well as chain entanglements or the formation of crystalline domains. These interactions are weaker than covalent bonds, but are often reversible, and can respond to environmental changes for stimulus-responsive gels.

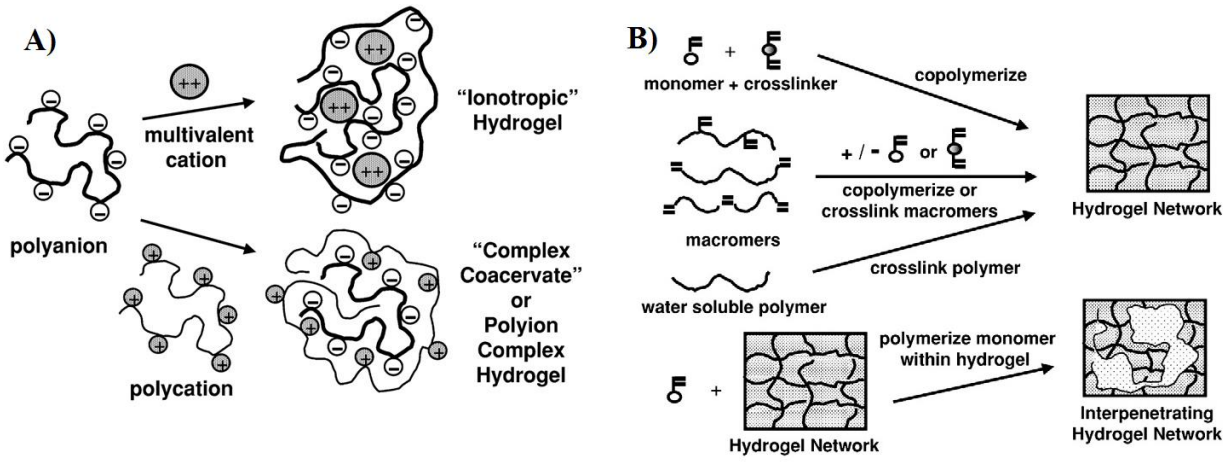

Figure 2-1. Example methods for forming hydrogels. (a) Physical hydrogels formed through polyelectrolytes, crosslinked by ions or polyelectrolytes of opposite charge; (b) Chemical hydrogels formed through covalent crosslinking of polymers. Adapted with permission from ref. [4]. Copyright 2012 Elsevier.

Another set of categories of hydrogels is whether they consist of homopolymers, copolymers, or interpenetrating networks (IPNs). Homopolymeric hydrogels are fabricated from a single species of monomer, while copolymeric hydrogels are formed from two or more monomer species. The copolymers formed from multiple monomer species can be arranged randomly, in an alternating pattern, or in a block configuration[3]. Interpenetrating network hydrogels consist of two separate polymer components that cross each other to form a single network. The second

component is synthesized or crosslinked in the presence of the first polymer, with several strategies illustrated in **Figure 2-2** – this first component can be already formed and crosslinked, or can itself polymerize/crosslink at the same time as the second component. If both components are crosslinked, then the resulting gel is a full IPN; if one component is uncrosslinked, the chains can still bed entrapped within the matrix of the polymer network, forming a semi-IPN[3,5]. The "double networks" of IPNs can be used to distribute stress and improve mechanical properties, to improve swelling/deswelling behaviour, or to modulate or incorporate the stimuli-responsive behaviour of the polymers[5].

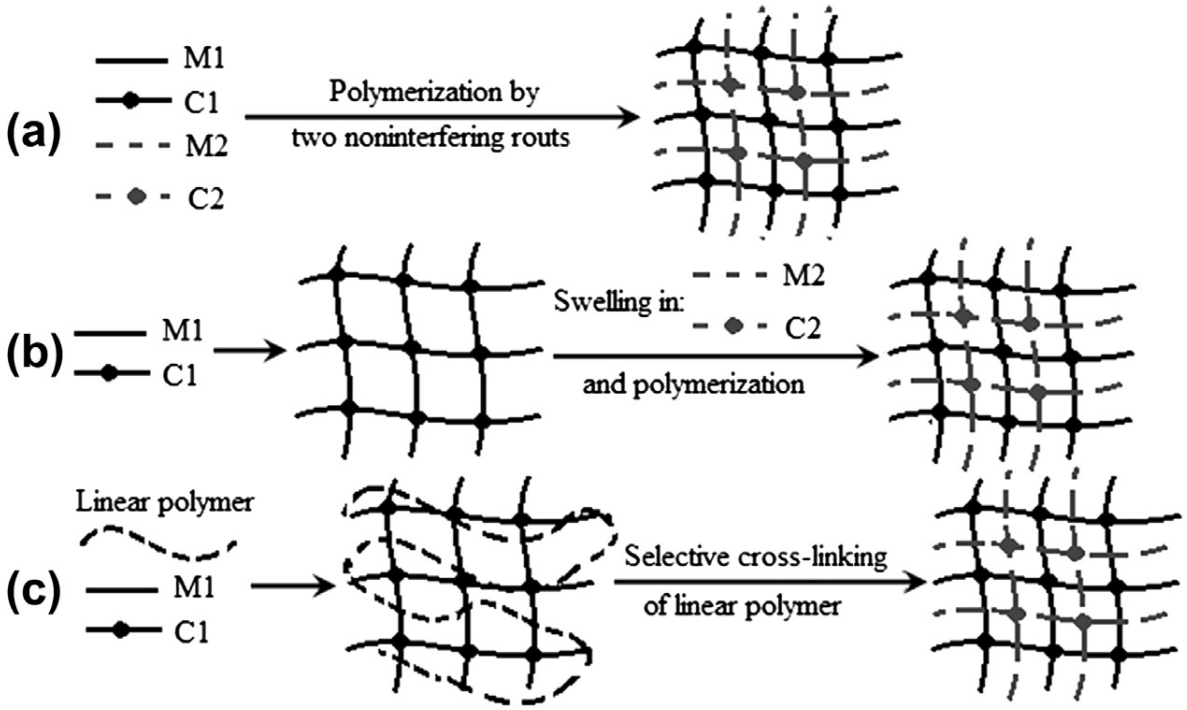

Figure 2-2. Strategies for forming IPNs. (a) Two polymers are simultaneously polymerized and crosslinked; (b) The first polymer network is swollen with a solution containing the second monomer and/or crosslinker components, which are then polymerized and/or crosslinked *in-situ*; (c) a semi-IPN with linear interpenetrating polymer chains is crosslinked within the first polymer network. Reprinted with permission from ref. [5]. Copyright 2014 Elsevier.

2.1.2 Applications of Hydrogels

The broad variety of hydrogels with differing chemical and physical properties means that hydrogels have found applications in a wide variety of fields where water is present, ranging from industrial to biological. In one example from the industrial side, functional groups in hydrogels can enable their use as adsorbents for removal of dyes and heavy metals[6,7]. Some hydrogels are able to absorb particularly large amounts of water (10-1000 times their original weight or volume); these superabsorbent polymers have been used in agriculture and disposable hygiene products (e.g., diapers), as well as for other applications where absorption of large amounts of water is desirable[8]. However, most hydrogel applications are in biomedical sectors. This is due to their favourable properties in biological conditions, particularly their hydrophilicity and ability to absorb large quantities of water. These two properties generally lead to good biocompatibility and favourable interaction with tissue and cells within the body[4,9]. Hydrogels have been used for purposes such as encapsulation for drug or cell delivery[10,11], wound dressings to promote healing[12–14], contact lenses[9,15,16], or scaffolding for tissue engineering[17,18]. Some hydrogels also possess the ability to respond to stimuli such as temperature or pH, allowing them to be used as sensors or actuators that (due to their biocompatibility) could be used in the body[19–21].

The crosslinking behaviour of hydrogels can also be exploited for novel applications. Some hydrogels are crosslinked with reversible bonds; depending on the nature of these interactions, the gels can self-heal after rupture. This behaviour can also be utilized to 'glue' together two fresh pieces of these hydrogels[22–24]. Injectable hydrogels have also been developed, where a prepolymer is injected with a crosslinking agent to form a gel *in situ*[25–27]. These injectable hydrogels lend themselves well to biomedical applications, as their insertion into the body does not require any invasive surgical procedures. This gelling behaviour allows these hydrogels to be applied towards

wound closure and tissue sealing applications[26,28]. In addition, when injected along with drugs, proteins, cells, or nanoparticles, this class of hydrogels can encapsulate these components *in-situ* after injection. When combined with tissue adhesion to prevent rapid removal, these gels can serve as depots for cell or drug delivery[28–30].

2.2 Alginates

Alginates are anionic polysaccharides and a family of copolymers consisting of units of β-D-mannuronic acid (M) and α-L-guluronic acid (G) residues[27,31,32]. These residues can form blocks consisting either entirely of one residue or alternating between the two, e.g., GGGGG, MMMM, or MGMGMG (illustrated in **Figure 2-3**)[33]. They are generally extracted from brown seaweed (though also produced by some bacteria), with the exact composition of the alginate depending on the species of seaweed and the part of the plant used for extraction. Alginate is able to form a gel in the presence of divalent cations, with calcium being the most commonly used. These ionic bridges are only able to be formed at GG sites on the alginate polymer (**Figure 2-3b**), meaning that the length of the G blocks is the main factor responsible for controlling the gel strength of the alginate[33]. A high-G alginate will give a stronger and harder gel with less swelling (due to stronger elastic forces from tighter crosslinking), as well as being more resistant to weakening from anti-gelling salts, e.g., Na^+. In contrast, an alginate with few G-blocks will be softer and more flexible, with greater water absorption and swelling[33]. Because there are so many varieties of alginate from different sources, and these varieties each have unique molecular weights, M/G ratio, and block length, choosing the right alginate for a particular application is essential.

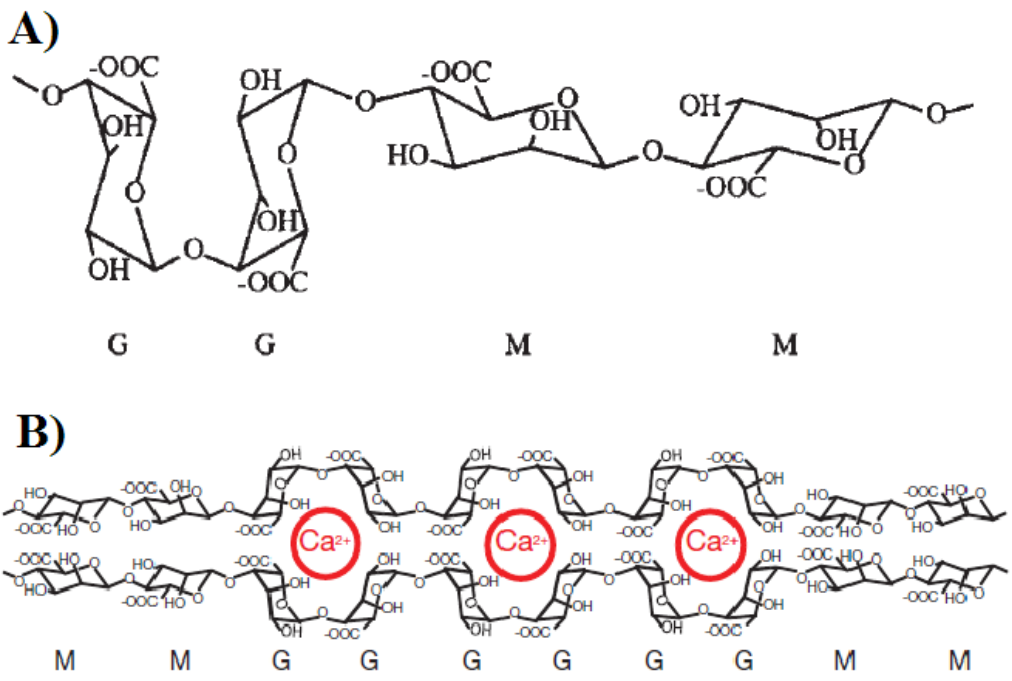

Figure 2-3. a) Structure of alginate, showing GG, GM, and MM blocks. Reprinted with permission from ref. [34]. Copyright 2004 Elsevier; b) Two alginate chains linked through Ca^{2+} ions at GG sites Reprinted with permission from ref. [32]. Copyright 2012 Springer Nature.

Due to its structure and ionic crosslinking, alginate exhibits several interesting behaviours that are different from many other hydrogels. The structure of alginate polymer networks can be described by the "egg-box" model, where crosslinking between chains occurs as multivalent cations fit into cavities between pairing G-blocks in alginate chains[35,36]. As such, crosslinks in alginate gels take the form of long junction zones, rather than individual crosslink points. This means that the general theory of rubber elasticity does not apply to these hydrogels, and could explain their unique mechanical behaviour (which includes a high fracture toughness)[37]. Combined with the ability of alginate's ionic crosslinks to break and reform, these hydrogels exhibit viscoelastic behaviour governed more by kinetics than thermodynamics, though they can behave elastically at low strains. The nature and structure of the ionic crosslinks in alginate hydrogels also leads to better dissipation of energy. Kong et al. proposed that since each crosslinked G-block

could have individual G-residues dissociating at lower stresses than those required for the entire block, G-blocks could partially de-crosslink in a stepwise fashion, leading to a larger plastic zone during deformation[38]. Webber and Shull used compression testing of alginate hydrogels (as compared with the shear and notched tension tests of Kong et al.), the results of which qualitatively agreed with these findings[37]. Together, these properties make alginate relatively unique in its behaviour, which could lead towards further specialized applications.

Besides its gelling properties, alginate is also a useful polymer due to its functional groups that act as potential sites for modification. The hydroxyl groups on the carbon ring can be oxidized and the ring broken to form alginate dialdehyde, which can then be crosslinked with gelatin in the presence of borax to rapidly form a covalently crosslinked gel[13,27]. The carboxylate group can act as a reaction site for crosslinking to other polymers or grafting of side chain groups. These modifications allow for potential novel uses for the resulting polymer, or changes to its properties to make it better suited for specific applications. For example, alginate can be covalently crosslinked with itself, rather than ionically, allowing for better control of gelling properties and a more resilient gel in physiological conditions[14,18].

2.2.1 Alginate Applications

Due to its biocompatibility, non-immunogenicity, and non-toxic nature, many applications for alginate are in the food or medical industries. In food, it is commonly used as a thickening agent for products such as jams, desserts, and sauces. It is also frequently used as a stabilizer or emulsifier in creams, beers (stabilising foam)[39,40], and mayonnaise[41]. One application that spans both the food and medical industries is encapsulation, particularly that of cells. Alginate is well-suited to cell encapsulation because of its gentle and rapid gelling behaviour; it does not require

harsh conditions for crosslinking, which helps prevent damage to cells during encapsulation. Alginate encapsulation has been applied to yeast[40,42] and other bacteria, such as probiotics[43]. Alginate has also been used in drug delivery, encapsulating drugs to provide immunoprotection and control drug release[4,44,45]. Externally, alginate has also been applied as a wound dressing, where it is most commonly used for its high absorption and ability to maintain a moist environment[46], while protecting the wound from maceration[47]. Alginate's gelling behaviour also lends it well to usage as a cost-effective and simple-to-use dental impression material[48].

Despite its advantages, one problem that alginate has – particularly for internal biomedical applications – is its low biodegradability and poor control of degradation. In particular, there are no enzymatic processes in the human body that will naturally break it down[49]. While this is not an issue in the food industry (as alginate will act as fiber in the diet when digested), it does limit its applications as a biomaterial, where a controlled lifetime is frequently desired[50,51]. Various techniques have been used to address this problem. One of the more common methods involves partial oxidation of the alginate, which renders it susceptible to degradation via hydrolysis. When a low degree of oxidation is used, a significant increase in degradation can be achieved without impacting the viability of cells in contact with the gel[27]. Another common method hydrolyzes alginate in acidic conditions to break down MG connections[50]. Polyguluronate can be isolated from the products and oxidized to form poly(aldehyde guluronate), which can then be crosslinked by adipic acid dihydrazide. The resulting hydrazone bond can degrade in aqueous conditions, with crosslinker density controlling the degradation kinetics[52]. Another potential issue with alginate as a biomaterial is poor cell adhesion[51,53]. This has generally been solved by covalent modification of the alginate polymer. This can include coupling of cellular adhesion molecules such as laminin, fibronectin, or collagen, or attachment of short peptides that mediate cell adhesion. The latter

strategy is preferable to control adhesion and avoid non-specific interactions, with a popular option for this being peptides containing the arginine glycine aspartic acid (RGD) attachment site and its subtypes[54,55].

2.3 Interfacial Forces in Hydrogel Adhesion*

2.3.1 Surface Energy and Work of Adhesion

The surface energy of a material (γ) arises from the disrupted bonds at the surface of a material, leading to an imbalance of intermolecular forces and an energy difference between the surface and bulk of the material. When considering the interface between two materials, the interfacial energy describes the energy to separate the materials. This makes the surface energy a useful concept in adhesion; it provides information towards the work of adhesion (W_A), which is defined as the change in energy per unit area associated with replacing a single interface with two separate surfaces:

$$W_A = \gamma_1 + \gamma_2 - \gamma_{12}, \quad (1)$$

where γ_1 and γ_2 are the surface energies of the two individual surfaces, and γ_{12} is the interfacial energy between them[56]. While this gives a broad, surface-scale level of information about interfacial adhesion, the sources of adhesion come from a range of interactions at this interface, as well as larger-scale effects such as mechanical interlocking. The next section covers many of the individual interactions that play a role in adhesion of hydrogels.

2.3.2 Interfacial Interactions

Many adhesive materials utilize nonspecific, noncovalent interactions to achieve adhesion. These noncovalent interactions include dipole-dipole, dipole-induced dipole, and dispersion forces

* This subsection is in preparation as part of a review paper for Chemical Society Reviews.

(with the latter three often grouped together as part of van der Waals forces), as well as electrostatic forces. Van der Waals forces are the most general of these interactions, resulting from a variety of sources such as permanent, instantaneous, and induced dipoles and multipoles. They are individually weak, but a high interfacial surface area can result in these interactions being numerous, and they are applicable to a broad variety of adherends. For example, the micro- and nanoscopic structures of gecko toepads lead to high real contact areas, enhancing van der Waals interactions and allowing them to stick to many surfaces and inspiring many works in dry adhesion[57,58]. Electrostatic forces are also quite nonspecific, relying on charges for attraction. These forces are defined by Coulomb's law:

$$F = \frac{q_1 q_2}{4\pi\varepsilon r^2}, \tag{2}$$

where q_1 and q_2 are the signed magnitudes of two point charges, r is the distance between them, F is the force between them (where a negative force indicates attraction), and ε is the permittivity of the medium. Many of these interactions (particularly electrostatic and van der Waals forces) are inversely proportional to the permittivity (or dielectric constant) of the medium (in the case of electrostatic forces, $\propto 1/\varepsilon$) or its squared value (for van der Waals forces, $\propto 1/\varepsilon^2$)[59]. For hydrogels, this medium is water, the dielectric constant of which is about 80 times that of air. As such, when considering hydrogels, many of these nonspecific interactions will, at best, be at only 1/80 of their strength in air.

Because of these effects of water, other interactions are frequently used to achieve underwater adhesive performance. For example, hydrophobic interactions come from the high entropy cost associated with water molecules arranging themselves around hydrophobic materials. This means that hydrophobic forces are strengthened underwater,

allowing two hydrophobic surfaces to repel water molecules when brought together. While uncommon in hydrogels due to their hydrophilicity, functional groups on the polymer chains could be hydrophobic and make use of these interactions[60].

Another form of interactions that is more commonly used is covalent bonding, where functional groups on the polymer chains are chemically reacted with groups on the adherend's surface. Covalent bonds are stronger than physical interactions; they rely on sharing of electrons, where orbitals of the corresponding atoms overlap. Since it involves chemical reactions, covalent bonding requires specific function groups on the surface, which are either already present or added through surface modification. This has been utilized by groups such as Yuk et al., who chemically modified surfaces so that tough hydrogels could covalently bond for them, resulting in high interfacial toughness[61]. Coordination bonds are a specific form of covalent bond where both electrons participating in the bond originate from the same atom. Coordination bonds are most commonly formed between organic ligands and metal ions or metal oxides. While they are most commonly used for crosslinking purposes in hydrogels[62,63], they can also provide adhesion to metal oxide surfaces[64–66], and may play a role in the adhesive strategies of some marine organisms to such surfaces[67]. However, because of this specificity of surface, coordinate bonds are generally used as one of multiple forms of interaction.

Hydrogen bonding is weaker than covalent bonding, but stronger than many other physical interactions, such as van der Waals forces. It is a specific form of dipole-dipole bonding that involves a hydrogen that is bound to a more electronegative atom or group, as well as another electronegative atom or group that possesses a lone pair of electrons. While typically stronger than many other physical interactions, they are also more specific. More

importantly for underwater adhesion, water itself is capable of hydrogen bonding, which can interfere with an adhesive based on these interactions. As such, many hydrogen bonding-based materials are used in dry conditions[66]. However, some forms of hydrogen bonds are stronger than those of water, making them good candidates for enhancing underwater adhesion. A good example is the catechol group; it can form bidentate hydrogen bonds, which are stronger and much more stable than those of water[67,68].

2.4 Biological strategies for underwater adhesion

While many entirely synthetic adhesives have been developed, especially for use in dry conditions, the subset of these that function underwater is significantly smaller. However, many marine organisms have developed their own strategies for adhering to surfaces in the ocean, attaching to surfaces that may be fouled with other biomatter, and enduring turbulence and the force of waves. Two organisms – benthic brown algae and marine mussels – serve as good models for developing novel underwater adhesives.

2.4.1 Adhesive strategies of brown algae

For brown algae, adhesion primarily occurs in the settling of algal spores and zygotes to the sea floor, with secretion of adhesive components over the entirety of the zygote's surface beginning shortly after fertilization[1,69]. The adhesive material consists of the same components that are found in the algae's cell walls: alginate, polyphenols, and sulfated fucans. Alginate is crosslinked by calcium ions to form calcium alginate gel, which provides cohesion for the overall adhesive. Polyphenols in brown algae consist of phloroglucinol units linked by carbon-carbon and ether bonds[70], and are responsible for initial adsorption onto the substrate, as well as subsequent adhesion. Sulfated fucans consist of a broad variety of highly branched and heterogeneous sulfated polysaccharides. Fucans possess a structural function in brown algae for both the extracellular

matrix of the cell walls and the adhesive material[71]. When initially deposited, these components are not linked to each other; crosslinking occurs during a separate "hardening" stage.

About 2 hours after binding to the substrate, zygotes of brown algae can begin to detect external stimuli. This results in the zygote transitioning to asymmetrical secretion of the adhesive material, preferring the best potential attachment site. At the same time, the adhesive begins transforming from the primary adhesive to the secondary adhesive. The components in the two stages of the adhesive are mostly the same; the major process delineating the two is one of covalent crosslinking, which results in the "hardening" of the adhesive. This covalent crosslinking is catalyzed by vanadium-dependent haloperoxidases, and results in the halogenation of the polyphenols[1]. This activates phenoxy radicals on the polyphenols, inducing covalent crosslinking between them, as well as crosslinking to the alginate chains[70]. The resulting final adhesive consists overall of alginate gel (providing cohesion) and polyphenol aggregates (providing adhesion), all covalently crosslinked together.

2.4.2 Adhesive strategies of marine mussels

Marine mussels adhere to a surface by forming a byssus: a bundle of individual threads, each formed by the mussel foot. These threads end in an adhesive plaque, which is responsible for adhesion to the substrate. During the formation of this plaque, proteins are secreted in liquid form by the mussel foot, in a manner resembling injection molding. These mussel foot proteins (Mfps) are commonly rich in glycine, contain Dopa, and are moderately to strongly cationic, though they do have some chemical diversity, and each possesses its own role in the plaque and thread. They also are localized to the portion of the byssus where they can serve their respective roles. For example, Mfp-3, Mfp-5, and Mfp-6 are generally found at the plaque-substrate interface, where Mfp-3 and Mfp-5 (both particularly rich in Dopa) provide adhesion, and Mfp-6 provides a reducing

environment for the other components. In contrast, Mfp-1 and Mfp-2 provide cohesion to the byssal cuticle and the plaque core, respectively. To do so, Mfp-1 and Mfp-2 utilize Dopa to provide crosslinking capability by coordinating with Fe^{3+} ions to form tris-catecholato-Fe^{3+} complexes.

While Dopa-based chemistry plays an important role in the mussel byssus, it is vital to also understand the processing steps used by the mussel to achieve adhesion. An illustration of the processes of plaque deposition by the mussel foot can be seen in **Figure 2-4**. During this protein deposition, the distal depression in the mussel foot seals a closed environment, wherein the mussel tightly controls a variety of conditions. This includes adjusting the pH (with experiments showing pH ranges of 2–4[72] or 4–6.5[68], compared to pH 8 of seawater) and the ionic strength (0.15 mol/L, compared to 0.7 mol/L in seawater), as well as maintaining a reducing environment. When the Mfps are secreted into this controlled environment, they can engage in coacervation: a form of fluid-fluid phase separation where two polyelectrolytes neutralize each other. In this form, they are better able to spread and wet the substrate, where Mfp-3 and Mfp-5 can engage in adhesion. In the low-pH conditions during plaque formation, interactions between these Mfps and the substrate are implicated to include bidentate hydrogen bonding, electrostatic attraction, and hydrophobic interactions (with coordination bonding also a possibility at pH values ≥ 5). The exact nature and strength of these interactions depends on the type of substrate, indicating the versatility of this adhesion. Before forming the final plaque, these coacervates likely undergo phase inversion, transforming from coacervate droplets in water to water droplets in coacervate. This would allow the plaque to form its observed porous solid structure after solidification.

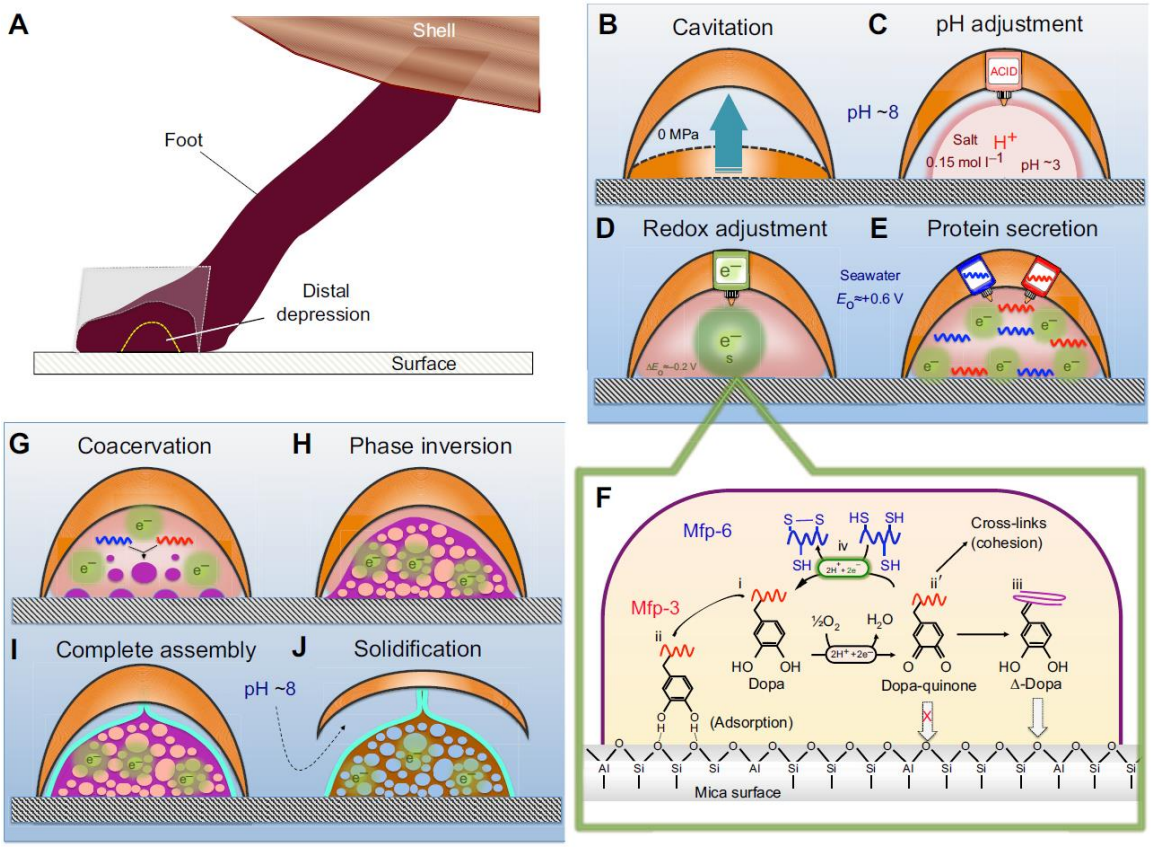

Figure 2-4. Deposition of plaque proteins by the mussel foot. Multiple stages are involved in plaque formation, which occurs in the distal depression of the mussel foot (a). These include cavitation to form a closed environment (b); adjustment of pH (c) and the redox environment (d); secretion of proteins to form the plaque (e); interaction of proteins with the surface (f); their subsequent coacervation (g); phase inversion of the coacervate (h) and coating with the mussel cuticle (i); with solidification occurring upon exposure to seawater (j). Reprinted with permission from ref. [67]. Copyright 2017 The Company of Biologists.

Importantly, the plaque does not majorly contribute to the strength of the overall mussel holdfast until after the mussel foot has been withdrawn. At this point, the plaque is exposed to seawater, which triggers the solidification of the plaque and thread – this is reminiscent of the "hardening" transition in brown algae from primary to secondary adhesive. This results in changes to both the adhesive and cohesive chemistry of the plaque and thread. Cohesively, the proteins in the coacervate precipitate out of the solution to form the solid porous structure of the plaque. Additionally, coordination bonding is activated at higher pH values, allowing Mfp-1 and Mfp-2 to

engage in coordinative crosslinking through Fe^{3+} ions to give strength to the plaque and thread. Dopa in the Mfps can also engage in covalent crosslinking after oxidation due to increased pH, which could improve long-term cohesive strength and stability. Adhesively, higher pH can induce coordinate or covalent bonding to a substrate (depending on surface chemistry of the substrate). However, the Dopa groups on Mfp-3 and Mfp-5 generally perform best when reduced. These catechols are protected from oxidation while interacting with the substrate surface, and Mfp-6 can rescue Dopa-quinone groups that form by oxidizing them, but this emphasizes the reliance of mussels on controlling their chemistry.

Overall, mussels engage in a careful and complex number of steps to achieve underwater adhesion. The chemistry behind their adhesion is important – while recognizing the need to control pH and redox potential – but the processing of their various components is essential to obtain strong adhesion. By combining both these aspects, new materials can be developed to adhere strongly underwater while resisting the conditions of this environment.

2.5 Bioinspired adhesives

2.5.1 Mussel-inspired adhesives

Marine mussels are probably the most studied and mimicked organism for obtaining adhesion to surfaces underwater. While recent research has highlighted the importance of mussels' adhesive process, almost all work in developing adhesives inspired by marine mussels has been centred on duplicating their chemistry[67]. In particular, the catechol group present in Dopa was identified as an important source of mussel adhesion. This is exemplified with studies of single-molecule adhesion of Dopa to a titanium surface, demonstrating a single-molecule pull-off force of ~800 pN, which is greater than typical hydrogen bonding forces in the tens of piconewtons, and not much smaller than the few nanonewtons required to rupture a covalent bond[64]. As such, much

research has been devoted to incorporating catechol functionality into polymers. This has been accomplished through many different means, with three main structures of incorporation (shown in **Figure 2-5**): polymerization of the catechols themselves, grafting of catechols as side groups on polymer chains, and grafting of catechols onto the end groups of polymer chains[73].

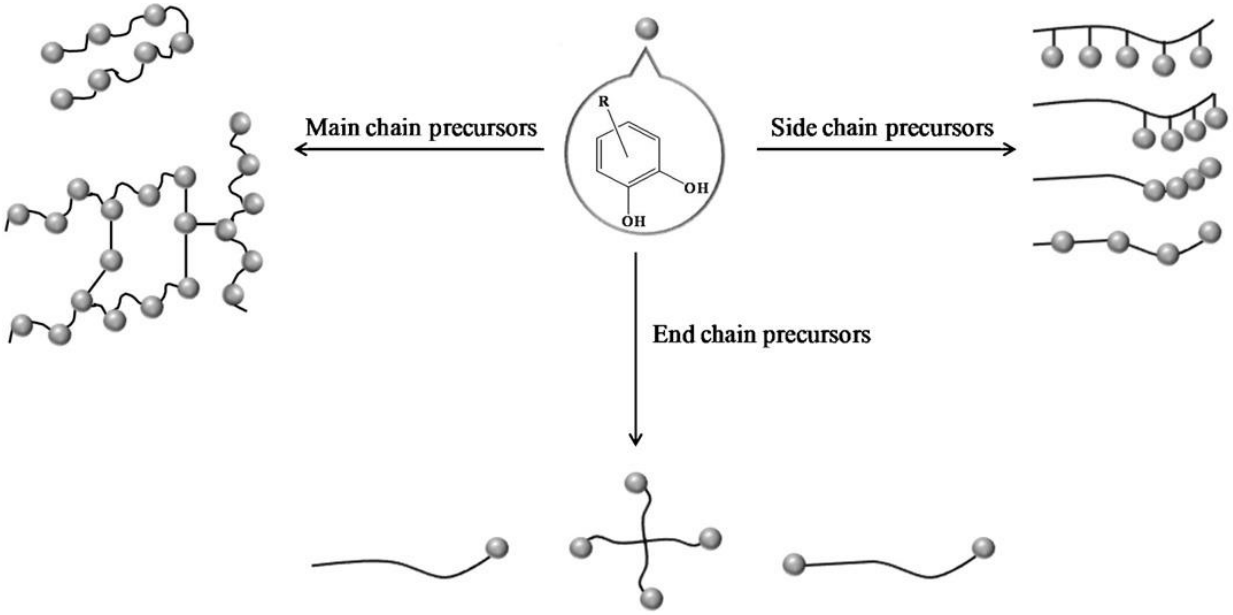

Figure 2-5. The three main ways that catechol groups can be incorporated into polymers, as part of the polymer backbone, or as side or end groups on polymer chains. Reprinted with permission from ref. [73]. Copyright 2013 Elsevier.

In the first method of developing catechol-bearing polymers, functional catechol molecules are themselves polymerized into poly(catechols), which frequently take the form of highly-crosslinked films. This is accomplished by converting catechol groups into quinones (typically utilizing a strong oxidizer or an enzyme), which are highly reactive, leading to the formation of poly(catechols). However, the most commonly used molecule for forming poly(catechols) is dopamine. Dopamine (DA) is a small molecule that is most commonly known as a neurotransmitter, playing a key role in reward and motivation, as well as other functions including motor control[74]. However, it is also a small molecule mimic of the components primarily

responsible for underwater adhesion in marine mussels. This is based on the observation that the proteins responsible for adhesion in mussels frequently display Dopa and lysine (Lys) amino acids in close proximity[75]. Messersmith et al. theorized that the close proximity of the catechol groups from Dopa to the amine from Lys was crucial to achieve strong adhesion to a wide range of materials, and proposed that DA, with both catechol and amine groups, could duplicate this functionality[76]. When dissolved in a basic (pH ~8.5) aqueous solution, DA will form a thin film of polydopamine (PDA) on almost any surface, including 'non-stick' surfaces such as polytetrafluroethylene (PTFE)[76]. Because of this capability, PDA films have been utilized in a multitude of coating applications. While PDA films have been used for their intrinsic properties – typically to improve cell adhesion to surfaces or even to encapsulate drugs – they also can be further modified in order to obtain a variety of surface functionalities. This includes utilizing PDA films in biomineralization[77], reaction of quinone groups with further functional groups[73], and grafting of polymers and proteins such as poly(ethylene oxide) for antifouling purposes[78] or bovine serum albumin to improve cell adhesion[79].

Compared with direct polymerization of poly(catechols), adding catechol functionality to the side chains of polymers allows greater flexibility in the properties of the polymers that can be combined with the adhesion from catechol. This is particularly true of copolymer systems, where the catechol-rich component allows for adhesion to a substrate, and the other component can be chosen for a particular functionality, allowing for functionalization of that substrate. An example of this process can be seen in **Figure 2-6**, where attached catechols allow for adhesion to a metal substrate. The second component of the copolymer can be chosen to promote or reduce adhesion, allowing for the surface to be made adhesive or anti-fouling[80].

One method for incorporating catechols as side chains is to start with vinyl monomers that bear a catechol functional group, and then to polymerize these monomers into a polymer with a catechol group on each unit in the chain. These vinyl catechols can be copolymerized with other monomers to acquire different properties in the resulting copolymer, with catechol groups on some fraction of the units in the polymer. Some of the most common examples of this include the use of Dopa methacrylamide[81] or dopamine methacrylamide[82]. In these methods, whether the catechol group is protected or unprotected is important, as unprotected groups can lead to the formation of branched polymers, as opposed to the linear polymers formed with protected groups[73].

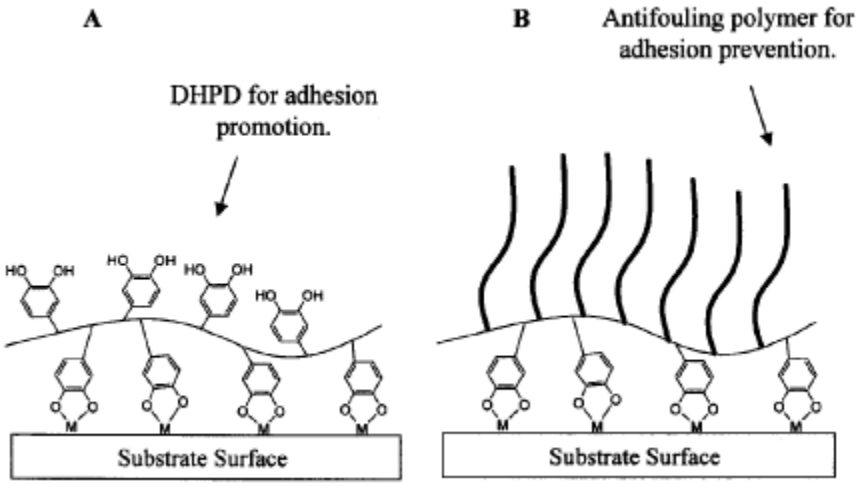

Figure 2-6. Catechols incorporated as side groups on a polymer to increase adhesion to a substrate, to provide a) increased adhesion to other materials; b) reduced adhesion to other materials Reprinted with permission from ref. [83], originally adapted from ref. [80].

A different method to acquire polymers with catechols as side groups is to modify biopolymers, such as peptides or proteins, bearing tyrosine (Tyr). This amino acid can be oxidized by the enzyme tyrosinase to form catechol or quinone groups, depending on the conditions of the reaction. In aerated and reducing conditions, tyrosinase can convert Tyr groups into Dopa amino acids[84]. These biopolymers more closely follow the original inspiration of mussel adhesive

proteins, and commonly possess Lys and Tyr groups in close proximity to one another, duplicating the effect of nearby Dopa and Lys after conversion of Tyr by tyrosinase[84].

One particularly useful method for grafting DA onto a polymer is through carbodiimide crosslinker chemistry. Carbodiimide coupling is a commonly used technique for attaching DA to polymers, and has been used for grafting of catechol functionality to alginate and heparin by Haeshin Lee's group[18,85]. This reaction links the primary amine on DA to a carboxylic acid on the polymer chain to form an amide bond (this reaction can also link a catechol with a carboxylic acid to a primary amine on a polymer chain). The most frequently used carbodiimide for aqueous crosslinking is 1-ethyl-3-(3-dimethylaminopropyl) carbodiimide (EDC); N-hydroxysuccinimide (NHS) or N-hydroxysulfosuccinimide (Sulfo-NHS) are commonly used to form a stable intermediate during the reaction. **Figure 2-7a** shows the mechanism behind amide coupling through EDC/NHS chemistry. Step (1) shows the reaction of the diimide with a carboxylic acid group (the first of two components that will be linked), then subsequent formation of the NHS ester intermediate. Step (2) shows the reaction with a primary amine (the second component) to form an amide bond between the two components. EDC/NHS act as zero-length crosslinkers here, as the final result is a direct link between the carboxylate and amine, with no part of the crosslinkers being incorporated into the final product. Step (3) is optional, where ethanolamine is added to deactivate the remaining NHS esters. These will also be deactivated by hydrolysis in the solution, with the rate of hydrolysis increasing with increasing pH. This can interfere with the step (2) reaction, reducing the efficiency of the final reaction, but can also serve to remove leftover NHS ester groups after the reaction is complete. Balancing pH is essential for this reaction, as the diimide reaction is most efficient in acidic conditions (pH ~4.5), while the NHS ester formation is most efficient at neutral conditions (pH ~7.2). Another consideration is the DA itself, which will

oxidize in aqueous conditions of neutral or higher pH. With the amine/amide group present, this can lead to irreversible formation of PDA and loss of some of the functionality. Due to all of these factors, most EDC/NHS reactions using DA are performed at intermediate pH values, often pH ~5.5[11,18,85,86].

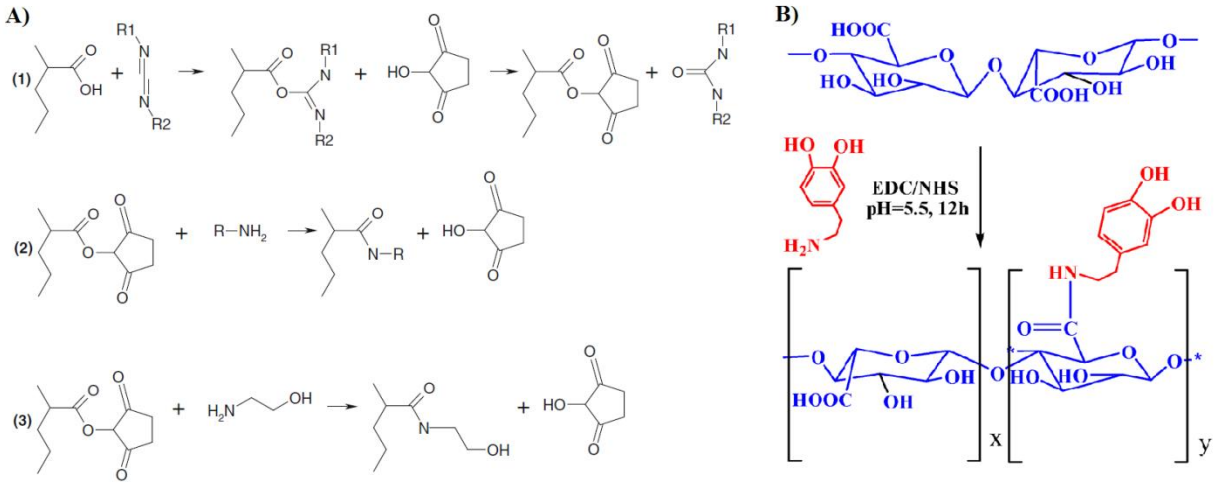

Figure 2-7. a) The mechanism of amide coupling through EDC/NHS chemistry. Reprinted with permission from ref. [87]. Copyright 2010 Springer Science; b) Schematic showing the attachment of dopamine to alginate polymer through EDC/NHS chemistry. Reprinted with permission from ref. [11]. Copyright 2012 American Chemical Society.

2.5.2 Algae-inspired adhesives

While there has been a great deal of interest in developing mussel inspired-adhesives, algae-based adhesives are less well-studied. Similarly to mussels, most work has been focused on duplicating algal adhesive chemistry using synthetic materials. Calcium alginate has been used as the primary cohesive component, which directly mimics the alginate network in brown algae adhesives. Phloroglucinol is commonly used to take the place of the adhesive polyphenol component, as it is the monomeric unit of the polyphenols present in brown algae[88,89]. However, other phenolic compounds (e.g., hydroquinone and pyrogallol) have been utilized for adhesion as well[90]. In some versions of algae-inspired glues, phloroglucinol was oxidised in the presence of

bromoperoxidase, KI, and H_2O_2. This was to duplicate the oxidative crosslinking present in the "hardening" stage of algal adhesive[88,91]. These glues have been targeted for medical applications – particularly as tissue adhesives[92] and tissue sealants[90] – due to their biocompatibility and low toxicity (though this is only true of the non-oxidised form, due to the use of H_2O_2[92]). However, biodegradability can be a concern, as the human body does not produce enzymes that will break down alginate.

2.6 Characterization techniques

2.6.1 Indentation

Indentation testing is one method of testing the mechanical and adhesive properties of hydrogels and thin films[32,93–95]. When an indentation probe is pressed into a sample in compression, the forces it feels can be used to determine elastic modulus[32,93,94]. In addition, when the probe is pulled away from the sample, if there is any adhesion between the two surfaces, an additional pull-off force will be felt before the probe separates from the sample surface. This pull-off force can be used to determine the adhesion between the probe and the sample. **Figure 2-8** shows a typical indentation curve for adhering surfaces, with the pull-off force visible on the unloading curve. Indentation can be performed on various length and force scales, with different probes, depending on the nature of the substrate. An atomic force microscope (AFM) tip can be used as a probe on the nano-scale, or a soft polymer tip for conformal contact at the micro-scale, or a hemispherical steel probe for rigid contact. The choice of probe material is also dependent on what is being measured. Common probes used in testing include glass[96], polydimethylsiloxane (PDMS)[95], or AFM tip probes[32]. In less common cases, adhesion between two specific materials could be tested with a probe and substrate of the respective materials. For example, adhesion of a polymer to metal could be tested with a metal probe indented into a flat piece of polymer. Adhesion

of the same polymer to a thin film could be tested either by coating the metal probe with the film, or (if the coating process is limited to flat surfaces) using a hemispherical probe made of the polymer with the coated material as the substrate.

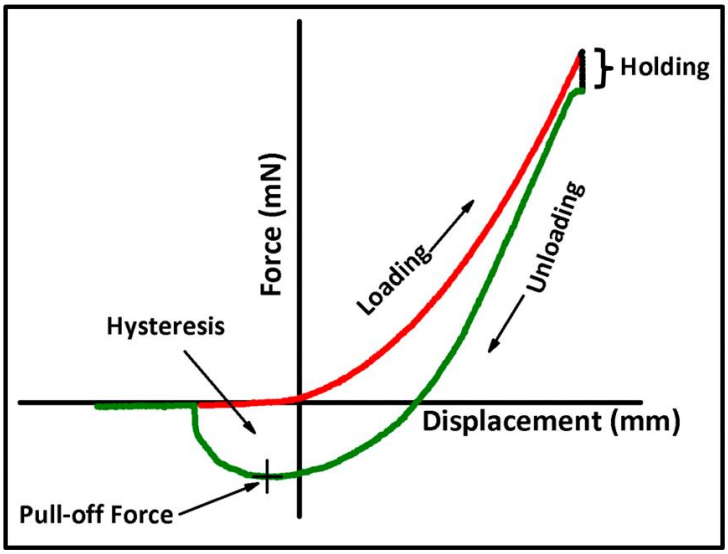

Figure 2-8. Typical force loading and unloading curve for an adhesive sample, highlighting stress relaxation during holding, pull-off force from adhesion, and hysteresis from time-dependent behaviour. Adapted with permission from ref. [93]. Copyright 2013 American Chemical Society.

When studying the mechanical properties of the sample through indentation, either Hertzian contact theory or JKR theory can be applied to the system. Hertzian contact assumes non-adhesive contact between the two surfaces, and works well for rigid materials. Using this model, the loading force, F, is related to the radius of the circle of contact, a_0, through the following equation:

$$a_0^3 = \frac{3}{4}\frac{RF}{E^*}, \tag{3}$$

where R is the combined radius of the two surfaces, $R = R_1R_2/R_1 + R_2$ (for a sphere and a plane, $R_2 \to \infty$, so $R \to R_1$), and E^* is the reduced Young's modulus of the two materials, defined as:

$$\frac{1}{E^*} = \frac{1-v_1^2}{E_1} + \frac{1-v_2^2}{E_2}, \tag{4}$$

with v_1 and E_1, and v_2 and E_2 the Poisson's ratio and Young's modulus of material 1 and 2, respectively[97]. Eq. (3) can be rewritten to provide a relationship between the load and the displacement, d, of:

$$F = KR^{1/2}d^{3/2}, \tag{5}$$

where $K = \frac{4}{3}E^*$. In situations where adhesion can be neglected, this theory works well and can provide relationships between modulus, stress, and deformation of the contacting solids[96]. However, where adhesion does play an important role, such as in the contact of soft materials, the theory is insufficient.

Johnson, Kendall, and Roberts took Hertz's theory and extended it to take adhesion between the two contacting surfaces into account. This led to JKR theory, which relates deformation of the solids to both the externally applied load and adhesion forces between them[98]. **Figure 2-9** illustrates the difference between the two models, where two spheres with radii R_1 and R_2, respectively, are pressed together to a displacement δ with a force P_0. a_0 shows the radius of the contact area if there is no adhesion between the surfaces, while a_1 is the contact area radius with adhesion present. These additional forces require changes to be made to the original Hertz equation of Eq. (3). When modified to incorporate the work of adhesion between the two surfaces, the Hertz equation becomes:

$$a^3 = \frac{R}{K}\left(F + 3W_A\pi R + \sqrt{6W_A\pi RF + (3W_A\pi R)^2}\right), \tag{6}$$

where W_A is the work of adhesion between the two surfaces. This can be particularly useful in indentation tests where the contact area can be seen (e.g., with a transparent or translucent substrate and a camera underneath the contact point), allowing for direct measurement of a as it changes with increasing F. Note that when $W_A = 0$ (i.e., there is no adhesion between the two surfaces), Eq. (6) becomes simply $a^3 = RF/K$, which is the same as the original Hertz equation as seen in Eq. (3). Another important consideration is that even at zero applied load, due to adhesion, the contact area is nonzero, and given by:

$$a^3 = \frac{R(6\pi W_A R)}{K}. \tag{7}$$

With there still being contact between surfaces at zero applied load, the force of adhesion can be determined by the required force to completely separate the two surfaces. Eq. (6) can be solved to find this point, and the required force to separate the surfaces, F_s, is:

$$F_s = -\frac{3}{2} W_A \pi R = -F_{ad}. \tag{8}$$

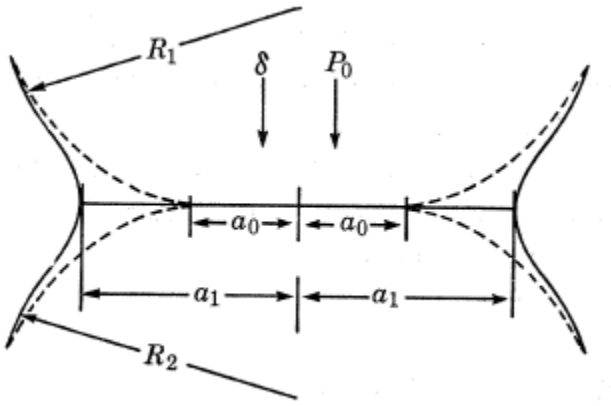

Figure 2-9. Contact between two convex surfaces with ($\boldsymbol{a_1}$) and without ($\boldsymbol{a_0}$) surface forces. Reprinted with permission from ref. [98]. Copyright 1971 Royal Society.

2.6.2 Alternate Adhesive Testing

While indentation is one method for determining the adhesion between two surfaces, it is not the only technique that is used. One other useful method is peeling one surface away from another (as shown in **Figure 2-10**). This is a method commonly used to test adhesive tapes, and applies well to testing adhesion of films or fabrics. The test is carried out by applying the adhesive material to the substrate, letting it set for a specific duration, and then pulling it off the substrate at both a constant rate and angle. By using a materials tester to pull the material, and assuming that this material is flexible but not extensible, the force required to peel off the dressing at this constant rate could be calculated. This force can be related to the work of adhesion between the two surfaces through Equation (9) [99]:

$$F = \frac{bW_A}{1 - cos\theta}, \tag{9}$$

where b is the width of the contact area (perpendicular to the pulling force), F is the measured pulling force, and θ is the pulling angle (between the substrate and film being peeled). As peeling force can be dependent on the velocity, this parameter is important to report when performing peeling tests.

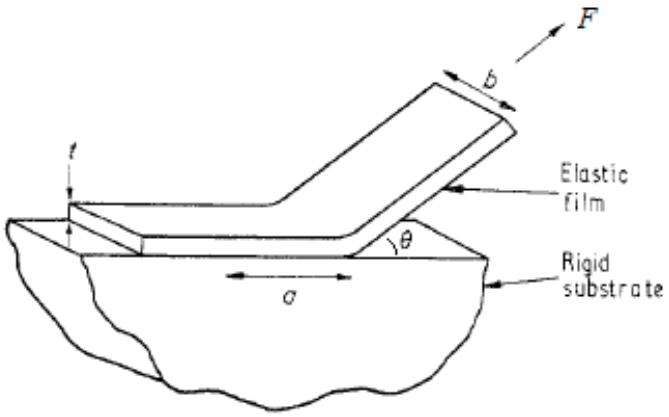

Figure 2-10. Schematic of the peeling test for adhesion of tapes or films. Reprinted with permission from ref. [99]. Copyright 1971 IOP Publishing.

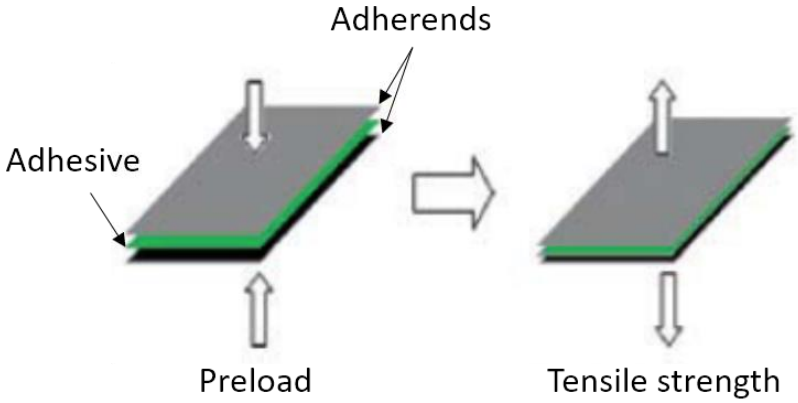

Figure 2-11. Schematic of testing geometry for tensile adhesive strength. Adherends are pressed together (with adhesive in between, or with one being adhesive itself), then pulled apart in the normal direction to the interface. Adapted with permission from ref. [100]. Copyright 2012 Royal Society of Chemistry.

Another method of adhesive testing is tensile (or pull-off) testing, illustrated in **Figure 2-11**. In this method, the two surfaces are bonded together and then pulled directly apart, in a direction normal to the plane of contact. As the two materials are pulled away, the force and displacement can be measured. When the adhesive fails, either at the interface (adhesive failure) or within itself (cohesive failure), the force at which this occurs can be measured. This total force

is a measure of the overall tensile adhesive strength, and can be converted to a stress through dividing by the contact area[101].

2.6.3 Scanning Electron Microscopy

Scanning electron microscopy is an imaging technique using similar principles as reflective optical microscopy, but using electrons as the image source. Because electrons have a much smaller wavelength than visible light ($\lambda_e = \frac{h}{p_e} = \frac{h}{\sqrt{2 \cdot m_e \cdot e \cdot V_a}}$ for an electron experiencing an accelerating voltage of V_a, where λ_e is the de Broglie wavelength p_e is the momentum of the electron , h is the Planck constant, and m_e and e are the mass and charge of an electron, respectively), this enables scanning electron microscopes (SEMs) to image materials at a much smaller scale. In an SEM, the sample is bombarded with an electron beam, which consists of electrons emitted by a thermionic or field emission source. When these electrons interact with the sample surface, multiple responses occur, which are detected separately and each used in a different aspect of SEM; these include secondary electrons (SE), backscattered electrons (BSE), and X-rays[102]. Secondary electrons are generated by inelastic scattering interactions between the electron beam and the sample; the energy lost in these interactions is able to excite electrons in the conduction or valence bands of sample atoms, which can then be picked up by a detector. Since these electrons do not possess much energy, they can only escape from a depth of a few nanometers below the surface. This makes SE emission highly sensitive to the topography of the surface. As such, SE are commonly used to image the structure of a surface with resolution on the order of nanometers or less[103]. In contrast, backscattered electrons – electrons from the original beam, reflected by elastic scattering interactions with sample atoms – are much higher energy and less sensitive to topography. Their energy depends more strongly on the atomic number of the atoms they are interacting with, as atomics with higher atomic weights backscatter electrons more

strongly[102]. A separate detector – commonly an annular detector in a ring around the electron beam source – is used to pick up BSE, and they are often used to detect contrast in elemental compositions over an area.

Escaped and reflected electrons are not the only results from the electron beam that can be detected and used in analysis. When electrons are ejected from the inner shells of atoms in the sample, electrons from higher states fill the vacancy, giving up energy to do so – this change in energy releases X-rays characteristic to that element, which can then be picked up by an X-ray detector. These X-rays can escape from deeper parts of the same than SE and BSE, and are used in energy-dispersive X-ray spectroscopy (EDX) and wavelength-dispersive X-ray spectroscopy (WDX). In WDX, an X-ray analyzing crystal collects X-rays of specific wavelengths at a time (using Bragg's law to diffract X-rays of specific wavelengths to reach the detector) – this is a slower method, but leads to higher resolution and lower background noise. EDX is the more commonly-used technique, wherein the X-rays are collected by the detector all together, measuring both their energy and intensity for identifying elements and determining their relative quantities, respectively.

2.6.4 Environmental Scanning Electron Microscopy

An environmental scanning electron microscope (ESEM) is similar to an SEM in overall function (using an electron beam to probe the sample and detecting signals that are released), but is able to examine specimens under gaseous environments at a relatively high pressure (with pressures up to 10-20 torr) and in the presence of liquid. This allows for imaging of objects in a more natural state, which is particularly useful for biological samples[104]. In order to accommodate for 'environmental' conditions, an ESEM requires multiple changes in its structure, particularly in its internal chambers and its secondary electron detection. In an ESEM, the specimen chamber is

kept separate from the electron source; the specimen chamber itself is kept at relatively high pressure, with two or more narrow apertures separating it from the high vacuum in the electron optics column containing the electron gun. Pumps are used to remove gases that escape each aperture; assisted by the pumps, a drop in pressure of multiple orders of magnitude across an aperture can be obtained, allowing for the electron gun to be kept at the high vacuum it requires. While the electron beam itself will be scattered by the higher pressure in the specimen chamber, a useful portion can reach the sample, producing similar signals as in a regular SEM.

While the electron beam outputs similar signals to SEM, an ESEM requires different detectors to catch secondary electrons. The conventional secondary electron detector in SEM, an Everhart-Thornley detector, will electrically discharge in a gaseous environment; a gaseous secondary electron detector is used instead[105]. This detector has a positive bias applied (typically several hundred volts) to attract electrons, and is positioned relatively close to the sample so it can be reached by the electrons. In fact, when secondary electrons escape the sample, they can interact with gas molecules on the way to the detector, releasing additional secondary electrons. This avalanche of releasing electrons serves to amplify the signal, allowing electrons to be detected even in the relatively high pressures of an ESEM. The presence of gas, particularly water vapour, in the system has other advantages as well. ESEMs are well-suited for non-conductive samples, as they do not suffer the same issues with charging as in conventional SEM. This charging typically results from the buildup of negative charge on the surface, due to the bombardment by negatively charged electrons, combined with an inability to carry away the charge for an insulating sample; the negative charges can deflect the electron beam from its target, causing imaging issues and artifacts. However, in an ESEM, the gas is ionized by the electron beam and the released secondary

and backscattered electrons; these positive ions are driven towards the sample by the electric field of the gaseous secondary electron detector, neutralizing any negative charges on the surface.

2.6.5 X-ray Photoelectron Spectroscopy

Inversely to EDX, X-ray photoelectron spectroscopy (XPS) uses X-rays to excite the electrons of atoms in a material, giving some enough energy to escape. The number and kinetic energy of these electrons is captured and recorded by a detector, and this gives useful elemental and chemical analysis of the sample. The kinetic energy of the electrons comes from their original binding energy to the atoms; this generates characteristic peaks for specific elements and their energy levels (e.g., C 1s, O 1s, and O 2p), which combined with a count of these electrons provides the elemental analysis of a sample[106]. By accounting for the difference in intensity generated by different elements (using a relative sensitivity factor), quantitative atomic percents can be found. Additionally, different oxidation states or types of chemical bonding can shift the elemental peak by a known amount, which means XPS can be used to provided chemical analysis as well. However, due to the distance of the detector from the sample, XPS systems require ultra-high vacuum to increase the mean free path of escaped electrons. Excited electrons also lose a lot of energy as they interact with the sample while passing through it, reducing the number that can escape[106]. Since this decay in energy is exponential, it can be used to estimate the depth of elements, which is of interest for inhomogeneous and layered samples.

2.6.6 Fourier Transform Infrared Spectroscopy

Fourier transform infrared spectroscopy (FTIR) is a subset of infrared spectroscopy, which uses infrared light to probe the structure of chemicals. Infrared spectroscopy exploits the fact that molecules will absorb specific frequencies of energy corresponding to specific vibrational modes of the molecule itself[107].. The resulting change in absorbance/transmittance can lead to a peak at

that specific frequency; acquiring values of absorbance or transmittance over a range of frequencies will give a spectrum that acts as a 'fingerprint' for specific molecules and functional groups. While some infrared spectroscopy techniques scan over a range of individual wavelengths to acquire these spectra, FTIR allows for exposing a sample to an entire range of wavelengths at once, which possesses several advantages, including a shorter scan time and higher signal-to-noise ratio.

FTIR utilizes a Michelson interferometer, with which an incident beam of light is split into two by a beam splitter, where one beam is sent to a fixed mirror and the other to a movable mirror. When the beams are recombined, they will engage in constructive or destructive interference, depending on the difference in path length – the movable mirror is shifted over the range of path lengths, and the combined light reaches first the sample and then the detector. The resulting map of intensity vs. path length is called an interferogram, which can then be converted into an absorbance or transmittance spectrum by Fourier transformation (with the resulting spectrum plotted against wavenumber, cm^{-1})[108].

2.6.7 Raman Spectroscopy

Like FTIR, Raman spectroscopy is another light-based technique that examines vibrational and rotational modes. However, Raman spectroscopy uses light in the visible, near-infrared, or near-UV ranges, and relies on the shift in energy of a small fraction of light by the change in vibrational mode. When light (with frequency ν_0) interacts with molecules in the sample, they become excited to a higher rovibrational state. Most of these excited molecules, when they relax, return to their original state, releasing light with the same frequency (ν_0) as the excitation source; this interaction is known as elastic Rayleigh scattering. However, a small fraction of molecules engage in inelastic scattering, returning to a different vibrational state from their state before

excitation – starting from the basic vibrational state and returning to an excited state (with energy corresponding to ν_m) releases light with a lower frequency ($\nu_0 - \nu_m$), referred to as a Stokes shift, while starting from an excited state and returning to the basic vibrational state releases light with a higher frequency ($\nu_0 + \nu_m$), referred to as an anti-Stokes shift[109]. These Stokes and anti-Stokes shifts can provide information on chemical bonds and groups present within a sample, as well as identifying specific chemicals by using the fingerprint region. Additionally, Raman spectroscopy provides a complementary technique to IR spectroscopy (like FTIR), as the signal strength in Raman spectroscopy depends on the change in polarizability of the molecule, which tends to be stronger in relatively neutral or symmetric bonds (contrasted with IR spectroscopy, which sees a stronger signal from higher polar bonds).

2.6.8 Ultraviolet-Visible Spectroscopy

Ultraviolet-Visible (UV-Vis) spectroscopy uses light in the visible and UV wavelengths to examine molecules present in a specific compound. The general principle behind UV-Vis spectroscopy is the ability of light to excite electrons. The wavelengths of visible light (and those near this range) are able to excite electrons into a higher electronic state. The main electrons able to absorb light at these wavelengths are electrons involved in π-bonds or non-bonding electrons in lone pairs, as both these types of electrons are less stable than σ-bond electrons, and require less energy to excite[110]. Each electron and its respective excited state require a specific amount of energy, meaning that they will absorb a particular wavelength of light that possesses this energy. Thus, plotting the wavelength vs. the absorbance/transmittance at that wavelength can give information as to the bonds present in a compound. This enables the detection of specific functional groups, which is particularly useful when attempting to modify a polymer, to detect the presence of the desired group. This has been used when attempting to graft catechol functional groups onto

hydrogels, as the catechol functional group has an absorbance peak at 280 nm[18,85,111]. The presence of this peak (and its absence in the unmodified polymer) serves as a strong indication that catechols are present. Additionally, when the group is oxidized to a quinone, the peak broadens and shifts to ~350 nm, meaning that both attachment of the catechol and its oxidation can be detected[112].

2.6.9 Nuclear Magnetic Resonance Spectroscopy

Nuclear magnetic resonance (NMR) spectroscopy is a powerful technique that allows analysis of the nuclei in a molecule, allowing for detailed information about the groups within that molecule, as well as their states and chemical environment. NMR spectroscopy exploits the nature of nuclei with (either half or whole integer) spin in a magnetic field, which exhibit splitting of the energy levels, each with an associated magnetic quantum number, m. As the population in the lower energy level will be slightly greater, due to alignment with the field and thermal agitation, these nuclei can be excited by electromagnetic radiation, with the required wavelength dependent on the energy difference, ΔE, between these levels. This energy difference depends heavily on the bonds and local environment of the nuclei being investigated. This is mostly because of the nature of the electrons surrounding the nuclei. These partially shield the nuclei from the applied magnetic field, and can be involved in bonds or have reduced effect due to electron withdrawing groups. For example, the hydrogens in CH_4, CH_3F, and -CH_3 will all require a different amount of energy to excite the nucleus, giving a different signal. The most common nuclei used for NMR spectroscopy are those of ^{1}H, due to its high abundance and sensitivity. Other useful nuclei include ^{13}C, ^{19}F, and ^{31}P. Deuterated solvents (with ^{1}H replaced by an isotope, deuterium, ^{2}H or D) are used to dissolve samples for NMR, to reduce the large absorption that would come from a non-deuterated solvent[113,114].

Most NMR spectroscopy uses Fourier transform NMR instruments, which send out a pulse containing all the frequencies in a spectrum (the older continuous wave method increments the energy to excite each nucleus in turn). All the nuclei in the sample are excited by this pulse, which provides a radio frequency signal. The nuclei then relax, resulting in this signal decaying with a frequency consisting of the sum of the individual frequencies of the nuclei. When mixed with a lower frequency signal, this output is called the free induction decay (FID). A Fourier transform of the FID provides a spectrum in the frequency domain, with peaks corresponding to the excitation energy of the different nuclei[114]. This has been applied by Lee et al. and Kastrup et al. for detection of successful addition of dopamine to the side chains of alginate[18,30]. As shown in **Figure 2-12**, the presence of attached dopamine results in the appearance of several new peaks of the NMR spectrum, meaning these peaks can help to confirm successful modification of alginate with dopamine. An additional note is that the peaks marked (a) are shifted from those marked (b), due to the different groups attached to the (a) and (b) carbon atoms.

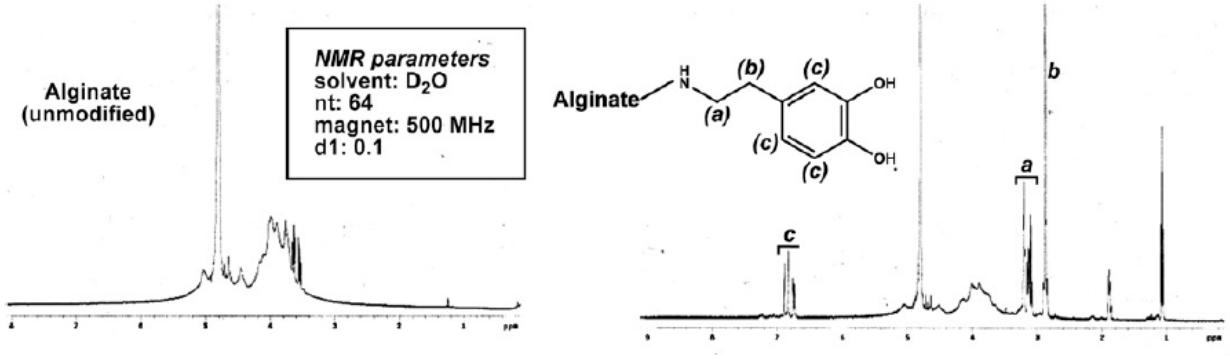

Figure 2-12. NMR spectra for unmodified alginate (left) and alginate with dopamine attached (right), with relevant peaks for dopamine marked Reprinted with permission from ref. [30]. Copyright 2012 National Academy of Sciences

Chapter 3 Underwater Contact Behaviour of Alginate and Catechol-Conjugated Alginate Hydrogel Beads[†]

3.1 Introduction

As mentioned in the previous chapter, hydrogels are a class of material consisting of crosslinked networks of hydrophilic polymer chains surrounded by a large amount of water. They often have similar properties to tissues in the human body, and so have been studied for a variety of applications, including artificial tissues, drug delivery, wound dressings, and medical implants[4,17,115]. With many biomedical applications, adhesion of hydrogels to tissue surfaces and other soft materials is of importance. When this adhesion is desirable, it is important to particularly improve wet adhesion to these surfaces, due to the large fraction of water both within the gels and in their applied biological environment.

One hydrogel of interest, particularly in biological applications, is alginate. Alginate is a linear polysaccharide copolymer consisting of 1,4-linked α-L-guluronic acid (G) and β-D-mannuronic acid (M) residues. These groups vary in their percentage and sequence, depending on the source of alginate; the combination of these factors determines its properties. Alginate interacts with multivalent cations through the G blocks, i.e. the portions consisting of consecutive G residues. These interactions are responsible for alginate's well-known ability to rapidly form ionically cross-linked gels when multivalent cations (most commonly divalent cations such as Ca^{2+} and Mg^{2+}) are added. The physically crosslinked hydrogel can break and re-form bonds to dissipate external mechanical stress[37]. Alginate's low toxicity allows for its use in various biomedical applications, and its ability to gel quickly and gently has found it utilized in drug encapsulation[30] and dental implants[51]. Alginate has also found uses as a wound dressing, where its high absorption

[†] This chapter is partially reproduced from Cholewinski, A., Yang, F. K. & Zhao, B. Underwater Contact Behavior of Alginate and Catechol-Conjugated Alginate Hydrogel Beads. *Langmuir* **33**, 8353–8361 (2017).

and gas permeability make it well-suited for heavily exuding wounds[46,47,116]. When crosslinked with calcium, it is also able to form a soft gel through ion exchange with Na^+ in exudate or saline solution[14]. While alginate gels have little adhesion on their own, they can be modified to improve surface adhesion. For instance, they have been modified by grafting cell- adhesive peptides to improve their adhesion to cell and tissue surfaces and used in tissue engineering such as regulating bone tissue regeneration[117] or promoting growth of neurites for spinal cord repair[118].

One way to extend the usefulness of alginate in biomedical applications is incorporating wet adhesion, particularly to tissue-like surfaces. For other hydrogels, catechol modification has been a subject of interest since the discovery of the important role of catechol chemistry in mussel adhesion[73,76,83,119,120], where the addition of catechol functionality is intended to provide improved adhesion that can function in aqueous environments. This has been applied successfully in forming a variety of novel tissue adhesives from catechol-modified hydrogels[26,28,120]. While catechol has been incorporated into alginate, which has led to a variety of potential applications in drug delivery[30] and wound closure[121], it has generally been limited to providing alternative methods of crosslinking[18,122] or improving cell viability[18,121,122]. Modifying the crosslinking behaviour of alginate is of interest because the ionic crosslinks of alginate are quick to form, but also easy to break, and stronger long-term behaviour may be desired. For example, catechol modification has been used to introduce covalent crosslinking between alginate chains (through oxidation of the catechol groups, which can then react with each other to form crosslinks), which can provide strength and longevity[122], as well as greater control of gelation and swelling[18]. Catechol modification has also been added to allow for coordination bonds with metal ions, which can be used as another alternative form of crosslinking[120,123] or in layer-by-layer deposition[11]. With this focus in the applications of catechol modification of alginate, its use to incorporate adhesion into

alginate is far less common, and is worth investigating. In addition, excepting cases where it is deliberately incorporated to improve gel strength, the effects of catechol modification on mechanical properties – and subsequently on adhesion – has not been greatly studied.

In this article, we report a systematic investigation of the contact behaviour of alginate gels, with the particular objective to elucidate the role of catechol modification on the wet adhesion of alginate on tissue-like substrates, such as gelatin. For this, we set up an indentation-based contact adhesion measurement, which allows us to test gels formed ex-situ and their mechanical properties, as well as soft-on-soft contact[81,124,125]. We used alginate hydrogel beads as the testing probe, allowing the substrate to vary, and performed the tests in aqueous conditions so as to investigate the time- and pH-dependent adhesion behaviours. While modified alginate gels showed poor adhesion to most hard substrates, improvements were seen across the protein-based systems. Our results reveal the dynamic adhesion at the alginate/gelatin interface, and how this can be improved and extended to other tissue surfaces through catechol conjugation. They also highlight the roles of conjugated catechol in modulating the mechanical and adhesive properties of physically crosslinked alginate hydrogels.

3.2 Experimental

3.2.1 Modification of Alginate with Catechol

Catechol-modified alginate was synthesized through carbodiimide coupling, using 1-ethyl-3-(3-dimethylaminopropyl) carbodiimide (EDC) and N-hydroxysuccinimide (NHS). First, 0.5 g of alginate (Protanal HF120RBS, FMC Biopolymer) was dissolved in 50 mL of 50 mM phosphate buffered saline (PBS, pH 5.5) at a concentration of 1% (w/v). 0.54 g of EDC (Sigma-Aldrich) and 0.33 g of NHS (Sigma-Aldrich) were added for an equal molar ratio to the alginate. The solution was then stirred, with argon being bubbled through, for 45 minutes. After that, 1.08 g of dopamine

(Sigma-Aldrich) was added at a 2:1 molar ratio to alginate. The vessel was sealed and left overnight for the reaction in the solution to complete. In order to remove unreacted components and PBS ions, the reaction solution was dialyzed against deionized (DI) water (acidified to pH 4) over two days, using UV-Vis spectroscopy (Agilent) to determine when all unreacted dopamine molecules had been removed. Following this, the mixture was freeze-dried and stored for later use. Successful formation of catechol-conjugated alginate was confirmed using NMR (Avance 500, Bruker) and UV-Vis spectroscopy. The conjugation efficiency of catechol to alginate was determined by monitoring the absorbance of the 280 nm peak in UV-Vis spectroscopy with a 1 mg/mL concentration of modified alginate, against a calibration curve of controlled dopamine concentrations.

3.2.2 Fabrication of Alginate Beads

Modified alginate beads were formed by taking the lyophilized powder and dissolving it in DI water at a concentration of 2% (w/v). This solution was mixed, and then centrifuged to remove bubbles. The solution was taken up into a 1 mL syringe, which was connected to a syringe pump (NE-1000, New Era Pump Systems). The gel was pumped out of the syringe at a rate of 0.05 mL/min, resulting in droplets that would quickly gel in the solution, forming beads in a 20 mL vial containing a solution of 0.5 M $CaCl_2$ in DI water. The vial containing the beads and $CaCl_2$ solution was kept in the fridge over two nights to anneal the beads, ensure gelation was complete, and to prevent any microbial degradation[126]. The procedure was the same for unmodified beads, except Protanal HF120RBS alginate powder was directly used.

3.2.3 Preparation of Gelatin Substrate and Solution Conditions

Gelatin substrate was prepared by dissolving 0.5 g of gelatin powder (175 bloom, from porcine skin, Sigma-Aldrich) in 5 mL of DI water in a ceramic container at a temperature of 35 °C

for 30 minutes. 50 μL of formaldehyde solution (37% (w/v) in water, Sigma-Aldrich) was added to the dissolved gelatin and stirred into the solution for 5 minutes. This mixture was then removed from heat and allowed to gel at room temperature overnight, forming a gel with final thickness of ~3 cm. Finally, the gel was allowed to soak for 24 hours in the respective testing solution that it would also be immersed in for the actual tests. These testing solutions contained 0.5 M $CaCl_2$ in either 0.1 M tris(hydroxymethyl)aminomethane (Tris, Sigma-Aldrich), acidified to pH 8.56, or in DI water. The solution was replaced at three times evenly over the total soaking period. Except for testing where the pH was varied, all experiments were carried out in the solution containing 0.5 M $CaCl_2$ and 0.1 M Tris.

3.2.4 Testing Procedure and Experimental Conditions

The overall system used for indentation testing consists of a wire loop (3.3 mm inner diameter) holding the hydrogel bead, with the wire glued to a small screw. This could be screwed into a 100 mN load cell (Transducer Techniques) for force measurement at 50 Hz, which is attached to two motorized stages. These consist of a micro-stage (MFA-CC, Newport) for controlling and recording larger-scale displacement (~0.1-20 mm) at 8 Hz and a nano-positioner (P-611.XZS, Physik Instrumente) for small-scale displacement (0.01-100 μm) at 50 Hz. The displacement recording rate for the micro-stage was artificially increased to 50 Hz by linear interpolation within each recording step. The substrate is immersed in aqueous solution beneath the probe. A side camera is used to capture images of the beads' size and shape before and after indentation. A custom-written LabVIEW program is used to control the motorized stage, force sensor, and camera, and to record collected data from these instruments. A custom MATLAB program is used to acquire the bead radius from side view images.

Indentation experiments were performed by taking an alginate (modified or unmodified) bead out of the $CaCl_2$ solution and inserting it into the wire ring holder. This was then attached to the force sensor, and a 'before' image was taken of the bead using the side camera. The substrate – gelatin or glass – was placed under the probe, and the testing solution – 0.5 M $CaCl_2$ in either DI water or 0.1 M Tris – was added. In the case of gelatin substrate, the solution it had been soaking in was removed and a fresh solution added; a barrier wall was placed onto the glass slide substrate with polydimethylsiloxane (PDMS) sealing the joint to contain the liquid. The probe was immediately brought down into the solution to minimize the exposure of the hydrogel in air. Next, the probe was moved towards the substrate at a rate of 5 μm/s, until just in contact with the substrate – a 'touch' force of 0.1 mN was used to determine when contact was achieved. The probe was then brought 100 μm into the substrate at a speed of 10 μm/s; a speed of 500 μm/s was used for elastic modulus measurements to minimize time-dependent behaviour. After indentation, the alginate probe was held in contact for varying amounts of time, with 15 minutes the standard contact time. For experiments where time was varied, contact times of 30 minutes and 60 minutes were also used. Once the wait time was complete, the probe was withdrawn from the substrate at a rate of 100 μm/s. For the tests with direct investigation of mechanical properties, there are several deviations from the standard procedure. First, a glass slide substrate was used to investigate alginate, while a hemispherical glass probe was used to investigate the gelatin substrate. Also, these tests were performed in 0.5 M $CaCl_2$ in DI water, with no contact time between indentation and retraction. Glass slides were sputter-coated with gold for gold-coated substrates. Pork and beef cuts were purchased from a local supermarket and rinsed thoroughly, then cut into ~3 cm cubes before use.

For indentation experiments with varied substrate elastic modulus, 'rigid' and 'soft' polyacrylamide (PAAm) substrates were formed using the following method. For the 'rigid' PAAm gels, 2.5 g of acrylamide (AAm, Sigma-Aldrich) and 0.25 g of N,N'-methylenebisacrylamide (MBAA, Sigma-Aldrich) were dissolved in 5 mL of DI water. 50 μL of 10% (v/v) diethoxyacetophenone (DEAP, Sigma-Aldrich) in dimethyl sulfoxide (DMSO, Sigma-Aldrich) was added to the solution, which was poured into a ceramic container (the same as for gelatin), then exposed to UV light (365 nm) for 30 minutes to form the PAAm gel. This gel was then exposed to excess 0.5 M $CaCl_2$ aqueous solution overnight in preparation for testing. For preparation of the 'soft' PAAm gels, the procedure was the same, except 0.5 g of AAm, 1.25 mg of MBAA, and 25 μL of DEAP in DMSO were added to 5 mL of DI water. The elastic modulus of the PAAm gels was measured using a hemispherical glass probe, travelling 100 μm into the gel at an indentation rate of 500 μm/s. Adhesion testing was performed on the 'rigid' and 'soft' PAAm substrates using standard testing conditions and parameters, except a solution of 0.5 M $CaCl_2$ in DI water (rather than in 100 mM Tris) was used.

3.2.5 Statistical Analysis

All tests were performed with at least 3 samples per condition. For results where values were similar or errors were large, two-tailed t-tests were used to confirm if the difference in the means was significant. Error bars for all figures show the standard deviation for that condition.

3.3 Results and Discussion

Figure 3-1a illustrates the modification of alginate polymer by conjugating with the catechol group of dopamine through the standard carbodiimide coupling of EDC/NHS chemistry. EDC and NHS first activate the carboxyl groups on alginate, which are then coupled to the amine group of dopamine. The visible difference in the final gel can be seen in **Figure 3-1b**, where after

exposure to basic solution (pH 8.5) for 15 minutes, the modified bead is clearly darker in colour. Since the catechol structure gives a clear absorbance peak at 280 nm[28,127], UV-Vis spectroscopy was used to confirm that the dialysis has removed all excess small molecules after coupling and the presence of the catechol functional group in the modified alginate. As seen in **Figure 3-2a**, a 280 nm absorbance peak is visible for the first dialysis solution and the modified alginate, but not the final dialysis solution, suggesting any catechol present in the modified alginate was successfully attached. In order to estimate the conjugation efficiency of the reaction, UV-Vis spectra were used to collect a calibration curve of known dopamine molar concentrations and compare this to the 280 nm absorbance of 1 mg/mL modified alginate. This provided a molar concentration of catechol that could be divided by the known amount of alginate in the solution, determining that about 2.9% of the alginate groups were conjugated with catechol. This percentage can be increased by varying the ratio of [dopamine]:[alginate] (similar to the work done by Lee et al.[18]), but in this work, we will focus on this degree of conjugation as a first step for investigating its effects. NMR spectroscopy was used as a second source of confirmation for catechol attachment, as seen in **Figure 3-2b-c**; the modified alginate showed additional peaks at ~7 ppm, corresponding to the aromatic ring in the catechol group. Additional peaks were visible closer to 3 ppm, which could be attributed to the CH_2-CH_2 group linking the catechol and amide groups. These peaks agree with those reported by Wu et al.[111] and Lee et al.[18], further confirming attachment of catechol functionality to the alginate backbone.

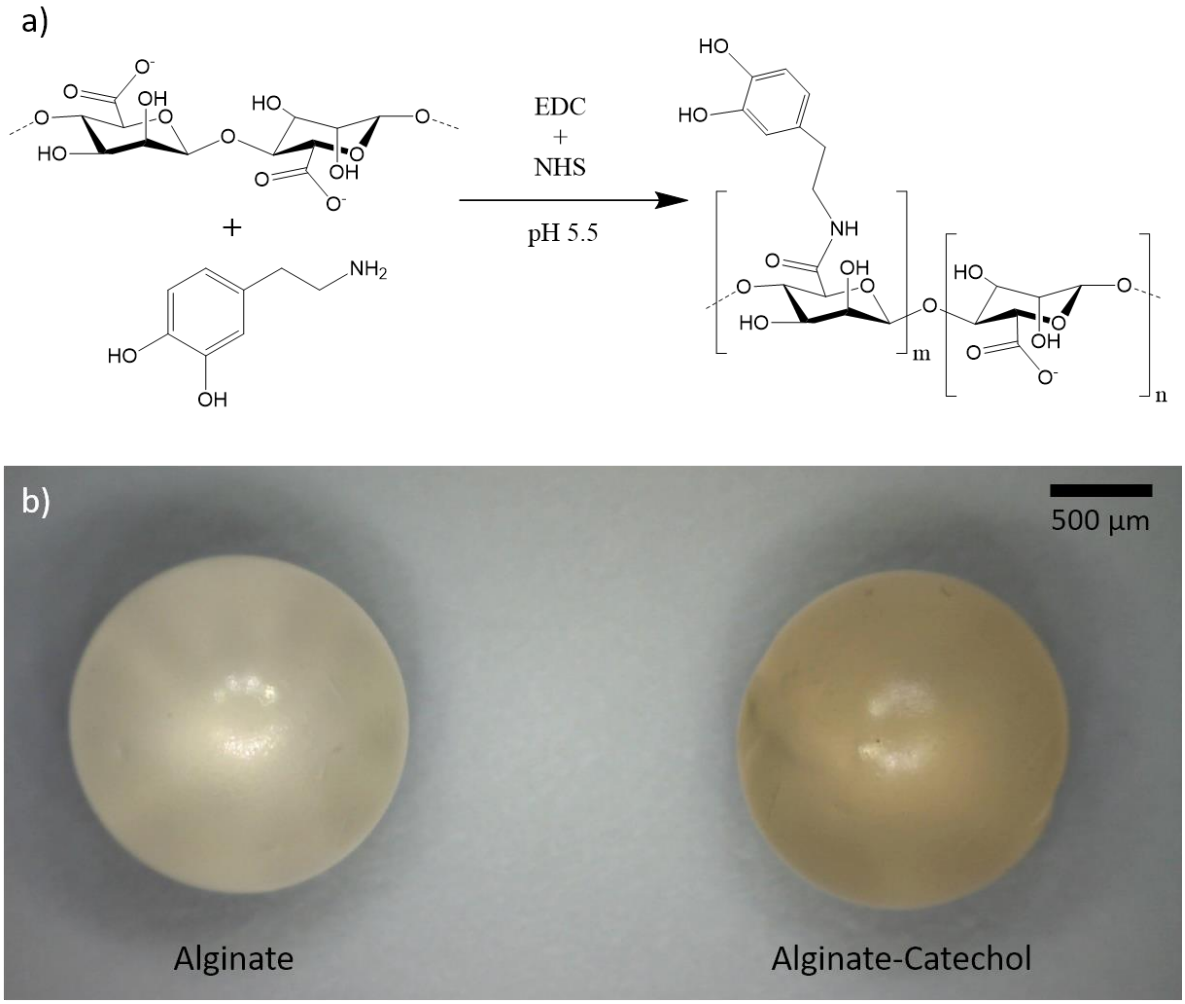

Figure 3-1. Chemical modification of alginate: (a) the basic schematic for the conjugation of dopamine onto the alginate backbone through carbodiimide coupling utilizing EDC and NHS; (b) the resulting beads, with unmodified alginate on the left, and modified alginate post-oxidation on the right, highlighting the colour change for oxidized alginate-catechol.

Measuring hydrogel adhesion underwater is a challenge. Hydrogels are complex, heterogeneous systems that frequently exhibit time-dependent mechanical properties[93]; testing in water can cause additional sources of error[124]. There are several methods available for testing underwater adhesion, each with their own advantages and disadvantages. The sphere-on-flat indentation was adapted in this work for testing underwater hydrogel adhesion. To have a direct measurement of the contact behaviour of alginate hydrogel with substrate, our indentation measurement used the hydrogel bead as a spherical probe; this feature allows for the testing of its

interactions with varied surfaces either rigid or soft. As a note, in this work, we use 'soft' and 'rigid' to refer to substrates with an elastic modulus significantly below or significantly above that of the hydrogel probe, respectively (i.e., $E_{substrate} \ll E_{probe}$ for 'soft' and $E_{substrate} \gg E_{probe}$ for 'rigid'). Herein, glass was used as a general-purpose rigid substrate, while gelatin was used as a soft substrate to provide an approximate model for human tissue, as many applications of alginate are biomedical in nature. A schematic of this setup can be seen in **Figure 3-3**.

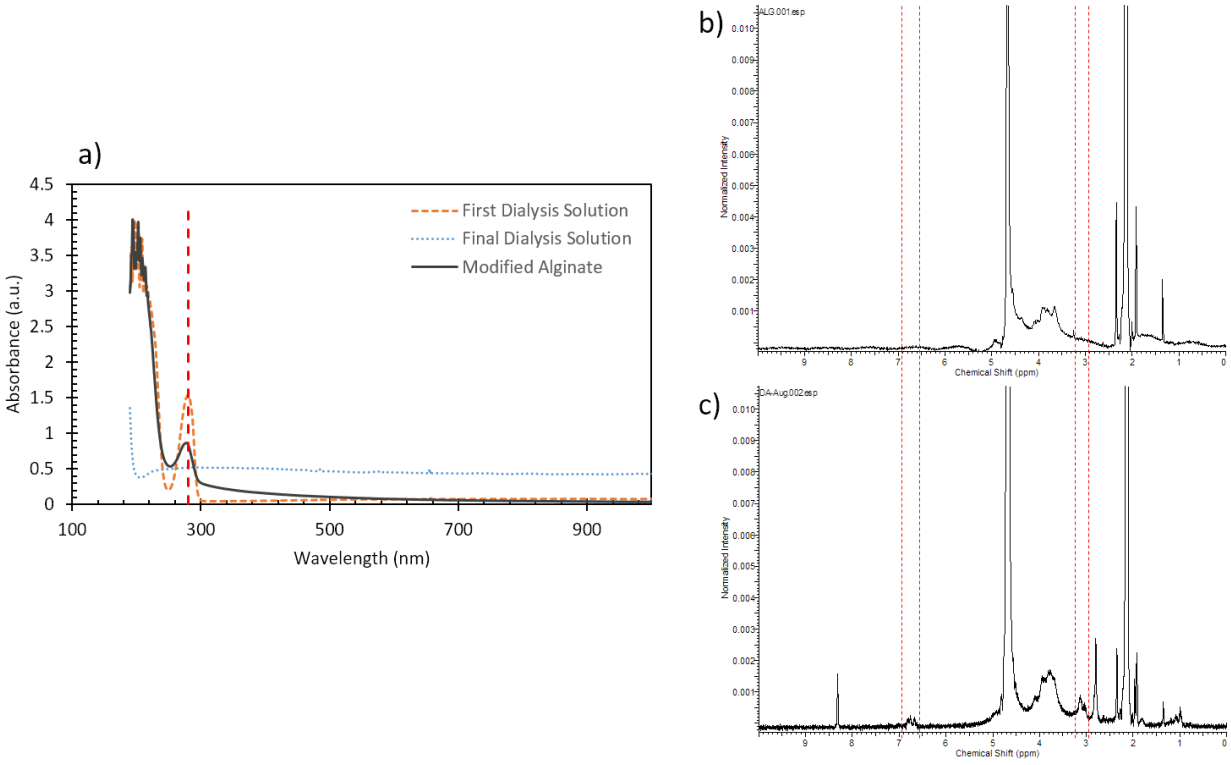

Figure 3-2. Confirmation of successful addition of catechol to alginate: (a) UV-Vis spectra for the first and last dialysis solutions – indicating dialysis has removed loose dopamine – as well as for modified alginate – indicating catechol is present on the polymer; (b-c) NMR spectra for (b) unmodified and (c) modified alginate powders dissolved in D_2O, with new peaks from catechol modification marked between dotted lines.

The gel probe is created by forming a hydrogel bead through drops of pre-gel into crosslinking solution for fast-gelling hydrogels, or potentially through molds for slower gelation. Originally, this bead was cut into hemispheres, which were glued onto a metal cylinder for use as

a probe. However, difficulty in cutting and ensuring uniformity of the hemispheres led us abandon this method and use the whole bead as the probe. To attach the gel bead to the force sensor, a metal wire is looped to form a circular holder with a diameter just smaller than that of the bead, and is glued to the end of the screw with epoxy. In this way, we avoided the gluing of hydrogel beads so as to minimize the possible damage of the gel bead. The bead can be fitted into the wire loop with only minor deformation, allowing for the force it feels to be transmitted to the sensor.

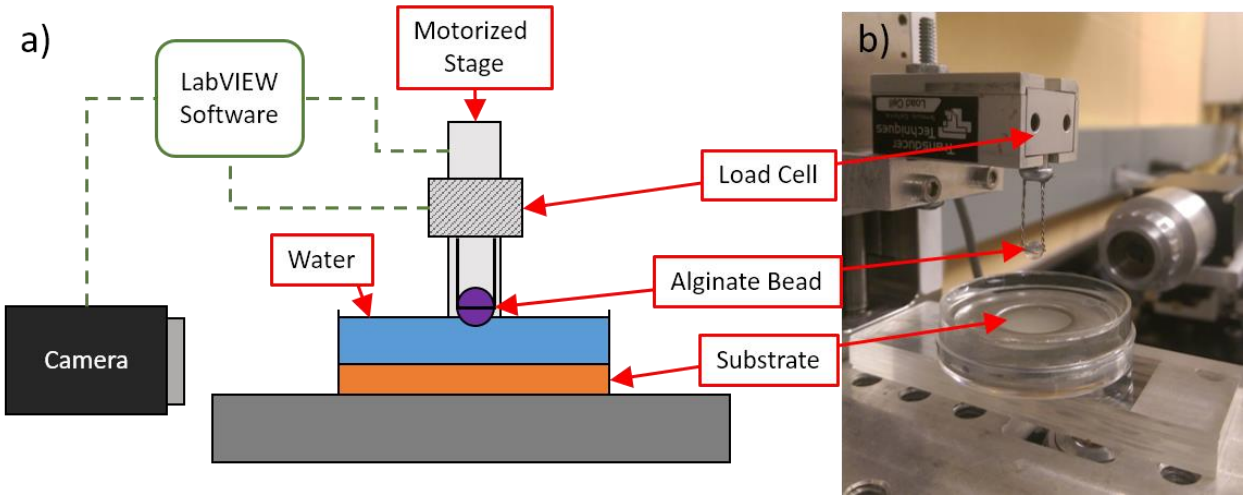

Figure 3-3. Gel indentation testing: (a) a schematic of the experimental setup, where the alginate bead is held by the wire loop, connecting it to the load cell (for measuring force) and motorized stage (for loading and unloading). A side camera is used to acquire side-view images of the bead before and after indentation to measure the size of each bead. (b) a corresponding view of the real setup – note the water is deeper than the bead diameter, so only the wire above the bead is exposed to air.

While using a wire loop to hold the gel bead probe helps to protect the bead shape and integrity, there is a risk of applied forces causing the bead to slip in position within the loop. In an attempt to avoid this behaviour, the loop was formed with a similar, but slightly smaller radius than that of the beads. The wire loop has an inner diameter of 3.2 mm (radius 1.6 mm), while the alginate and alginate-catechol beads were measured to have radii of 1.68 ± 0.06 mm and 1.73 ± 0.12 mm, respectively.

In addition, in order to address the possibility of slippage in the wire loop occurring during indentation, two types of experiments were carried out to investigate when this behaviour would occur. These were used to explore differences in slippage during both pushing and pulling on the beads. In the first set of experiments, alginate beads were inserted into the wire loop as per the standard procedure. They were then indented into a glass slide in 0.5 M $CaCl_2$ aqueous solution at varying rates until the force stopped increasing or the limit of the force sensor was reached, whichever happened first. Alginate beads attached to a screw with superglue were used as a control, as slippage should not occur until failure of the glue. These glued beads were also indented into the substrate at the same rates, and the resulting force-displacement plots (normalized by bead radius) were directly compared with those for the beads in the wire loop. It was expected that slipping of the bead could be observed in deviations from the control curve. Examples of these force-displacement curves for slow (10 μm/s) and fast (500 μm/s) indentation rates can be see in **Figure 3-4a** and **Figure 3-4b**, respectively. As seen in these plots, deviation from the control occurs at ~20 N/m preload. Since the highest testing preload on hard substrates is 10 N/m, this is deemed to be within the 'safe' region for holding the bead.

The second set of experiments was used to investigate when slippage of the bead would occur during pulling. As the bead was pushed into the wire loop to be held in place, it was theorized that slippage would occur at lower forces when pulling the bead. In order to test the behaviour during pulling, alginate beads were inserted into the wire loop as normal. They were then indented into a thin layer of superglue on glass substrate, to a total indentation depth of 100 μm. After waiting for 2.5 minutes of contact time for the superglue to partially cure, 0.5 M $CaCl_2$ solution was added. After an additional 2.5 minutes waiting time, the beads were withdrawn at a rate of 100 μm/s, as this was the standard condition for pull-off in the main set of experiments. As with

the previous tests, a control was used consisting of a bead glued to a screw. Similarly, this bead was indented into a thin layer of superglue on glass, with the same waiting and withdrawal procedure. Also as before, the resulting force-displacement curves for the glued and wire loop cases were directly compared, with the start of deviation between the two indicating that the bead was slipping in the loop. As seen in **Figure 3-4b**, this slippage appears to begin at ~4N/m. While this is significantly lower than the preload for pushing the bead, the adhesive forces encountered in the main set of experiments were all less than 3 N/m. As such, slippage should also not be occurring during the pulling of the bead.

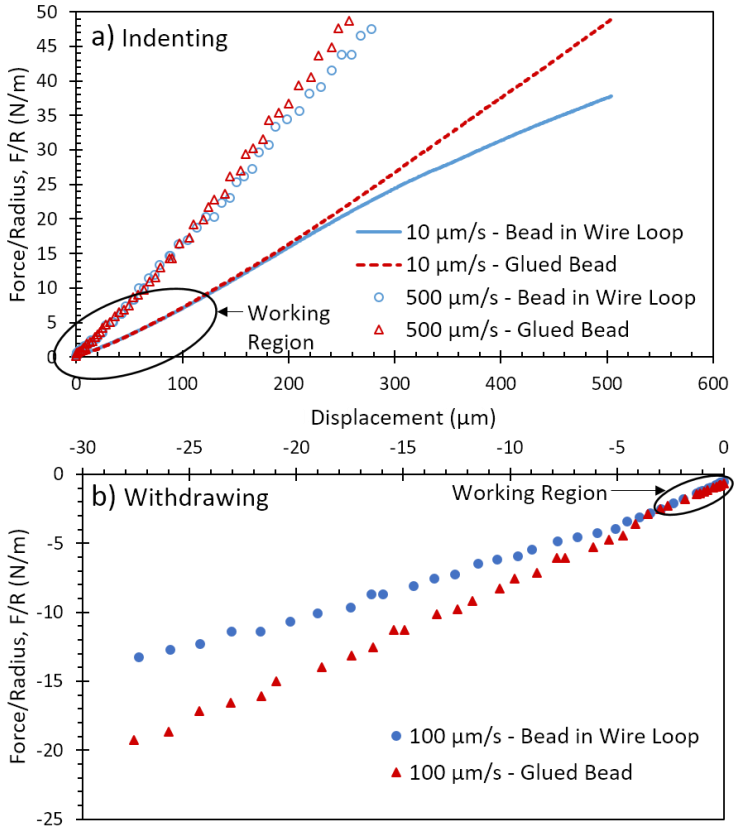

Figure 3-4. Plots of force (normalized by bead radius) vs. displacement for beads held in a wire loop (blue solid line and circles) and glued to a screw (red dashed line and triangles). The region within which the main set of experiments are performed is circled in black. (a) plots for indentation force, where the bead was indented into a glass substrate at rates of 10 µm/s and 500 µm/s; (b) plots for withdrawal force, where the bead was glued to the substrate, then pulled away at a rate of 100 µm/s.

Figure 3-5 shows typical force vs. time curves for alginate with and without catechol on gelatin. The compressive force increased rapidly to the maximum force at the pre-set indentation depth. The slope and the value of the maximum force reflect the mechanical properties of the gel. During the holding period maintained at the indentation depth, the compressive force relaxed with time to reach a lower plateau; likely the polymer chains of the hydrogels had re-arranged to partially release the stress, causing some plastic deformation. This plateau was reached for the gels within a 15 minute contact time. As such, in order to remove the additional time-dependent behaviour of relaxation, 15 minutes was used as the minimum contact time for all tests. During unloading, the compressive force dropped rapidly and became negative (i.e., tensile) to give a pull-off force; this pull-off force is directly related to the hydrogel adhesion to the substrate surface.

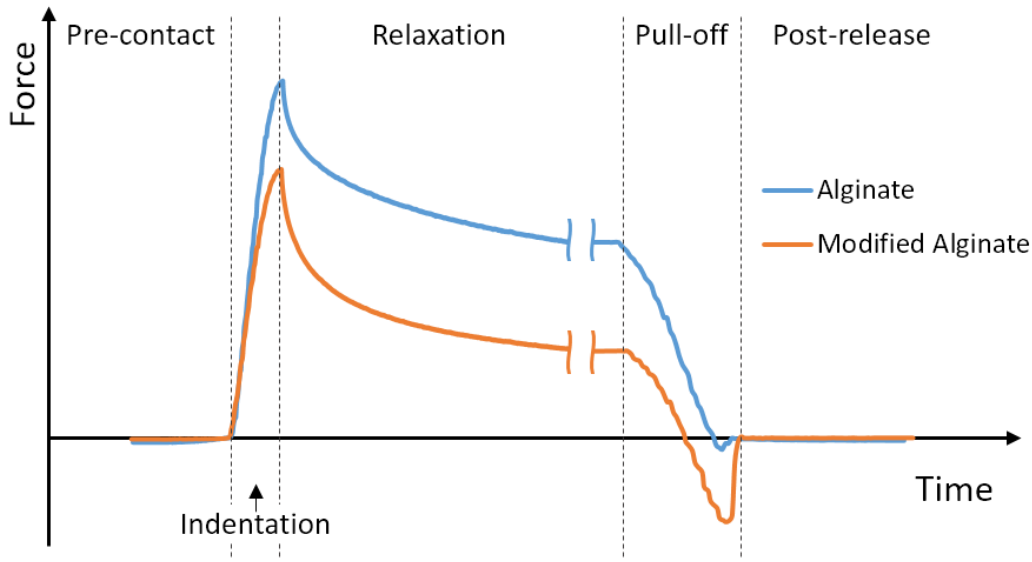

Figure 3-5. Representative indentation and pull-off curves for catechol-modified and unmodified alginate, indicating the behaviour during each step over time. Portions of the curves are expanded or compressed to appear on similar scales.

The contact area during the indentation could be measured from the bottom-view images if the test were performed in air or with different materials. However, for hydrogels immersed in

water, the similarity in refractive indices between the hydrogel and water makes directly measuring contact area difficult[124]. Hence, Hertz theory was applied to the indentation curve to estimate both the contact area and combined modulus of the system, using the following equations:

$$F = \frac{4}{3}E^{*}R^{1/2}d^{3/2}, \tag{10}$$

$$d = \frac{a^2}{R}, \tag{11}$$

where F is the applied load, a is the contact radius, d is the displacement, R is the radius of the probe (here, the alginate bead), and E^{*} is the combined or reduced Young's modulus of the probe and substrate together. E^{*} is related to the Young's modulus and Poisson's ratio of the probe, E_p and ν_p, and the substrate, E_s and ν_s, through Eq. (12):

$$\frac{1}{E^{*}} = \frac{1-\nu_p^2}{E_p} + \frac{1-\nu_s^2}{E_s}. \tag{12}$$

Gelatin is well-known to be quite elastic and incompressible, and its Poisson's ratio was assumed to be 0.5[128]. Similarly, the Poisson's ratio for alginate was assumed to be 0.5, based on work done by Wang et al.[129].

When glass is used as the substrate, the loading curve in the indentation tests can give an estimation of the elastic modulus of the hydrogels. Glass is rigid and has a high elastic modulus (generally on the order of tens of GPa), which is much greater than that of a hydrogel. This situation allows the contribution of the substrate in Eq. (12) to be ignored, and E_p to be directly acquired from E^{*}. Similarly, for quantifying the modulus of the gelatin used as a substrate, a glass hemisphere was used as the testing probe. Assuming ν for alginate and gelatin to be 0.5 – at least for the duration of the initial indentation – the elastic modulus for the neat and modified alginate, as well as for the gelatin substrate, could be estimated if the compressive force F varies linearly

with $d^{3/2}$ [130,131]. **Figure 3-6a-b** plots the force vs $d^{3/2}$ curves for the alginate hydrogels and gelatin, showing an overall linear relationship. Thus, the elastic modulus of alginate, modified alginate and gelatin were estimated and shown in **Figure 3-6c**. The modulus for the gelatin substrate is only 15-20% of modified alginate, reflecting its tissue-like softness. Considering the low modulus of gelatin, the combined modulus of alginate/gelatin (E^*=14.3 kPa) is actually similar to that of catechol-alginate/gelatin (E^*=12.4 kPa). That is, the elastic modulus of the gelatin substrate comprises the majority of the reduced modulus of the system. However, it was also observed that catechol modification significantly reduced the overall elastic modulus of the final hydrogel, with a reduction of ~50% compared with neat alginate. This effect is most likely due to replacement of crosslink-capable carboxylate groups with catechol; ionic crosslinking of alginate requires multiple G-residues in succession, and the disruption of these blocks can result in a lower extent of crosslinking. It is of interest to note that elastic properties may not be the only mechanical properties affected by catechol modification. The viscoelastic properties are likely to be affected as well, such as the loss modulus, G", and the dissipation factor ($\tan\delta$), and their change with frequency. While this effect was not greatly studied in this work, it was observed in preliminary experiments that pull-off velocity changed the measured adhesion, with a general trend of adhesion decreasing with lower pull-off velocities.

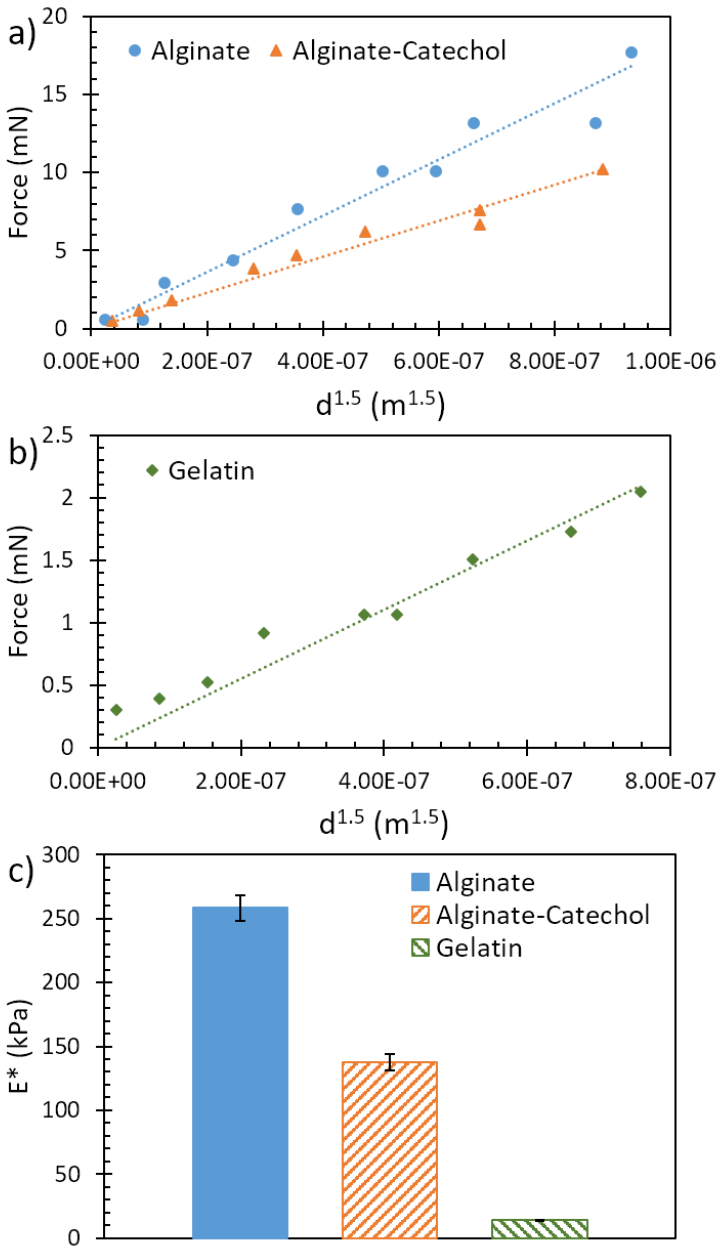

Figure 3-6. Results of elastic modulus measurements. (a) and (b) show example plots of $\boldsymbol{F}$ vs. $\boldsymbol{d^{3/2}}$ for: (a) catechol-modified and unmodified alginate probes on glass; and (b) a glass probe on gelatin substrate. (c) shows the final calculated Young's modulus values for unmodified and modified alginate probes, as well as the for gelatin substrate, assuming $\boldsymbol{\nu = 0.5}$ for these materials.

One major focus of this work was to investigate the nature of the adhesion interactions between the two gels, particularly when catechol groups are introduced onto the alginate chains. For this, the pull-off force from the indentation curves gives a direct measure of the adhesion

between the alginate beads and the substrate. To provide a quick comparison in adhesive behaviour for both modified and unmodified alginate, indentation tests were first performed on both gelatin and glass in 0.1M Tris and 0.5M $CaCl_2$ solution, and 15 minutes contact time. As seen in **Figure 3-7**, the adhesion of catechol-modified alginate on gelatin is 0.24 N/m under these conditions, which is greater than that of unmodified alginate by half an order of magnitude. This indicates that adhesion has been greatly increased, which is of particular interest because the alginate and gelatin are already solid gels before contact. As a control, similar tests were performed on glass surfaces. The adhesion of both modified and unmodified alginate on glass is always greater than adhesion on gelatin, likely because glass is rigid and has higher surface energy.

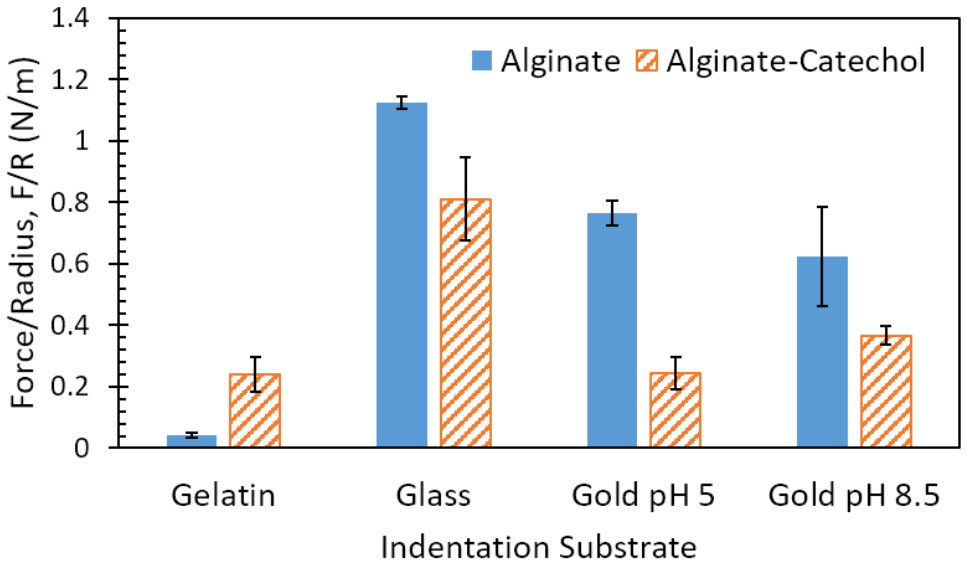

Figure 3-7. Differences in the final adhesive pull-off force between catechol-modified and unmodified alginate on gelatin and glass in aqueous solution at pH 8.5, and gold-coated glass at pH 5 and pH 8.5, with a standard holding time of 15 minutes.

It is interesting to note that catechol modification of alginate appears to decrease the adhesion to glass. The lack of any expected specific interactions may account for a smaller improvement in adhesion, but an overall drop compared to neat alginate is surprising. In order to verify this unexpected observation, we performed indentation tests on gold-coated glass, also

shown in **Figure 3-7**. For pH 8.5, the overall adhesive force for both alginate and alginate-catechol dropped by about half compared to on glass, with the ratio between them remaining similar. Here, again, catechol modification appeared to result in an overall decrease in adhesive strength. In case it was the reduced catechol form that might be responsible for adhesion to gold, additional tests were performed at a lower pH of 5. While results for unmodified alginate were slightly higher at this pH, the adhesive force of alginate-catechol to gold was even lower than at pH 8.5, dropping by ~30%. This confirms that, like on glass, the overall adhesion for alginate-catechol in either form is lower than unmodified alginate on gold.

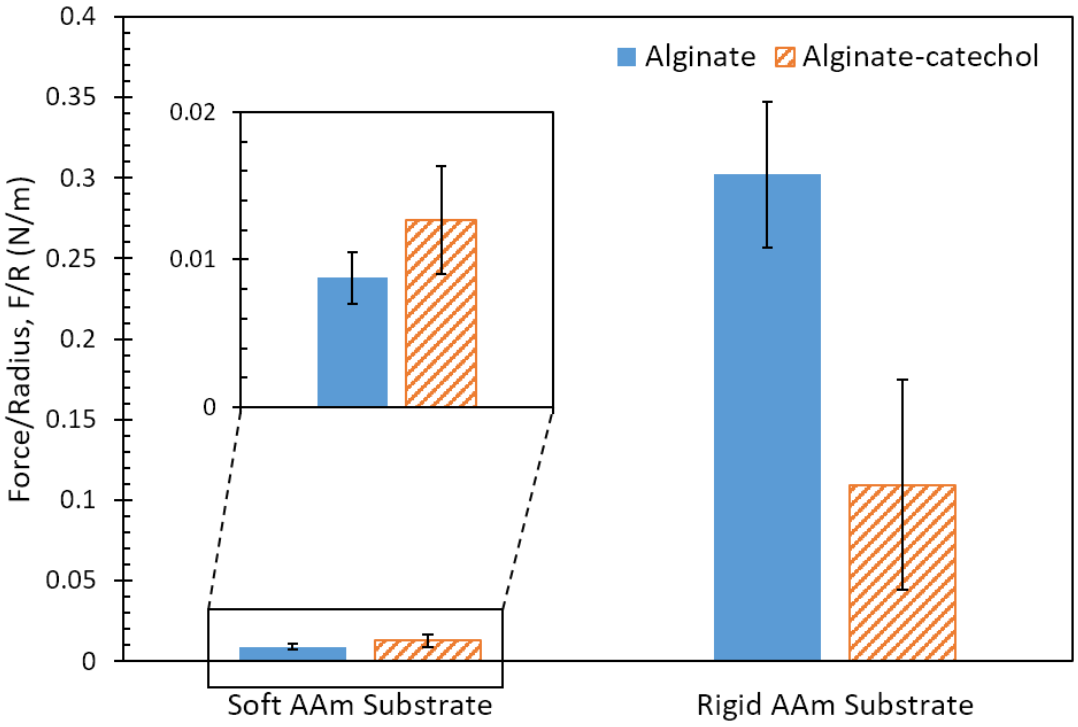

Figure 3-8. Pull-off force values for catechol-modified and unmodified alginate on polyacrylamide substrates with different elasticities (1.8 ± 0.3 kPa for Soft PAAm, and 678.7 ± 65.2 kPa for Rigid PAAm) in aqueous solution with pH 5. The insert shows a closer view of the pull-off force on the Soft PAAm substrate.

It was suspected that the lower adhesion of alginate-catechol to substrates like glass and gold was a result of the decreased elastic modulus of the modified beads. If this is the case, then

this would only be apparent on substrates with an elastic modulus similar to or greater than that of the probe (as for 'soft' substrates, where $E_s \ll E_p$, it results that $E^* \sim E_s$, and E_p does not play a role). This effect would be greatest on 'rigid' substrates, with $E_s \gg E_p$, as in this situation, Eq. (3) simplifies down to $E^* \sim E_p$, meaning the modulus of the probe has the greatest effect. To see if this was indeed the case, tests were performed on two polyacrylamide (PAAm) substrate with different initial monomer concentrations and degrees of crosslinking to provide substrates with similar chemical composition, but drastically different elasticities. This allowed us to explore a situation where the difference between the two substrates was almost entirely mechanical elasticities, and to probe the two cases mentioned above, with $E_s \ll E_p$ and $E_s \gg E_p$. The 'rigid' PAAm substrate had a measured elastic modulus of 678.7 ± 65.2 kPa (over 3x the elastic modulus of the unmodified alginate beads, so $E_s \gg E_p$), while the 'soft' PAAm substrate had a measured elastic modulus of 1.8 ± 0.3 kPa (almost two orders of magnitude lower than the elastic modulus of alginate-catechol beads, so $E_s \ll E_p$). We were then able to probe the adhesive strength of both alginate and catechol-alginate on both surfaces, and how they changed between 'soft' and 'rigid' substrates. **Figure 3-8** shows the difference between the 'rigid' and 'soft' PAAm substrates for the adhesive behaviour of the alginate gels. On the 'soft' PAAm substrate, the adhesive strengths of modified and unmodified alginate are quite similar, with alginate-catechol slightly higher. However, on the 'rigid' PAAm substrate, the unmodified alginate has more than twice the adhesive strength of the alginate-catechol gel. The overall adhesion of both alginate gels is lower on the softer PAAm substrate, likely from its higher water content. While there is little change in the substrate apart from its modulus, we see a significant change in the relative adhesion between catechol-alginate and unmodified alginate. This supports our hypothesis that on 'rigid' substrates, the elastic modulus of the beads plays a role in adhesion, and the lower modulus from catechol modification

could be responsible for the unanticipated lower adhesion observed on substrates like glass and gold.

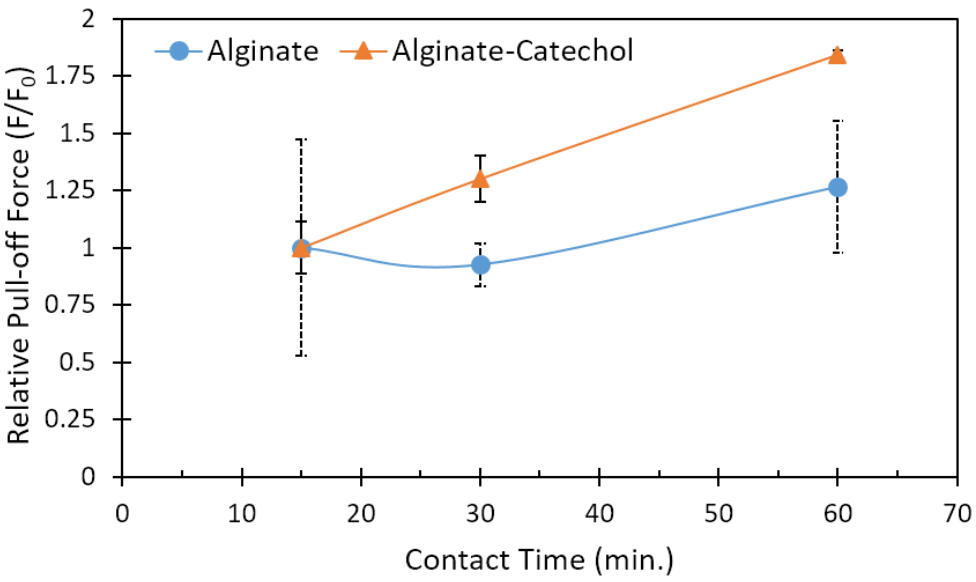

Figure 3-9. Pull-off force values for catechol-modified and unmodified alginate in aqueous solution at pH 8.5, with varying contact times between the probe and gelatin substrate before retraction. All values are normalized against the pull-off force for 15 minutes contact time. Dotted line error bars correspond to alginate, while solid line error bars are for catechol-alginate. Solid curved lines are used as a guide for the eyes.

In order to elucidate the nature of the interfacial adhesion between catechol-alginate and gelatin, we performed a systematic investigation on the effect of contact time and solution pH on the adhesive pull-off force. **Figure 3-9** shows the change of adhesive pull-off force with time at pH 8.5 for both modified and non-modified alginate on gelatin. It is clear that the adhesion of the alginate-catechol beads increases with time. This increase in adhesive force with contact time might be related to three possible dynamic interactions: a) time-dependent oxidation of catechol into quinone group; b) time-dependent formation of chemical bonding at the interface, for which kinetics of the reaction play a role; c) interdiffusion of polymer chains. This is in contrast with the unmodified alginate beads, which display far less time-dependence in their behaviour, particularly

with their large variations in adhesive strength. The error scale for alginate is large, partly because of the variation of alginate beads, partly because of the intrinsically low adhesion of alginate. For the alginate catechol, the error scale is relatively much smaller due to its higher adhesion. This behaviour of alginate suggests that interdiffusion at the interface is not the main source of the time-dependent behaviour for alginate-catechol. As such, it was expected that quinone formation from catechol and/or chemical bonds forming with the substrate were responsible for the majority of adhesion.

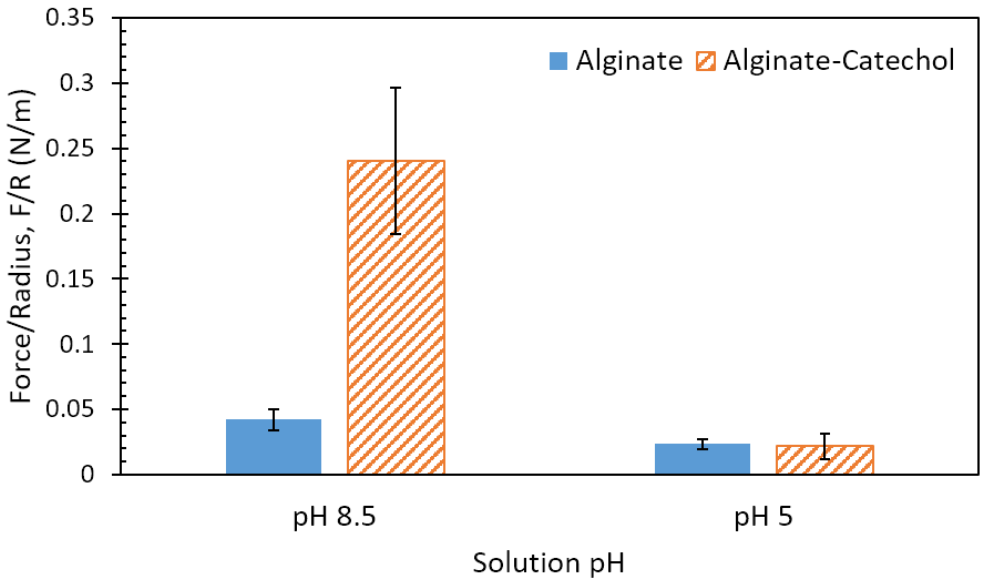

Figure 3-10. Adhesive pull-off force for catechol-modified and unmodified alginate on gelatin substrate in aqueous solutions with a pH of either 8.5 or 5, for a standard holding time of 15 minutes.

Due to the differences between catechol and its oxidized quinone form, particularly regarding their mechanism of adhesion – mainly hydrogen and coordination bonding for catechol and covalent bond formation for quinone[64] – it is useful to investigate the effect of pH on the adhesive pull-off force of alginate-catechol beads to gain insights into the dynamic interfacial adhesion behaviour. Two solution pHs were chosen for testing: DI water with 0.5 M $CaCl_2$ and

0.1 M Tris buffer at pH 8.5, and DI water with only 0.5 M $CaCl_2$ at pH 5. These two conditions were used to investigate the catechol functional groups in their reduced and oxidized states, in acidic and basic pH solutions, respectively[64]. pH 8.5 in particular was chosen for the basic condition, as dopamine is known to auto-oxidize and form polydopamine at this pH[76,132]. **Figure 3-10** show the comparisons of adhesion at these two different pHs for both catechol-alginate and alginate. It can be seen that the adhesive force for the modified beads drops by an order of magnitude, from 0.24 N/m to 0.022 N/m, when the solution pH is lowered from 8.5 to 5. In contrast, the unmodified alginate beads only drop by about half, from 0.042 mN to 0.023 mN. The large drop in adhesive strength with lower pH cannot be account for by changes to alginate itself, suggesting that it is the oxidized form of the catechol groups that is primarily responsible for the adhesion to gelatin.

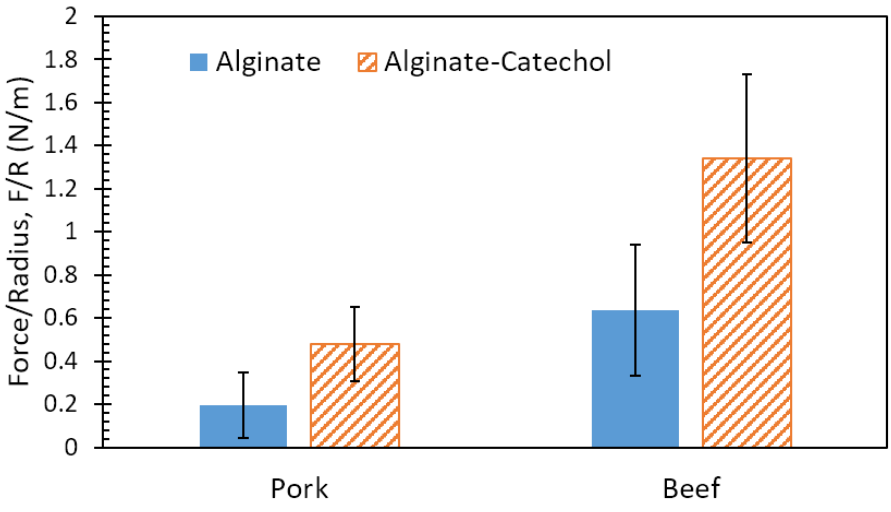

Figure 3-11. Pull-off forces from indentation testing for catechol-modified and unmodified alginate on pork and beef tissue at pH 8.5, for a standard holding time of 15 minutes.

Additional tests were performed to check if the observed increase in adhesion of alginate-catechol to a soft gelatin surface could also be effective for other soft, protein-based tissue substrates. Cuts of pork and beef were used to further investigate the hydrogel behaviour on soft

tissue. Both substrates are softer than the hydrogel beads and, in a similar manner to gelatin, their elasticities composed the majority of the system. **Figure 3-11** shows results for indentation tests on both pork and beef substrates; due to the inhomogeneity of the tissue, the error is quite large for these systems. As such, while there is still a noticeable increase in adhesion for alginate-catechol over unmodified alginate on both substrates, t-tests can only confirm a difference in the means on pork substrate. Both substrates show a smaller increase in adhesion than pure gelatin, likely indicating that their additional components do not interact with catechol. Also, both modified and unmodified alginate adhere more strongly to the beef substrate. While the overall adhesion was lower on the pork substrate, the difference in adhesive strength between alginate and alginate-catechol was generally similar to that on beef. Though only confirmed on pork, catechol modification of alginate appears to result in a stronger adhesive force on these biological substrates, reinforcing the suggestion from gelatin that catechol incorporation can result in greater tissue adhesion.

3.4 Conclusions

Catechol functionality was added to alginate polymer, and the mechanical and adhesive behaviours of the resulting hydrogel were investigated. In order to do this, we developed a setup using a hydrogel bead as the probe, allowing for testing of interactions with rigid (glass) and soft (gelatin) substrates. Catechol modification of alginate greatly improved the adhesion to soft or biological substrates. However, this modification also resulted in an unexpectedly large decrease in the elastic modulus of resulting catechol-alginate gels, which particularly impacted their adhesion to rigid substrates. Reduced adhesion of alginate after catechol modification was observed on glass and gold substrates, and was further investigated by testing adhesion to polyacrylamide gels with varying elastic modulus. Additionally, adhesion of catechol-alginate to

gelatin substrate exhibited time- and pH-dependent behaviour not seen in unmodified alginate; this change in behaviour is most likely due to oxidation of the catechol group and/or reaction kinetics. Further tests indicated that the strong adhesion of catechol-alginate to gelatin substrate can extend to other protein-based substrates, such as animal tissue. These results show the important effects of catechol modification on the mechanical and adhesive properties of alginate hydrogel. In addition, with gelatin as the model substrate, they could be useful for predicting behaviour of modified hydrogels in and on the body, supporting potential applications in bioadhesion such as tissue adhesives and adherent wound dressings.

Chapter 4 Algae-Mussel-Inspired Hydrogel Composite Adhesive for Underwater Bonding‡

4.1 Introduction

While conjugation of catechol groups can be an effective strategy for improving wet adhesion of polymers, chemical synthesis can be complex and time-consuming, and can have its own set of limitations for mussel-inspired adhesives. For example, the protection and deprotection of catechol during synthesis imposes strict restrictions that can be difficult to meet[133]. For catechol-alginate, the limiting factor has been the low degree of modification, as seen in Chapter 3 (typically around 5%)[11,18,30,121–123,134–137]. This restricts its applicability as an adhesive, as found by ourselves and others[135]. A strategy that can overcome these shortcomings would broaden the list of hydrogels that can possess adhesive functionality, and such a strategy would be more capable of significantly improving alginate's adhesion without reducing its cohesive strength.

To establish bonding between two adherends, the adhesive needs to penetrate surface boundary layers, spread and develop intimate interfacial contacts with the adherends' surfaces, and cure and set within a reasonable period. These requirements are especially difficult to meet in the presence of water because water as a boundary layer can weaken the interfacial adhesion of the adhesive and as a solvent can undermine the adhesive's integrity. This is the reason why synthetic adhesives developed for dry applications perform poorly on wet surfaces or underwater. However, adhesion in wet and moist environments is an important concern for many construction, biomedical and marine applications[26,138,139]. There has been an interestingly large amount of

‡ This chapter is partially reproduced from Cholewinski, A., Yang, F. K. & Zhao, B. Algae–mussel-inspired hydrogel composite glue for underwater bonding. *Mater. Horizons* **6**, 285–293 (2019).

research activities on the development of adhesive materials that can work effectively in wet and even underwater conditions.

In order to develop this strategy for improving alginate adhesion, it is important to examine not just the chemistry of mussel adhesion, but their overall adhesive strategy, as well as that of benthic algae. These organisms have each developed their own methods for adhering to a variety of wet surfaces in underwater environments[1,70,140]. Brown algae obtain adhesion from polyphenol aggregates, with phenolic residues possessing two or three hydroxyl groups that enhance adhesion to a substrate by forming hydrogen bonds, as well as displacing water molecules at the surface. However, the bulk of the adhesive is a separate network of alginate, which is gelled by calcium ions to provide cohesion; these phenolic and alginate groups are secreted separately, then crosslinked together to form the final adhesive[1,70]. One important concept to learn from this strategy is that adhesive functional groups do not need to be initially present on the polymer itself, and the adhesive and cohesive portions can begin as separate components, as long as they are linked together in a 'curing' or 'hardening' process. Marine mussels, for their part, use catechol groups (which are also phenolic residues with multiple hydroxyl groups) as part of their adhesive strategy. Unlike with alginate, these adhesive phenolic groups are present in proteins that also serve as the structural fiber of the adhesive plaque; L-3,4-dihydroxyphenylalanine (DOPA) in particular is a major component in adhesive mussel foot proteins[83,140]. This amino acid is present both in the adhesive proteins (particularly mfp-3 and mfp-5) at the interface between the mussel foot and the substrate, and in the cuticle protein (mfp-1), where it complexes with Fe^{3+} ions to crosslink protein chains in this protective exterior of the byssal thread[62,141]. Important concepts that can be learned from the adhesive strategy of mussels include the localization of adhesive

components at the interface with the substrate, as well as the applicability of catechol groups to improve adhesion (through surface interactions) and cohesion (through cation complexation).

Other works have looked to take inspiration from algae or mussels for underwater adhesion, with most taking a more direct approach. For example, there have been very few studies mimicking algal adhesion, and groups have often focused on directly adapting algae chemistry and small-molecule mimics[88,90,92]. Part of the reason for these studies being less common has been the weak adhesion associated with the polyphenols specifically used by algae, with the resulting biomimetic adhesive utilizing phloroglucinol only outperforming pure alginate by less than twice the strength[88]. In contrast, mussel chemistry has been much more widely studied as an adhesive strategy due to the high underwater adhesive strength of catechol[64], which has inspired a large number of works in developing underwater adhesives. These works achieve adhesion either by incorporating catechol into polymers[73,135,142] or by expressing recombinant mussel adhesive proteins[120,143]. However, looking at these organisms together, the adhesive strategies of algae demonstrate that adhesive functional groups do not need to initially be present on the polymer.

We believed that by synergistically combining the two strategies of algae and mussels (especially incorporating the concepts learned above), we could overcome the limitations of biomimetic glues inspired by purely algae or mussels. We hypothesized that alginate, dopamine, and ferric ions could be used together to form a novel hydrogel composite glue[144]. This is because these components, when combined, could serve to mimic beneficial aspects of each organism's adhesive strategy. Dopamine mimics the adhesive components of both organisms, first since it has functionalities (catechol and amine) that can duplicate mussel chemistry. Second, under alkaline conditions, it auto-oxizides to form polydopamine, which can coat virtually any surface[76]; this polydopamine formation is also reminiscent of the polyphenols present in algae adhesive. Alginate

serves as the cohesive backbone of the adhesive secreted by algae, and its ionic crosslinking ability is particularly useful in this work. Fe^{3+} ions were used to link together the adhesive and cohesive elements of the gel. This exploits the ionic crosslinking of alginate, used by algae (Ca^{2+} is used by algae, but Fe^{3+} is also known to crosslink alginate chains[145]), as well as the formation of catechol-Fe^{3+} complexes within the mussel cuticle[62,146]. These catechol-Fe^{3+} complexes have been exploited to create injectable polymers with tunable elastic moduli and degradation behaviours[25], as well as to incorporate reversible crosslinks into self-assembling networks to improve mechanical properties and retain self-healing behaviour[147]. Based on this, we believed Fe^{3+} ions could link together the adhesive and cohesive elements of our gel. Fe^{3+} ions were expected to be able to provide cohesion through crosslinking alginate and through coordinating with dopamine, as well as providing sites that could interact with both the alginate and dopamine components of the adhesive gel. A schematic detailing the way the dual inspirations of algae and mussels are combined together is presented in **Figure 4-1a-c**, with **Figure 4-1c** illustrating the expected interactions between alginate and catechol, linked by Fe^{3+}. This form of crosslinking is in contrast to typical methods for incorporating catechol adhesion, which frequently involve chemical conjugation of catechol groups to polymer backbones[28,73,135]. It should offer a simpler method for introducing catechol adhesion that does not require chemical conjugation or modification.

In this work, we also took inspiration from both benthic algae and marine mussels in developing the process for applying the adhesive. Dopamine adhesive and alginate polymer components are initially separate when added; polydopamine formation and ferric ion coordination give structure to the adhesive and link the components. This resembles the nature of the components in algae adhesive, which are separate, then linked together. This also follows the two stages of algae adhesion, where the adhesive is first in liquid form to spread over the surface, then

hardened in a second stage through polymerization and crosslinking[1]. Further mimicking the exposed nature of algae adhesion (which takes place in seawater for both stages of adhesion), application of the adhesive takes place between two adherends, but in an open environment in bulk solution (in contrast, mussels secrete their adhesive proteins in a closed and controlled environment at a low pH, only exposing the components to the higher pH of seawater for the final hardening step[67]). While this makes the glue innovative, stronger, and easier to use, it does make it more difficult to control exact amounts at the surface, and will be more sensitive to environmental factors in solution. To account for this, care was taken to ensure each set of experiments was performed under the same conditions. Additionally, the adhesive dopamine/polydopamine components are injected at the surface of the adherends, providing adhesion where it is needed most – mussels also localize the adhesive proteins at the surface they are trying to adhere to, with the rest of the plaque and thread providing cohesive strength. The overall concept of this adhesive application method is illustrated in **Figure 4-1d**: dopamine is localized at the surface to provide adhesion, alginate is injected in between to provide bulk cohesion, Fe^{3+} ions link everything together, and the components diffuse and harden to form the final glue.

We performed analytical microscopic examination of the adhesive materials and elucidated the roles of each component, as well as their effects on the final adhesive performance. Environmental factors relating to this open delivery system were also investigated. Through these techniques, we demonstrated the effectiveness of this approach, particularly that of sequential delivery. The resulting composite glue outperforms pure alginate by almost two orders of magnitude, effectively turning alginate into an adhesive, which was not possible through traditional chemical conjugation of alginate with catechol.

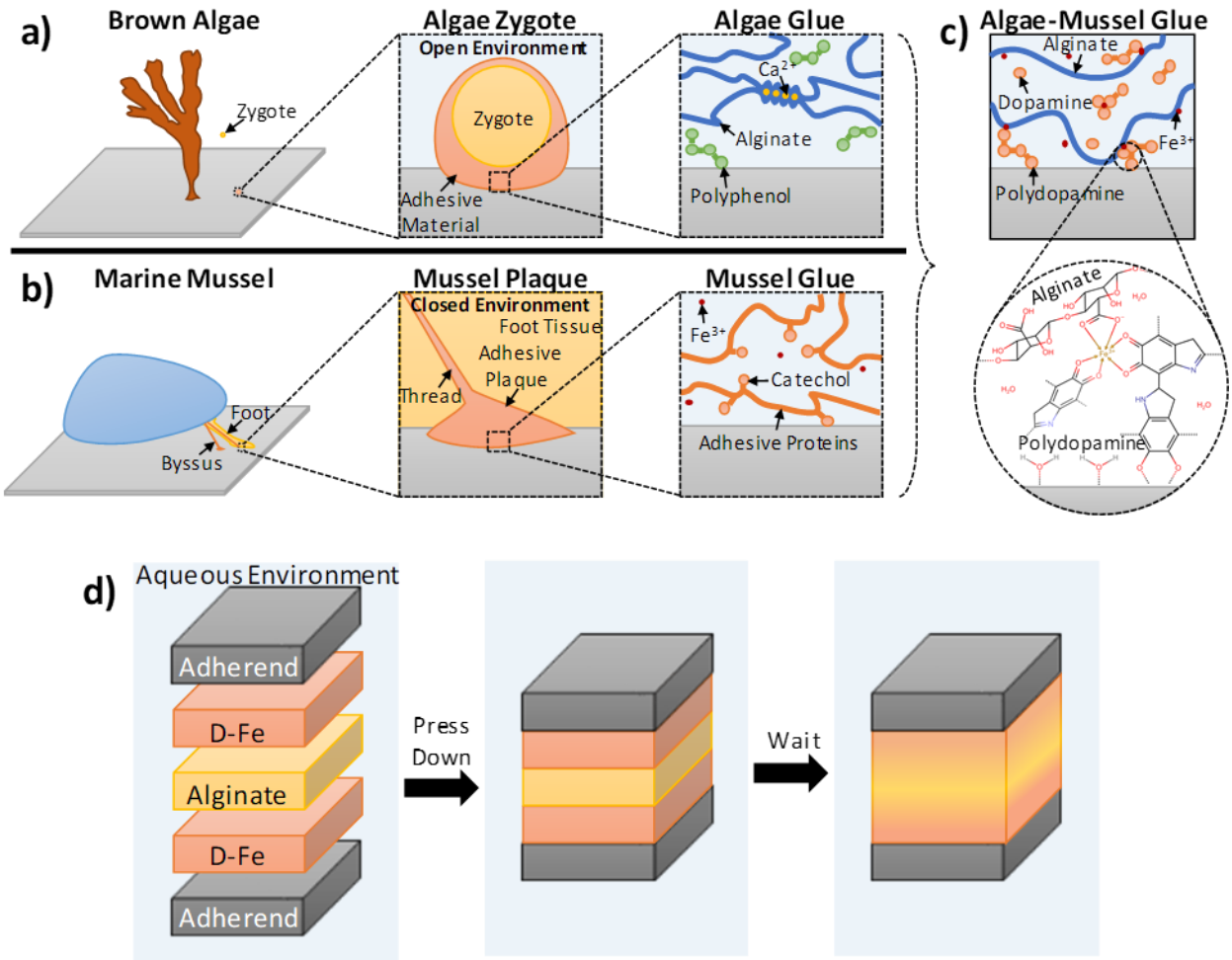

Figure 4-1: (a-c) Illustration of the algae-mussel hydrogel composite adhesive: components of brown algae adhesive system (a) and marine mussel adhesive system (b) were combined to form algae-mussel glue (c). The zoomed view shows the hypothesized molecular interactions between the components: namely, the coordination bonds between the catechol functional group of dopamine with the ferric ion, the ionic bonds between the alginate and the ferric ion, the self-polymerization of dopamine, and the chemical bonding of polydopamine to the adherend's surface through its catechol functionality. (d) illustration of the sequential application of algae-mussel glue. The two solutions used are a dopamine-iron-Tris solution (D-Fe-Tris) and a 5 wt% alginate solution in deionized water. The adherends' surfaces are exposed to the D-Fe-Tris solution, and alginate solution is injected in between, then the adherends are pressed together; this takes place while the system is exposed to a bulk solution of 10 mM Tris.

4.2 Experimental

4.2.1 Preparation of Gel Precursor Solutions

Adhesive gel was formed in two parts. Solution (1) was prepared by mixing together 17.8 mg of iron (III) nitrate nonahydrate (Sigma-Aldrich), 50 mg of tris(hydroxymethyl) aminomethane

(Tris, Sigma-Aldrich), and 100 mg of dopamine hydrochloride (Sigma-Aldrich) in 70 μL of deionized (DI) water. This solution was used immediately after mixing. Solution (2) was prepared by dissolving 5 wt% sodium alginate (HF 120RBS, FMC Biopolymer) in DI water. This solution was either used immediately after mixing or prepared in advance and refrigerated at 4.4 °C to store for up to a month.

4.2.2 Fabrication and Testing of Adhesive Gel

For the sequential application method, directly after mixing solution (1), 20 μL of solution (1) was taken up by a syringe and 18 gauge needle, then dropped onto a substrate (typically a glass slide) immersed in 50 mL of 10 mM Tris-HCl solution (prepared by acidifying 100 mM Tris solution with HCl to a pH of 8.56, then diluting 10x). The second adherend (typically an aluminum SEM stub) was then immersed and agitated within the concentrated region of solution (1), which has a higher density and remains at the bottom of the Tris-HCl solution. Finally, the second adhered was brought up out of the Tris-HCl solution, 30 μL of solution (2) was dropped (via a syringe and 18 gauge needle) onto its surface, and it was then pressed onto the surface of the first adherend. This glued-together system was left in the Tris-HCl solution for 2 hours before tensile testing.

The pre-mixed application method utilized the same substrates, solutions, and final wait time before testing as the sequential method. The major difference is that instead of applying solutions (1) and (2) in separate steps, these two solutions were added together and mixed by vortex to form a viscous pre-gel solution. Approximately 40 μL of this pre-gel solution was then spread onto the surface of the second adherend, which was then pressed onto the immersed surface of the first adherend.

Tensile pull-off testing was performed using a universal materials tester (UMT, CETR), using a glass slide and an aluminum SEM stub (6.6 mm head, Ted Pella) as the first and second adherends, respectively. The aluminum stub was fitted into a custom holder to be attached to the UMT system, and then glued to the glass slide using either the sequential or pre-mixed application methods. After the 2 hour waiting period in Tris-HCl solution, samples were immediately withdrawn and attached to the UMT. The stub was then pulled away from the glass slide substrate (which was restrained from moving) at a rate of 500 mm/min, until the two surfaces were fully separated from one another. The force was recorded during this time, and the maximum force achieved at pull-off was used as the adhesive pull-off force, then normalized by the contact area to determine the tensile strength.

For varying conditions, all tests except that labeled "Full System Pre-mixed" used the sequential application method, with deviations from this technique listed below. For the "pure alginate" case, only solution (2) was used. For the "no dopamine" case, solution (1) did not contain dopamine. For the "catechol-alginate" case, solution (2) used 5 wt% alginate that had been chemically modified with catechol groups, as in our previous work[135]; also, solution (1) did not contain dopamine. For the "no iron" case, solution (1) did not contain ferric chloride. For the "100% humidity" case, the substrate was immersed in Tris-HCl solution and withdrawn prior to application, then the adhesive system was left at 100% humidity overnight. For the wet surface, the glass slide was immersed in DI water, then removed from the water immediately prior to gluing on the aluminum stub, with this system left at room temperature for three days. For the dry surface, the aluminum stub was glued to a clean, dry glass slide, with the system left at room temperature for three days. For water content tests, solution (1) had varying quantities of DI water instead of the standard 70 μL. For polydopamine formation time, solution (1) was left for a varying amount

of time after mixing before being dropped onto the glass slide surface for the sequential application.

4.2.3 Microstructure Characterization

For examining the microstructure, solutions (1) and (2) were directly added together in a separate mini-centrifuge tube and mixed by vortex. This tube was immersed in 50 mL of 10 mM Tris-HCL solution overnight, then the gel within was removed and either examined directly under optical microscope, or freeze-dried and examined using scanning electron microscopy (SEM).

4.2.4 Statistics

All experiments were carried out with $n \geq 3$ data points; the only exceptions are the "pure alginate" and "catechol-alginate" cases in **Figure 4-4a**, which only have 2 data points, as most samples were so weak as to detach before testing. For all figures, error bars represent the standard error of the mean.

4.3 Results and Discussion

X-ray photoelectron spectroscopy (XPS), Raman spectroscopy, scanning electron microscopy (SEM), and energy-dispersive x-ray spectroscopy (EDX) were used to examine the Fe^{3+} linking. XPS was used to determine if the alginate-iron-dopamine interactions were indeed present, with elemental atomic percents presented in **Table 4-1**, and an example of the resulting high-resolution Fe 2p spectra visible in **Figure 4-2g**. Examining the relative levels of each element, the dopamine-iron-alginate (D-Fe-Alg) gel shares more in common with polydopamine film than it does with the iron-alginate (Fe-Alg) gel. This may indicate that a majority of the final adhesive is polydopamine. In examining the high-resolution Fe spectra (**Figure 4-2g**) for Fe-Alg and D-Fe-

Alg gels, the two systems appear to share similar peak locations, which may suggest that Alg-Fe interactions are present.

Table 4-1: Surface chemical composition from XPS of pure alginate, polydopamine thin film, iron-alginate (Fe-Alg) hydrogel, and dopamine-iron-alginate (D-Fe-Alg) hydrogel.

atomic %	C1s	N1s	O1s	Fe2p3
Alginate	60.6	1.6	37.8	
Polydopamine	66.9	6.7	26.4	
Fe-Alg	54.5	3.7	40.2	1.6
D-Fe-Alg	66.2	6.6	26.7	0.5

A clearer indication of interactions between dopamine and Fe^{3+} ions was seen when using Raman spectroscopy. Resonance Raman spectra of dopamine-iron-alginate gel provided evidence of chelation of Fe^{3+} ions by the catechol group of dopamine, primarily visible in the 470-670 cm^{-1} Raman band (**Figure 4-2f**). In particular, peaks at ~590 cm^{-1} and ~633 cm^{-1} mark interactions between Fe^{3+} ions and individual oxygen atoms in the catechol group, while the peak present at ~528 cm^{-1} can be attributed to charge transfer interactions of the catechol-metal bidentate chelate[62,148]. The height of the charge transfer peak, compared with the other two peaks, indicates a high level of bidentate complexation, suggesting the dopamine-Fe^{3+} complexes are predominantly tris-catechol-Fe^{3+}. This is supported by the observation that the dopamine-iron solution was dark red in colour, which is typical of tris-catechol-Fe^{3+}[62].

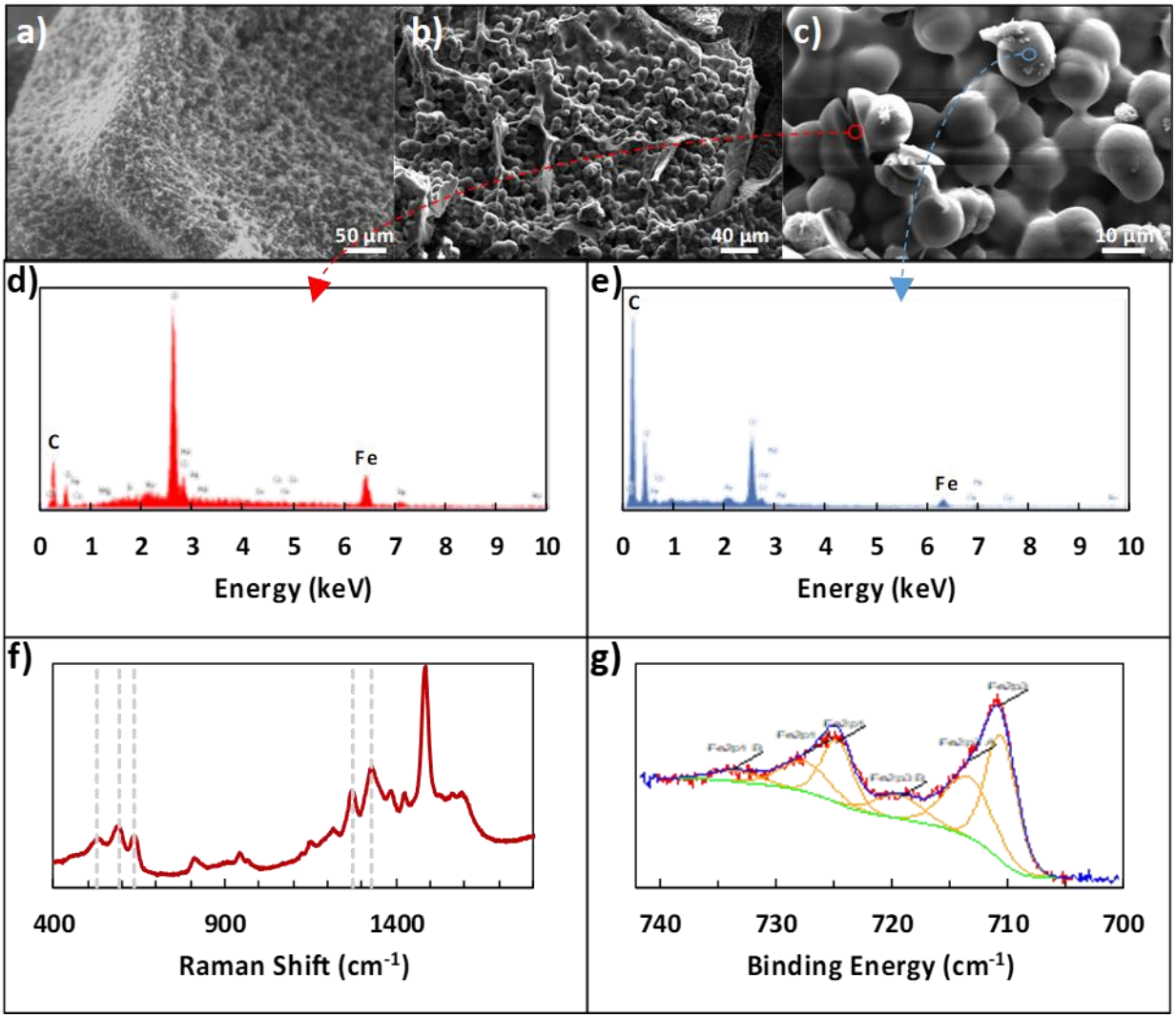

Figure 4-2: (a) ESEM image and (b-c) SEM images of spherical structures present in dopamine-iron-alginate gel. (d) and (e) show EDX analysis of the locations marked in (c), emphasizing peaks for carbon and iron, with (d) focusing on the interior of a cracked sphere, and (e) examining the surface of a sphere. (f) shows a Raman spectrum of dopamine-iron-alginate gel, with dotted lines marking peaks corresponding to catechol-Fe^{3+} interactions. (g) shows a high-resolution XPS spectrum of the Fe 2p peaks for iron-alginate gel.

One interesting evidence for alginate-iron-dopamine interactions was seen when the microscale structure of the adhesive gel was examined. To do so, the gel was formed by mixing together the components of dopamine, alginate, iron, and tris(hydroxymethyl) aminomethane (Tris). These gels were immersed in 10 mM Tris-HCl buffer overnight, and then examined using optical microscopy and environmental SEM (ESEM). In addition, a portion was freeze-dried and

examined using SEM. Three main components are visible with optical microscopy in the resulting hydrogel: pieces of the gel itself (alginate crosslinked by Fe^{3+} ions), irregular polydopamine particles, and other particles that are highly spherical in shape. These spherical particles were observable through optical microscopy, ESEM, and SEM, as seen in **Figure 4-2a-c**, and were determined to be 12.26 ± 0.75 µm in size. By excluding individual components from the hydrogel-forming pre-mixture (e.g., no addition of dopamine, or no alginate), it was determined that all components – dopamine, iron, alginate, and Tris – were required to form the spherical particles. Without alginate or iron present, only smaller, irregular particles could be seen, which are expected to be polydopamine particles. Without dopamine or Tris present, the solution became a solid gel rapidly, lacking the presence of any of the spherical particles.

Additionally, EDX was used to provide elemental analysis of the spherical particles, both on their surface and in the center, utilizing a large crack on the particles. Examples of the resulting EDX plots can be seen in **Figure 4-2d-e**, with their corresponding locations visible in **Figure 4-2c**. While preliminary images from optical microscopy and ESEM suggested the spheres may be mostly iron, the SEM images and EDX results clarify their nature. The surface of the spheres appears to be polymer, with the majority consisting of carbon and oxygen, and only very small amounts (1-2 atomic %) of iron present. In contrast, the cracked sphere, with analysis closer to the center, showed much higher levels of iron present (8.55 atomic %). This additional iron may be in a solid form, or present as an ion, interacting with the alginate and polydopamine in the rest of the particles. In particular, the polymer content of the spheres has a low amount of oxygen present, bearing more in common with the carbon:oxygen ratio of polydopamine than that of alginate. This further reinforces the suggestion from XPS results that the adhesive surface consists mostly of polydopamine.

While there is evidence of both Alg-Fe^{3+} and dopamine-Fe^{3+} interactions, the overall cohesion of the system is a balance of these interactions, as well as Alg-Fe^{3+}-dopamine linkages. In addition, there is another balance, one between cohesion and adhesion resulting from the Fe^{3+} ions; while their interactions with alginate and dopamine provide the system with cohesive strength, dopamine that is complexed with Fe^{3+} is unlikely to be able to directly contribute to adhesion. With the current composition of algae-mussel glue, the presence of Fe^{3+} appears to be more beneficial than harmful. However, attention should be paid when modifying the ratio of Fe^{3+} ions to the other components, since changing concentrations of Fe^{3+} ions has previously been used to manipulate mechanical properties and degradation behaviour of dopamine-Fe^{3+}-crosslinked elastomer[25].

After confirming the interactions between all components, tensile pull-off tests were used to evaluate the bonding performance of the composite glue for underwater joining of aluminum stubs to glass slides. The glue was applied by using two base solutions: (1) a solution of dopamine, ferric nitrate nonahydrate, and Tris in deionized (DI) water; (2) a solution of 5 wt% alginate in DI water. These two solutions were applied separately, here referred to as the ‘sequential’ method, which is illustrated in **Figure 4-1d** (with a detailed schematic in **Figure 4-3**). This separate addition means that the dopamine and alginate solutions were never directly mixed before application; however, there is time for the components to diffuse and interact during the curing stage, which mimics the adhesive deposition process of algae.

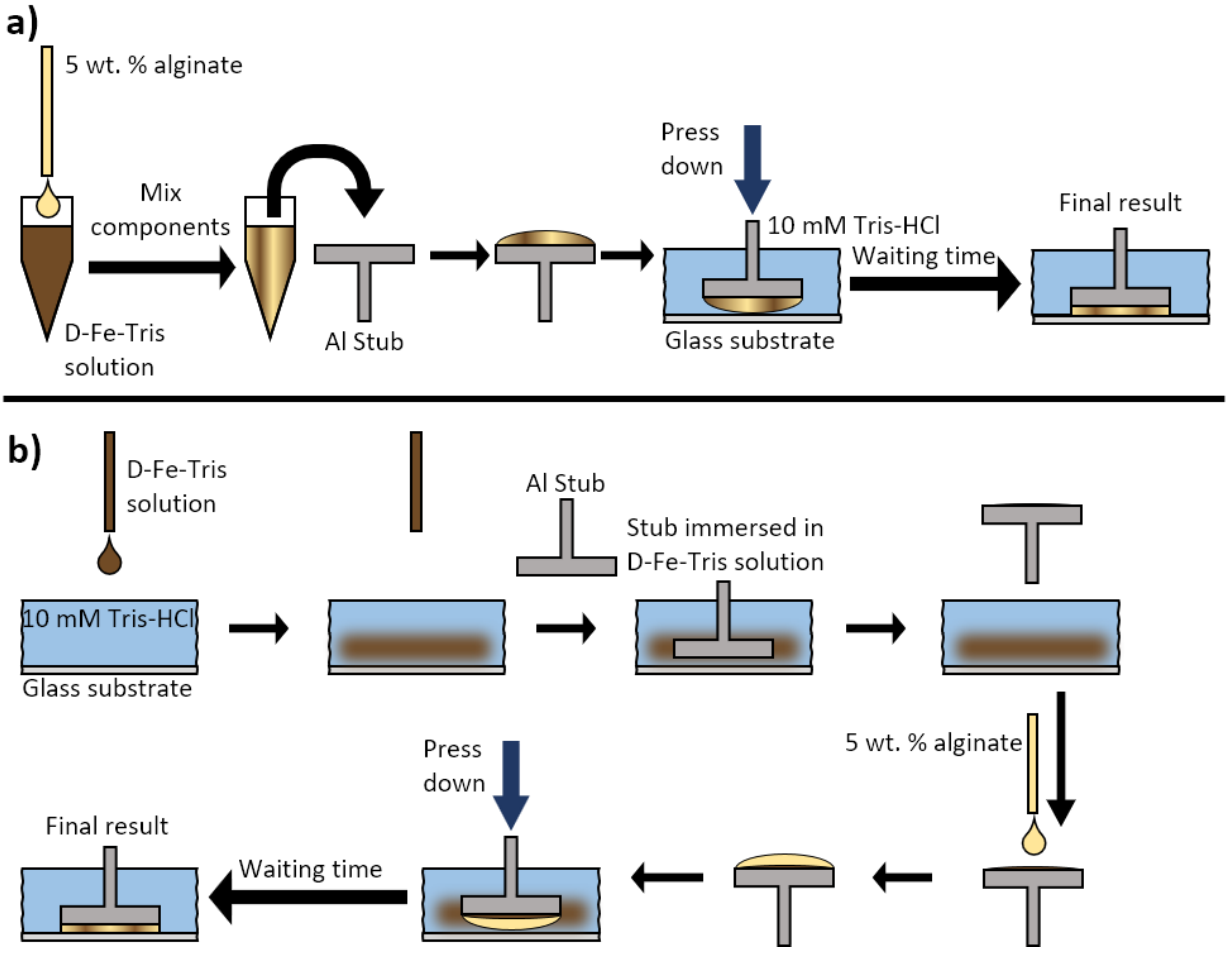

Figure 4-3: Schematic detailing the procedure for (a) pre-mixed application; and (b) sequential application of algae-mussel glue. The two solutions used are a dopamine-iron-Tris solution (D-Fe-Tris) and a 5 wt. % alginate solution in deionized water. For pre-mixed application, these two solutions are directly mixed together, then applied to an aluminum stub, which is subsequently pressed into a glass substrate underwater for bonding. In sequential application, the D-Fe-Tris solution is added to the surface of the glass substrate while underwater. The aluminum stub is then immersed in this surface D-Fe-Tris solution, after which the alginate solution is added to the face of the stub. Finally, the aluminum stub is pressed into the glass substrate underwater for bonding.

The tensile adhesive strength obtained from pulling apart these glued components can be seen in **Figure 4-4a**. In all cases where dopamine was not present (whether iron was present to cross-link alginate or not), adhesion of the gel was minimal (4-6 kPa). This is unsurprising, as alginate and its crosslinked gels are generally low in adhesion[121]; this also shows the viscous nature of pure alginate does not contribute significantly to adhesion. Alginate with conjugated catechol

groups also has poor adhesion, indicating the functionalization had little effect on the final adhesion. The gel also exhibited extremely low adhesion when no alginate was present in the system, which emphasizes how all the components must be present to achieve the adhesive properties of this composite glue. One interesting point of note was the surprising strength of the sequential application with no iron present. While still significantly lower than the full system, the strength of the iron-free case suggests that dopamine and alginate may still be interacting in some way, especially since there were no ions available to crosslink alginate. It is possible that the basic conditions from Tris induced covalent crosslinking between alginate and catechol. With a tensile adhesive strength of 400 kPa, the composite glue achieves an improvement of nearly two orders of magnitude over pure alginate.

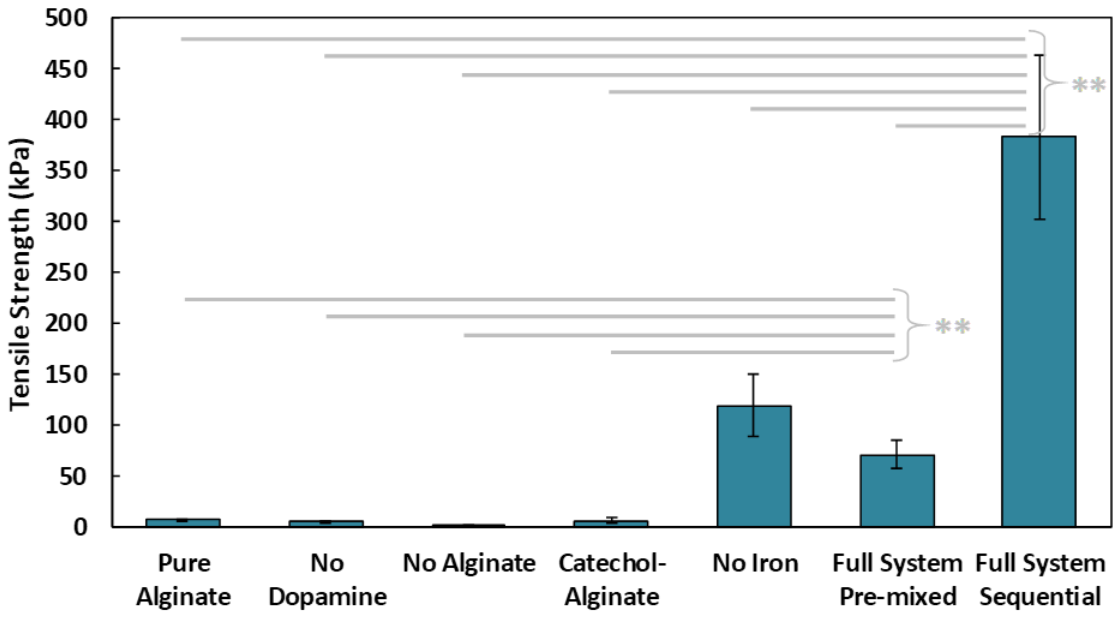

Figure 4-4: Performance of algae-mussel adhesive, shows the effects of varying formulations, including: using only 5 wt% alginate (Pure Alginate); using alginate, iron, and tris, but without dopamine (No Dopamine); using iron, dopamine, and tris, but without alginate (No Alginate); using catechol-modified alginate with iron and tris, but no additional dopamine (Catechol-Alginate); using alginate, tris, and dopamine, but without iron (No Iron); and the complete system with all components, applied using the pre-mixed (Full System Pre-mixed) or sequential (Full System Sequential) application methods. ** refers to a p-value < 0.01 between the pair of conditions.

Table 4-2. Summary of recent literature work in underwater adhesives reporting tensile adhesive strength.

Adhesive	**Nature**	**Adherends**	**Tensile Bonding Strength**	**Notes**	**Source**
Algae-mussel sequential	***Hydrogel***	***Aluminum-glass***	***382.6 ± 81.0 kPa***	***This work.***	***149***
Algae-mussel pre-mixed	***Hydrogel***	***Aluminum-glass***	***70.5 ± 34.3 kPa***		
Live mussel	Biological	Plaque-aluminum	0.13 ± 0.01 MPa	Salt water as medium.	150
		Plaque-aluminum	288 ± 110 kPa	Salt water as medium for establishing adhesion.	151
		Plaque-glass	171 ± 65 kPa		
Biomimetic cyanoacryl	Biomimetic adhesive	Bone-bone	125 ± 10.5 kPa	Glued at 100% humidity.	94
Poly(catechol-styrene)	Biomimetic adhesive	Aluminum-aluminum	2.2 ± 0.9 MPa	Salt water as medium.	150
Poly(allylamine)	Pressure-sensitive adhesive	Glass-glass	435 kPa	Formed before adhering	152
DOPA-like units + amino	Pressure-sensitive adhesive	Bone-bone	1.4 ± 0.3 MPa	Formed before adhering (5 N preload applied)	100
Protein from squid ring teeth	Protein melt-cool	Glass-glass	1.50 ± 0.23 MPa	Requires melting during application. Dependent on preload.	153
Anthracene-PEI glue with reversible anthracene dimerization	In-situ crosslinked polymer	Quartz-glass	~580 kPa	Reversible (heat lowers cohesion)	154

In order to put this strength into context, the performance of algae-mussel adhesive is compared with other underwater adhesives from literature in **Table 4-2**. There is a broad range of adhesive strengths reported for various underwater adhesives; sequential algae-mussel glue is close to that of live mussels. Considering the varying nature of both the glues and adherends, algae-mussel adhesive appears to achieve reasonable performance.

While the sequential method was inspired by algae and mussels, it is also possible to simply mix the components together. We tested a 'pre-mixed' system, which more closely resembles traditional two-part adhesives (where solution (1) and (2) were directly mixed before application to the adherends). The pre-mixed method only demonstrated an adhesive strength of 70 kPa, compared to the 400 kPa strength of the sequential method. Based on our observations, we suspect the difference in performance could be attributed to the gelling of the pre-mixed solution occurring before application; the surface localization of the adhesive components in the sequential case could also be playing a role in improving overall adhesion.

In contrast to the controlled environment mussels maintain for adhesion, brown algae attach to surfaces in more exposed and open conditions. For this reason, we wanted to investigate the effects of dilution or concentration of the glue on its adhesive capabilities. In order to do so, solution (1) was prepared with differing initial quantities of DI water. While previous strengths using 70 µL of water are overall higher than values acquired while varying water content, this is due to the variability of batches of the glue being fabricated. All tests over a set of conditions are performed on the same batch, meaning an overall trend can still be observed. As shown in **Figure 4-5a**, a peak in strength was visible using a water quantity of 50 µL. This adhesive strength was clearly higher than that when the water content was decreased further (30 µL). In addition, both the 50 µL and 70 µL cases demonstrated greater tensile strength than conditions where solution (1) was diluted further, particularly those of 120 µL and 180 µL. The effect of low water content can be explained by the high viscosity of solution (1), making mixing difficult and the application less homogeneous. The dilution from high water content would reduce the concentration of both adhesive and cohesive components, namely dopamine and Fe^{3+}, as well as causing solution (1) to spread more rapidly upon application, diluting it further. The combination of these effects would

lead to a significant reduction in the overall adhesive strength. This suggests that concentration of the initial adhesive solution, as well as its ability to avoid spreading too quickly, are essential factors in maximizing adhesion.

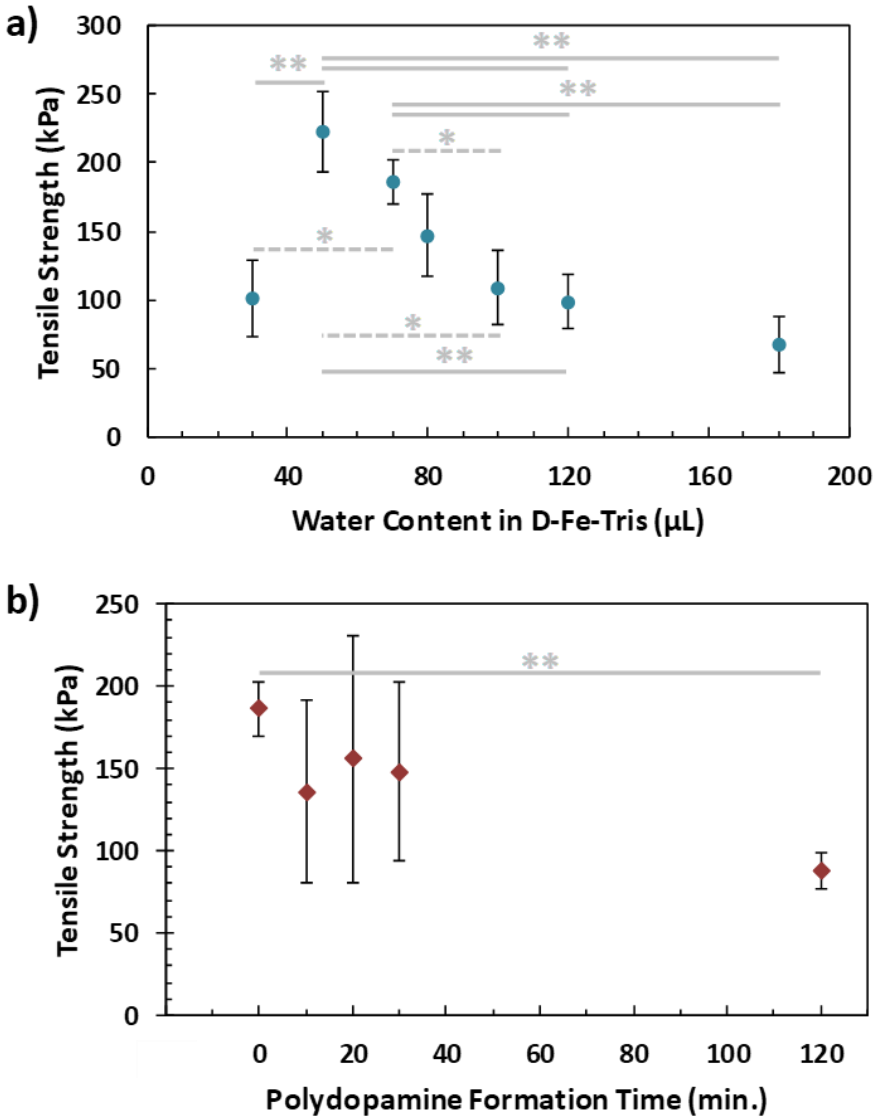

Figure 4-5: Effects on final underwater adhesive tensile strength of sequential algae-mussel adhesive for varying (a) water content of dopamine-Fe^{3+}-Tris (D-Fe-Tris) solution (effectively diluting or concentrating these three components before application) and (b) polydopamine formation time before application. In both plots, * refers to a p-value < 0.05, while ** refers to a p-value < 0.01, each between the pair of conditions.

After determining the importance of the concentration of the initial adhesive, we sought to investigate the water content of the gel at equilibrium by using samples of aluminum stubs glued to glass slides, which were made using the sequential method. The stubs and slides were weighed before forming the gel; after gel formation, the outside surfaces of the samples were gently dried with Kimwipes, with a second weighing to determine the mass of the swollen gel. Finally, the samples were dried in an oven at 90 °C overnight and weighed to determine the mass of the dried gel (with the difference between swollen and dried gels providing the mass of water). This was used to acquire a weight percentage of water, which was 64.0 ± 29.4 %.

Another factor to consider in algal adhesion is the nature of the polyphenol adhesive component. This is important for the composite glue because brown algae use polyphenol molecules in their adhesive strategy, while the adhesive presented in this work uses the small molecule of dopamine. The state of polydopamine depends on time, as dopamine self-polymerizes into polydopamine, growing over time. To investigate this, a waiting step was incorporated into the sequential procedure, where solution (1) was left for varying periods of time before application to the adherends. This was to allow the dopamine molecules to partially form polydopamine, resembling the polyphenols in algae. After this waiting step, the adhesive gel was formed using the sequential procedure, with results of tensile testing visible in **Figure 4-5b**. While variability was lower for waiting times of 0 and 120 minutes, samples tested at 10, 20, and 30 minutes demonstrated large variations. This could be from the dynamic process of polydopamine formation occurring during this timeframe; this could lead to greater inhomogeneity in samples. By 2 hours, polydopamine formation has nearly completed, leading to more stable and consistent results. Additionally, there is a significant difference in adhesion measured between waiting times of 0 and 120 minutes, indicating that polydopamine forming before application could weaken overall

adhesion of gel. This makes sense considering the two-stage adhesive of algae, where hardening/crosslinking only occurs after the adhesive has spread.

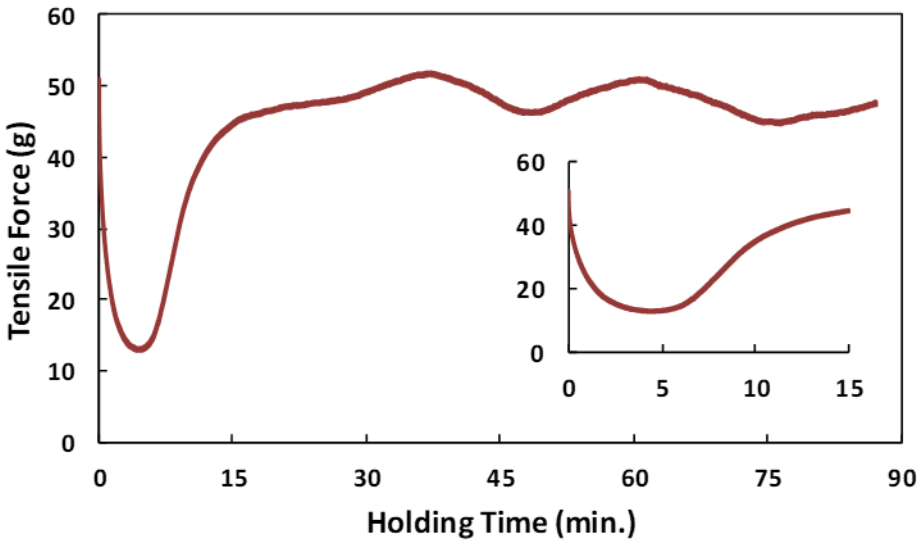

Figure 4-6: A plot of force vs. holding time for a constant strain applied to an aluminum stub bonded to a glass slide with sequentially applied algae-mussel adhesive. After adhesive application, the system is left in the 10 mM Tris-HCl solution for 2 hours, then gently rinsed and transferred to DI water, where it is pulled to a force of 50 g, then held at constant strain, monitoring change in force over the holding time. The insert shows a closer view of the first 15 minutes of holding time.

In order to investigate the viscoelastic behaviour of the algae-mussel glue, tensile holding tests were carried out, where aluminum stubs were glued to glass slides using the same technique as for general adhesion testing in this work. The method used was similar to that of stress relaxation tests, and the inclusion of the time domain was intended to give insight into viscoelastic properties. Instead of pulling on the stub until failure, the stub was pulled until a force of 50 g was felt, and then held at constant strain. At this fixed displacement, the change in force over time was measured and recorded, with **Figure 4-6** showing a typical force-time plot. One interesting behaviour that is immediately apparent from **Figure 4-6** is that while the force initially decreases over time, it then begins to increase again, reaching a value close to the initial force at the fixed strain. At first, the

force appears to drop to 25% of its initial value, before rising back up to 95% of the initial force. To make sure this surprising result is valid, we repeated the experiment multiple times, and performed additional tensile holding tests with cyanoacrylate-based glue in both dry and submerged conditions (to confirm this result was not due to external factors).

The lowering of the tensile force is likely due to the ionic crosslinks breaking to release the stress; however, the cause for the following increase in force is unclear. One possible explanation is that the alginate chains and dopamine complexes could tighten and pull on the gel when they reform in new positions. While this is not direct evidence of self-healing capability, it does suggest the composite glue has some ability to reform bonds that are broken – at least those that are broken as part of releasing stress.

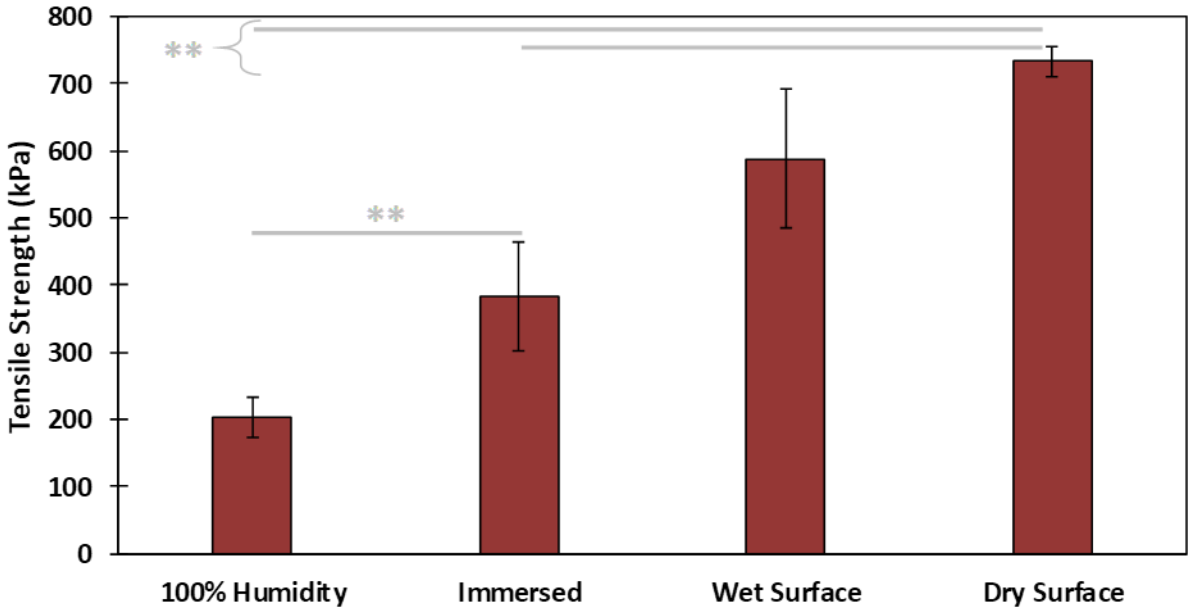

Figure 4-7: Performance of sequential algae-mussel adhesive in varying environmental conditions, including: applied to a wet substrate and kept in a 100% humidity environment overnight (100% Humidity); applied underwater, kept in aqueous conditions for 2 hours (Immersed); applied in air to a surface wetted by water, and left to dry at ambient conditions for 3 days (Wet Surface); and applied to air to a dry surface, and allowed to dry at ambient conditions for 3 days (Dry Surface). ** refers to a p-value < 0.01 between the pair of conditions.

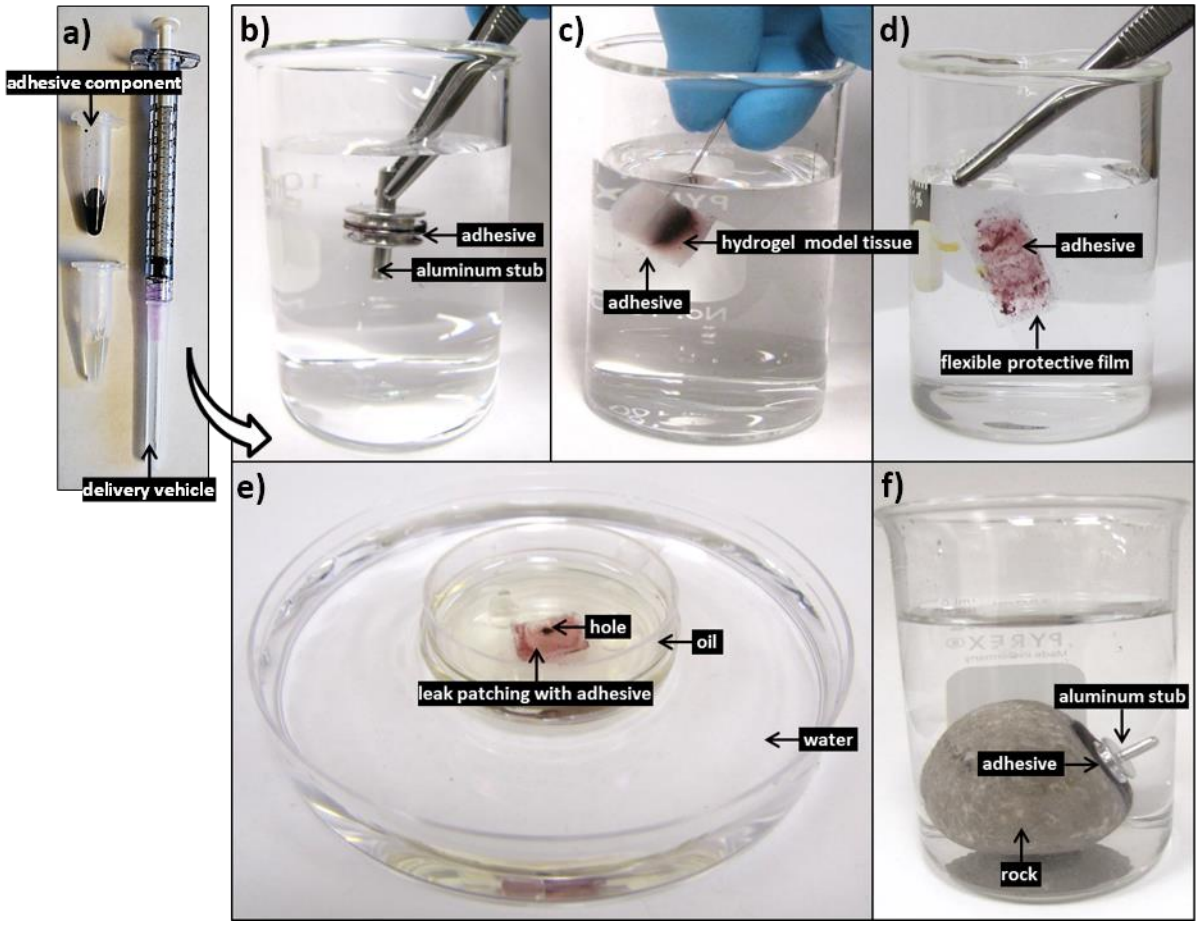

Figure 4-8: Photos of (a) solutions used for sequential adhesion, used to join together: (b) two rigid aluminum SEM stubs; (c) two pieces of soft PVA hydrogel; (d) two flexible plastic (PET) films; (e) a plastic film to a plastic Petri dish patch a hole in the Petri dish, preventing the oil from leaking into the water; and (f) an aluminum stub to a rock. Both cases were joined by the sequential algae-mussel adhesive in 10 mM Tris-HCl buffer at pH 8.5 for 2 hours of curing time. Note that the buffer solution was replaced by water for clarity.

Further tensile adhesive tests were carried out on the composite glue in different environmental conditions: in 100% humidity, as well as in air on wet and dry glass substrates, with results shown in **Figure 4-7**. Samples in 100% humidity were left overnight, while those in ambient conditions were left to dry over three days. The dry-applied glue demonstrated an adhesive strength almost twice that of the immersed, providing a high maximum strength to the glue. Application to a wet substrate resulted in adhesion similar to that of dry substrates. This indicates that the composite glue can tolerate varying levels of exposure to water. In addition, as we have shown previously, the glue can also tolerate varying pH levels, temperatures, and different surface

conditions[144]. Overall, the performance of this algae-mussel composite glue indicates that it could potentially find use in a variety of applications, including bonding and patching of soft and rigid materials. These potential applications are illustrated in **Figure 4-8**, where the algae-mussel glue is sequentially injected between varying materials to hold them together. These include rigid inorganic (aluminum to glass) or flexible organic (bonding two sheets of polymer film) materials, or even hydrogels.

4.4 Conclusions

In this chapter, we demonstrated a new strategy for constructing underwater adhesive, combining elements of algal and mussel adhesion. This method does not require complicated chemical modification, avoiding the pitfalls determined in the previous chapter; instead, Fe^{3+} ions are utilized as a bridge between the adhesive dopamine and cohesive alginate components. Good adhesive performance was achieved underwater, with reasonable tolerance to other environmental conditions. Sequential delivery of the components to focus adhesion at the interface, mimicking algal and mussel adhesive strategies, greatly strengthened the adhesive capabilities of the gel. The role of individual components was investigated, demonstrating the importance of incorporating dopamine for adhesion. Overall, our results demonstrate that the adhesive functionality does not have to be initially part of the polymer backbone, and connecting the components without chemical synthesis can still lead to strong bonding performance.

Chapter 5 Development of Algae-Mussel-Inspired One-Part Adhesive towards Practical Applications

5.1 Introduction

Taking cues from the adhesive strategies of both brown algae and marine mussels can allow for strong underwater adhesion that does not require chemical conjugation of catechol groups. However, while effective, sequential application of adhesive and cohesive components can be somewhat impractical and prone to human error. In contrast, one-part adhesives are frequently desired for their improved ease of use. Pre-mixing techniques should be able to provide this, but the resulting rapid gelation leads to inhomogeneous mixing and poor performance, and does not achieve any form of long-term stability before use. This lack of longevity before use is also true for sequential application of algae-mussel glue; while alginate is stable by itself in water, the other components (dopamine, ferric nitrate, and tris(hydroxymethyl)aminomethane (Tris)) will interact over time (e.g., oxidation of dopamine and complexation with ferric ions).

While underwater bonding is the primary objective of algae-mussel glue, the dissolving of its components in water before use may be a major source of issues with stability. An ideal case would be if all components were mixed together in the form of dry powders, which could then interact, gel, and form the final adhesive on contact with water. However, this answer gives rise to its own problems. Primarily, each granule of powder is still separate from each other, with grain sizes much larger than the molecular scale. Combined with the rapid gelation of alginate, this means that on contact with water, each granule will crosslink within itself, but interactions between powder particles is minimal. Additionally, each granule still contains a multitude of polymer chains, meaning the individual chains are not separate when dry powders are mixed together.

Because of these two issues, the resulting glue is still inhomogeneous, and is too weak to bond any surfaces together.

Dispersing the components in a different liquid would provide another alternative to dissolving them in water, while also avoiding the pitfalls of directly mixing the dry powders. Glycerol is a good candidate to act as the dispersant for a variety of reasons. First, a majority of the components of algae-mussel glue do not dissolve well in it, allowing it to disperse instead of dissolve them. Second, it has a high viscosity, which can slow down both settling out of the components, as well as diffusion of water (extending gelation time). Third, it has an extremely low vapour pressure, preventing most evaporation and allowing it to keep performing its role. Finally, it is completely miscible with water, allowing it to diffuse into the bulk phase when immersed in water, and allowing exchange of glycerol and water molecules to activate gelation.

In this work, we utilized glycerol as a dispersant for powders of alginate, dopamine, Tris, and ferric salts. We examined how the structure of the resulting gel changed, and used its freezing behaviour to confirm the exchange between glycerol and water. When mixing the components together, the dispersion remained stable overnight, while sequential or pre-mixed applications in water gelled in seconds. We also demonstrated a two-part formulation that remained stable for days, further extending the usability of this adhesive system. With this more practical application technique, the algae-mussel adhesive could be useful for commercial or industrial underwater adhesive applications.

5.2 Experimental

5.2.1 Vacuum Drying of Alginate in Glycerol

Alginate-glycerol dispersion was first prepared by dissolving alginate (HF 120RBS, FMC Biopolymer) in a mixture of 10 wt% deionized (DI) water and 90 wt% glycerol (EMD Chemicals).

Alginate was added at weight fraction of the glycerol component – typical quantities were 3 wt% and 5 wt% alginate. This solution was mixed on a vortex mixer until alginate was fully dissolved, then placed in a vacuum oven (VWR) and heated up to 70 °C under vacuum to remove water. To maximize water extraction, the mixture was heated under vacuum for 96 hours (cycling the vacuum twice a day). The masses of the empty container, as well as the full container before and after drying, were measured on a mass balance and recorded to estimate water loss. Pure glycerol was exposed to the same conditions in the vacuum oven as a control for mass loss during drying.

5.2.2 Preparation of Other Components

Iron (III) sulfate hydrate (Sigma-Aldrich) was converted into its anhydrous form through vacuum drying in a vacuum oven at 300 °C for 24 hours. Tris(hydroxymethyl)aminomethane (Tris, Sigma-Aldrich) was ground from small crystals into a fine powder using a mortar and pestle. All other chemicals were used as received.

5.2.3 Preparation of One-Part Glycerol Dispersion

All samples were prepared by adding dopamine hydrochloride (Sigma-Aldrich), anhydrous iron (III) sulfate, and powdered Tris components to alginate-glycerol. Components were added in weight percent amounts relative to the mass of glycerol, noted in a format of A-D-F-T (e.g., 5-5-5-5, where each component is included at 5 wt% of glycerol) referring to weight percents of alginate (A, referring to the alginate-glycerol dispersion), dopamine (D), anhydrous iron (III) sulfate (F), and powdered Tris (T), respectively. Due to the high viscosity of alginate-glycerol, components were mixed in by vigorous stirring with a wooden stick.

5.2.4 Preparation of Two-Part Glycerol Dispersion

For two-part glycerol dispersion, components were added to two separate mixtures. Part (1) consisted of the dopamine component added to the alginate-glycerol dispersion, while part (2) contained anhydrous iron (III) sulfate and powdered Tris added to pure glycerol. Each part had the same weight percents of the components as the respective one-part system; as such, once (1) and (2) were combined in equal parts, the final concentrations were half of their original (e.g., 5 wt% alginate in alginate-glycerol became 2.5 wt% alginate in the mixture of parts (1) and (2)). For preliminary testing, parts (1) and (2) were mixed directly with a wooden stick prior to use, similarly to mixing the D, F, and T components into each part. For the demonstration of the two-part adhesive, parts (1) and (2) were added to separate syringes, which were joined together with a syringe connector for mixing.

5.2.5 Testing of Adhesive Gel

Tensile pull-off testing was performed using a universal materials tester (UMT, CETR), using a glass slide and an aluminum SEM stub (6.6 mm head, Ted Pella) as the first and second adherends, respectively. The glass slide was immersed in a Petri dish (100 mm diameter, Fisher Scientific) containing 50 mL of DI water, with the bonding taking place underwater. The aluminum stub was fitted into a custom holder to be attached to the UMT system, and then either the one-part or mixed two-part glycerol dispersions was spread onto the stub's surface to a 0.5 mm thickness, after which the stub was then pressed onto the submerged glass slide. After waiting overnight, samples were withdrawn from the water and quickly attached to the UMT. The stub was then pulled away from the glass slide substrate (which was restrained from moving) at a rate of 500 mm/min, until the two surfaces were fully separated from one another. The force was

recorded during this time, and the maximum force achieved at pull-off was used as the adhesive pull-off force, then normalized by the contact area to determine the tensile strength.

Shear testing was also performed using a UMT, with a glass slide and nylon fabric (purchased from Len's Mill Store, Waterloo) as the substrate and peeled material, respectively. The ribbons of nylon fabric were obtained with a width of 15 mm, and were cut into 75 mm long strips. To perform the shear adhesion test, 200 μL of the one-part glycerol dispersion was spread onto a glass slide to a square area of 15 x 15 mm. A nylon strip was then placed to overlap with this spread area (such that the end of the fabric strip covered the glycerol dispersion), with the fabric oriented in the same direction as the glass slide. This entire sample was then submerged in a Petri dish containing 50 mL of DI water to allow gelation and bonding to occur. After waiting overnight, samples were withdrawn from the water and attached to two grips on the UMT. The glass slide and nylon fabric strip were then pulled apart at a rate of 2.56 mm/s with a 0° angle between the glass and fabric, until the two materials were fully separated from each other. The force was recorded during this time, and the maximum force achieved during peeling was used as the shear adhesive force, then normalized by the 15 x 15 mm area to determine the shear adhesive strength.

5.3 Results and Discussion

5.3.1 Fabrication of one-part algae-mussel glue in glycerol

In order to obtain a more stable one-part formulation of algae-mussel glue, components (alginate, dopamine, anhydrous ferric chloride, and powdered Tris) were dispersed in glycerol. However, we found that this could not be performed in a single step, as alginate would remain separate granules in pure glycerol, as opposed to being dispersed on a scale closer to individual polymer chains. We determined that with a small amount of water (10 wt%) in glycerol, alginate

would disperse extremely well – the mixture became evenly cloudy throughout and did not show macroscopic granules, but also did not exhibit the viscosity-increasing behaviour of dissolved alginate. However, the mixture could not be used in this state, as removal of water was important to minimize the solubility of components dispersed in glycerol. We speculated that, with the high viscosity of glycerol, water could be removed without aggregation of the alginate. To confirm this, we kept the mixture in a vacuum oven at 70 °C for 96 hours, recording the mass lost during drying. Water made up 9.52% of the original mass, and a total of 10.02 ± 0.11% mass was lost during drying. A control of pure glycerol was used, which itself exhibited a negligible mass gain, suggesting the mass loss of the alginate-glycerol-water mixture was not from glycerol. Based on these results, the remaining water was estimated to be negligible, leaving behind alginate dispersed in glycerol. At this point, dopamine, iron, and Tris components could be dispersed in the alginate-glycerol mixture.

Initially, anhydrous iron (III) chloride was used as the source of Fe^{3+} ions for the one-part algae-mussel glue. However, gelation still occurred rapidly when ferric chloride powder was added to the other components in glycerol. In order to investigate this behaviour, anhydrous ferric chloride powder was added to pure glycerol, either directly or after drying glycerol in a vacuum oven. It was observed that in either glycerol sample, when ferric chloride was added, the entire mixture became a clear yellow colour, which is in contrast with the translucent, cloudy appearance of any of the other components dispersed in glycerol. Based on this observation, it was thought that ferric chloride was too soluble in glycerol, and hence was being dissolved instead of dispersed, allowing it to interact with and gel the alginate in the system. Other sources of Fe^{3+} ions were investigated, and iron (III) sulfate was determined to be the most promising candidate, as it is

slightly soluble in aqueous conditions (for release of Fe^{3+} ions upon exposure to water), but only sparingly soluble in alcohols (to avoid ion release in glycerol).

5.3.2 Characterization

Differential scanning calorimetry (DSC) was used to investigate the thermal properties of the glycerol-based algae-mussel glue, as well as to determine if any glycerol was remaining. Glycerol-based glue samples were tested, both before and after immersion in water, as well as sequential and pre-mixed versions of the original algae-mussel glue (as prepared in 0). All samples were brought from 25 °C to -60 °C and back to 25 °C to observe their freezing and melting behaviour. The glycerol-based glue that was not immersed in water (and hence had only glycerol as the solvent) did not freeze during the entire experiment. This is expected, as while the freezing point of pure glycerol is 17 °C, it has an extremely high capacity for supercooling, preventing freezing when there is no seeding[155]. In contrast, glycerol-based glue after water immersion froze at -10.2 °C (**Figure 5-1a**). While this is a lower freezing point than pure water, it is very similar to the freezing points of the sequential and pre-mixed gels: -9.0 °C and -8.6 °C, respectively (**Figure 5-1b-c**). A lowered freezing point is expected for gels, as the depression of freezing points in solvated polymer and gel systems is a well-known phenomenon[156].

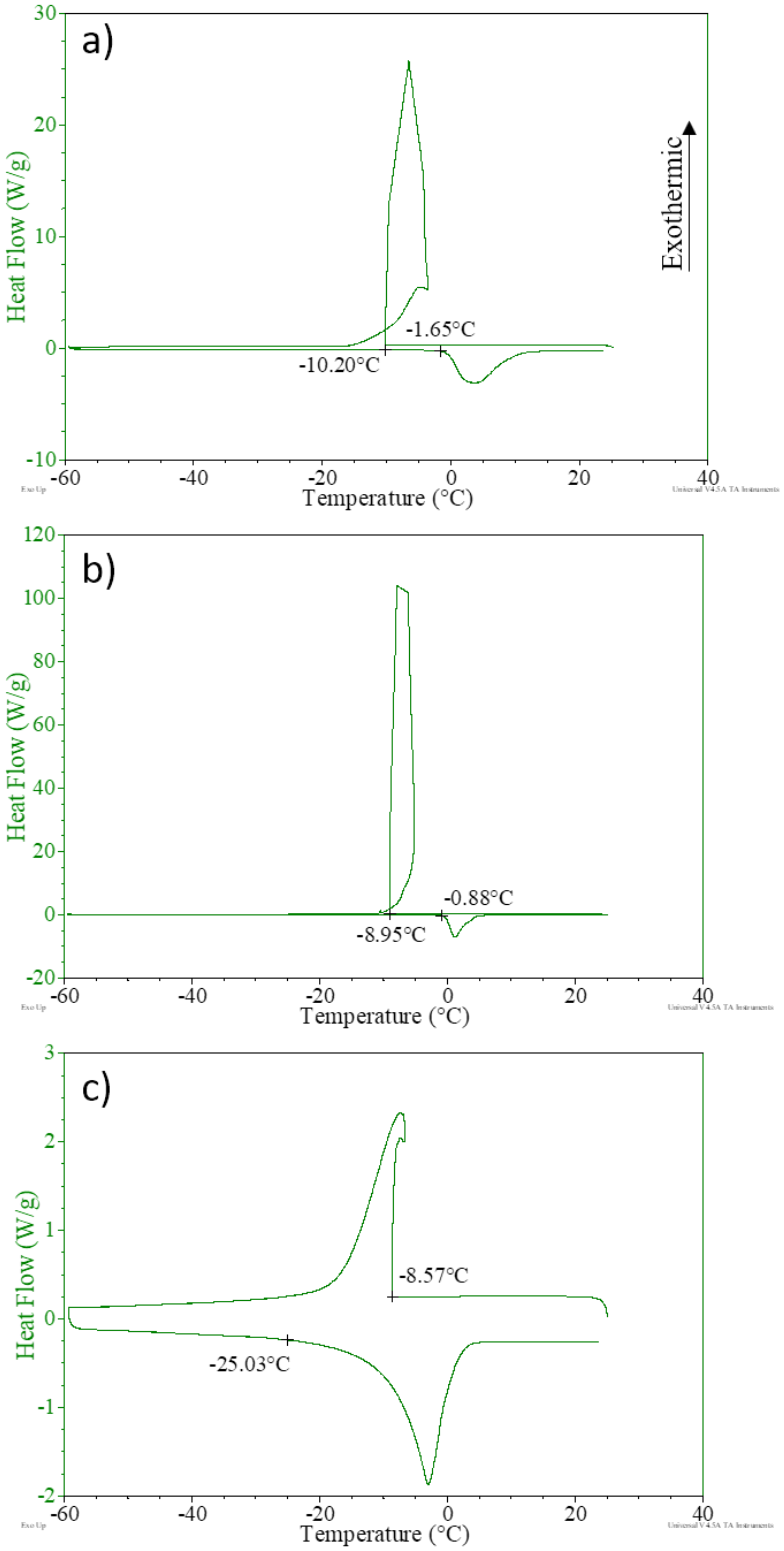

Figure 5-1. Preliminary differential scanning calorimetry curves for varying forms of algae-mussel glue; (a) glycerol-dispersed; (b) sequential application; and (c) pre-mixed application. Marked points indicate onset of freezing and melting peaks.

It is also important to note that melting of both the glycerol-based and sequential algae-mussel glues began at about -1 °C, which is very similar to water. In contrast, for the pre-mixed gel, melting begins at around -25 °C, which is a significantly lower temperature than its freezing peak. This could be explained by the forms that water can take inside hydrogels, which are based on interactions with the polymer network. In hydrogels, water can exist as non-freezable bound (where it interacts too strongly with the polymer to freeze), freezable bound (where it interacts strongly enough with the polymer to delay freezing), or non-bound (where its freezing behaviour is not significantly influenced by the polymer) forms[157]. The early melting point for the pre-mixed system is indicative of the presence of freezable bound water; however, since this is a single broad peak that stretches back to 0 °C, a broad continuum of melting peaks appears to be present. The other systems do not exhibit this behaviour, suggesting that for them, the majority of water may be present as free water.

Overall, the thermal behaviour of the glycerol-based algae-mussel glue suggests that the amount of glycerol remaining is too small to depress the freezing point. While there are likely interactions between the water and the gel, as indicated by the depressed freezing point, the melting point of water is not lowered in glycerol-based algae-mussel glue. Both of these behaviours are similar to the sequentially-applied algae-mussel glue, though pre-mixed algae-mussel glue displays a broader melting peak. These differences may result from different distributions of the components in the gel (as pre-mixed samples will partially gel before bonding).

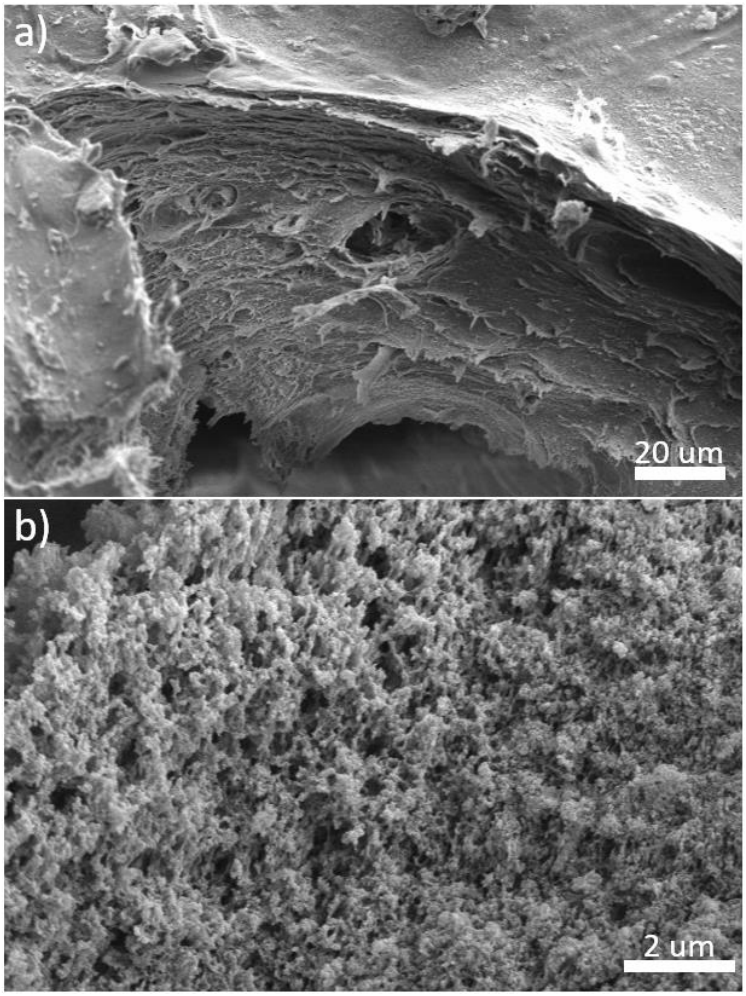

Figure 5-2. SEM images of glycerol-dispersed algae-mussel glue after immersion in water and freeze-drying. The images are from the (a) exterior and (b) interior portions of the bulk glue.

Along with characterizing the thermal behaviour, the structure of the one-part algae-mussel glue was investigated using SEM. The gel was cured by exposure to water, then freeze-dried for examination. Unlike the two-part algae-mussel glue from our prior work, the glycerol-based glue did not exhibit the formation of spherical structures. Instead, it appeared to possess a porous structure more similar to typical hydrogels. This could be seen in two forms, depending on the sample and the region. Some samples showed evidence of larger-scale (1-10 μm) collapsed pores that had formed into layered sheets (**Figure 5-2a**), while others still possessed smaller-scale (~100 nm) pore structures (**Figure 5-2b**). Chemical analysis using EDX confirmed that the gel was

comprised primarily of carbon and oxygen. Iron was also present, suggesting the crosslinking mechanism of algae-mussel glue was retained. Interestingly, the atomic carbon:oxygen ratio is lower in the glycerol-based glue (close to 2:1 carbon:oxygen). This is in between the atomic ratios for dopamine (4:1 carbon:oxygen) and alginate (1:1 carbon:oxygen), indicating that both of these components are still present in the final gel. As such, while using glycerol to disperse the components may affect the final structure of the algae-mussel glue, it retains all of the components that are important for providing both adhesion and cohesion.

5.3.3 Adhesion testing

In order to investigate the adhesive strength of the one-part algae-mussel glue, two types of adhesion tests were carried out. For tensile adhesion tests, aluminum stubs were glued to glass slides with algae-mussel glue, left overnight to set, then pulled directly away from the glass. For 0° peel tests (shear tests), nylon fabric was glued to a glass slide, left overnight to set, then pulled away in a direction parallel to the slide. These tests were carried out with a number of different formulations of algae-mussel glue, obtained by varying the concentrations of each component. Each formulation was noted by a series of four numbers: A-D-F-T, denoting the weight percents in glycerol of alginate (A), dopamine (D), ferric sulfate (F), and Tris (T), respectively. Several conclusions can be drawn from these tests, the results of which can be seen in **Figure 5-3**. One point of interest is the difference in trends between the tensile and shear adhesive tests for specific formulations, namely 5-5-5-8, 5-5-3-5, 5-3-3-3, and 5(MV)-5-5-5. Relative to the change in tensile adhesion for these formulations, the shear adhesion is markedly reduced (whereas for 5-5-8-8 and 5-3-5-5 shear adhesion is distinctly improved relative to the change in tensile adhesion). A clue towards explaining this behaviour comes from observations made during shear testing; for the above formulations with low relative shear adhesion, the gel appeared to suffer from cohesive

failure. Not only were there pieces of gel on both the glass slide and nylon fabric in these samples, but the gel appeared to be far less solid than for other samples. This suggests that for these formulations, the gel is much weaker cohesively than it is in other samples, with the tensile tests still probing adhesive behaviour, resulting in the discrepancy between the tests. For 5-5-5-8, this implies that too much Tris can interfere with the cohesion of the gel, perhaps through raising pH upon exposure to water, which might reduce the availability of Fe^{3+} ions. Lower amounts of Fe^{3+} ions relative to alginate polymer in 5-5-3-5 and 5-3-3-3 could explain why these form weaker gels. Finally, 5(MV)-5-5-5 uses a different source of alginate, which may have fewer or shorter G-blocks, leaving fewer sites for crosslinking of the gel network.

The results in **Figure 5-3** can also be used to evaluate the formulations against each other and against the algae-mussel glue described in Chapter 4. When determining the optimum formulation, both tensile and shear adhesive strengths had to be considered. This is particularly important for formulations like 5-3-3-5, which appeared to offer some gain in tensile adhesive strength, but significantly reduced shear adhesive strength. 5-5-5-5 and 5-5-8-8 appeared to offer the best overall performance, with 5-5-5-5 exhibiting lower variance and 5-5-8-8 showing higher shear adhesive force. These two formulations had similar tensile adhesive strength, and comparing with the adhesion of the sequential algae-mussel glue, the one-part adhesive in glycerol achieved about 37% of the performance. While this is a large decrease, it is still more than a 25 times improvement over the adhesion of catechol-modified alginate. Of particular interest, since this is a one-part mixture, the glycerol-dispersed glue showed double the adhesive strength of the pre-mixed version of algae-mussel glue. It also demonstrated far superior stability compared to either non-glycerol algae-mussel glue, both of which gelled rapidly when components were combined.

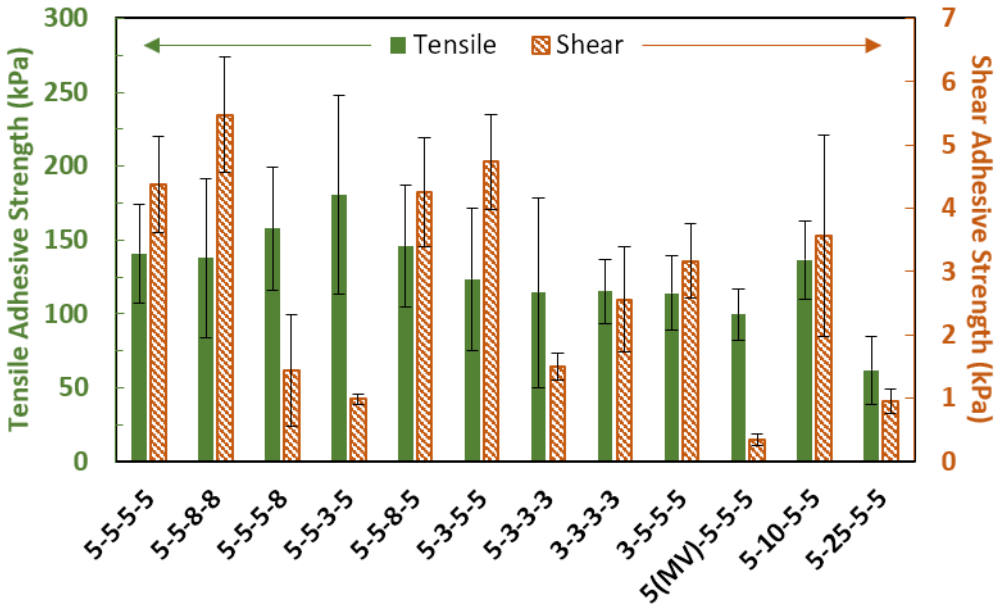

Figure 5-3. Tensile (solid green) and shear (dashed orange) adhesive strength values for algae-mussel glue in glycerol with varying compositions, each applied between an aluminum stub and glass slide in DI water and kept immersed overnight before testing. Samples are denoted as A-D-F-T, for the weight percent (compared to the mass of glycerol) of the alginate (A), dopamine (D), ferric sulfate (F), and Tris powder (T) components, respectively. Note that 5(MV) refers 5 wt% of alginate from a different source (medium viscosity alginate from Sigma-Aldrich).

While dispersion of A-D-F-T components in glycerol greatly delayed the reactions the components undergo in water – particularly the gelation of alginate by Fe^{3+} ions and the oxidation of dopamine, accelerated by high pH due to Tris – it did not prevent them entirely. While the mixture could last overnight without gelling, gelation would still occur after more than a day. This was suspected to be due to the iron (III) sulfate; while its low solubility in glycerol would greatly retard the release of Fe^{3+} ions, enough could eventually be released to gel the alginate. While the timescale of gelation was much improved by the one-part method, a two-part formulation was developed to fully resolve gelation and oxidation issues. Instead of all the components being dispersed together in the same glycerol mixture, alginate and dopamine were dispersed in glycerol to form part one (1) of the adhesive, while ferric sulfate and Tris were dispersed together in glycerol to form part two (2). This kept apart the pairs that were interacting too soon (alginate and

ferric sulfate as one pair, and dopamine and Tris as the second pair), greatly extending the lifespan of the adhesive.

The goal of this two-part adhesive was to be able to extrude the components in glycerol out of a two-part syringe through a mixing nozzle directly onto the adherends, then joining them underwater. However, this plan had two setbacks. Firstly, the nature of a two-part syringe is that equal volumes of mixtures are pushed out of the two barrels; when mixed together, this would result in an overall 2 times dilution of the components compared to their concentration in each barrel. Due to limitations on the solubility of alginate, the formulation used was 5-5-5-5 in the two barrels (5-5 A-D in the first, and 5-5 F-T in the second), resulting in an overall adhesive formulation of 2.5-2.5-2.5-2.5. Secondly, there was a large difference in viscosity between the two mixtures, with A-D dispersed in glycerol possessing much higher viscosity than F-T dispersed in glycerol. This negatively impacted the mixing of the two components – indeed, a short-length mixing nozzle (35 mm) was insufficient for mixing parts (1) and (2). Tensile adhesive measurements were performed using the two-part formulation. When applied to the adherends directly from the mixing nozzle of the two-part syringe, adhesion was particularly weak, about 65% that of the 3-3-3-3 one-part formulation (which possesses the closest concentrations of components). However, when parts (1) and (2) were further mixed after extrusion, then applied to the adherends, tensile adhesive strength was almost identical to that of 3-3-3-3 (115.24 ± 21.89 kPa for 3-3-3-3 and 116.29 ± 28.54 kPa for 2.5-2.5-2.5-2.5). These results confirm that the two-part formulation can perform similarly its one-part equivalent, but mixing issues negatively impact its usability and adhesive strength. As an alternative form of mixing, two separate syringes could be used; a syringe connector could allow for straightforward and thorough mixing of the components. This was demonstrated by mixing together separate alginate-dopamine-glycerol and

ferric sulfate-Tris-glycerol components within two syringes. The resulting mixtures was used to bond and lift a 96 g aluminum metal block underwater, as shown in **Figure 5-4**.

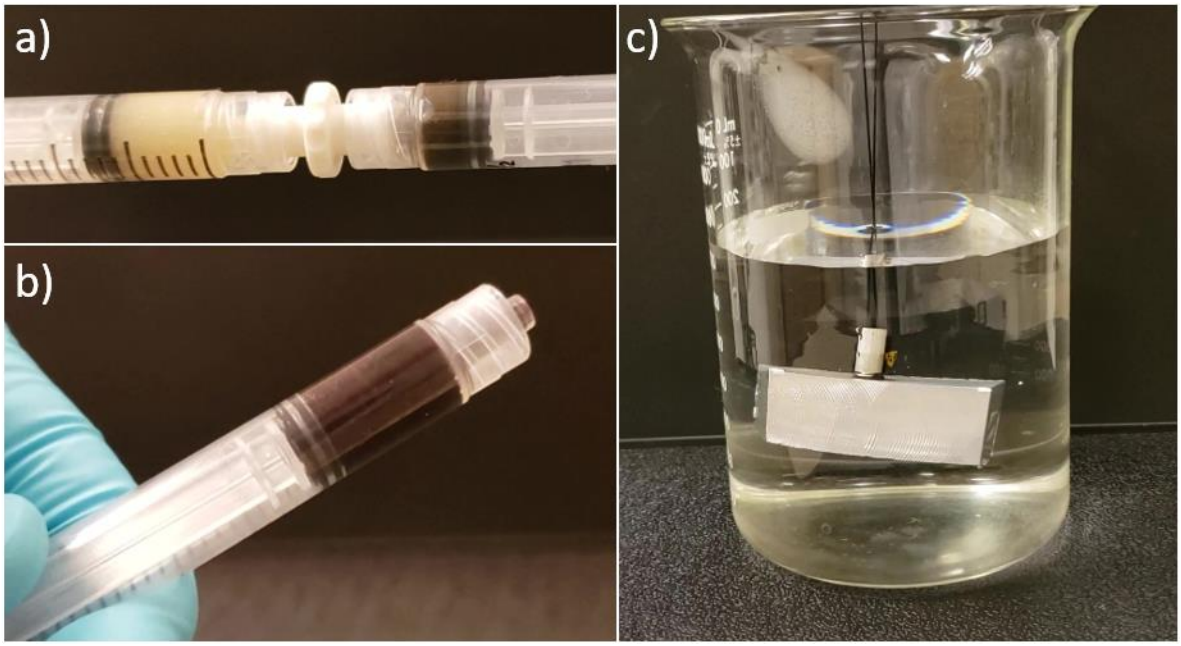

Figure 5-4. Demonstration of two-syringe mixing of glycerol-dispersed algae-mussel glue showing (a) the alginate-dopamine and ferric sulfate-Tris dispersions in glycerol in the left and right syringes, respectively; (b) the combined dispersion after mixing; and (c) the glue holding up a (96 g) block of aluminum metal after being applied underwater.

5.4 Conclusions

In this chapter, we demonstrated the ability to improve stability and usability of algae-mussel glue. By dispersing components in glycerol, we greatly delayed interactions between them, resulting in a one-part underwater adhesive. We also developed a two-part adhesive that was significantly more stable; dispersion of the components meant that it could be mixed without immediately curing, making it simpler to handle. After immersion in water, the glue forms a nanoporous gel containing all the components; glycerol's high miscibility with water also allows for it to successfully exchange with the medium for bonding. This results in an underwater adhesive that is itself water-activated, allowing for stability and ease of use.

Chapter 6 Concluding Remarks and Recommendations

6.1 Summary of Contributions and Concluding Remarks

The main objective of this thesis research was to explore underwater adhesion, in particular, to take inspirations from the adhesive strategies of two sessile marine organisms: benthic brown algae and marine mussels, focusing on the studies of alginate-based hydrogel adhesive systems. The chemistry of both mussels and algae play an important role in their ability to adhere to surfaces – the catechol group at the interface is primarily responsible for mussel adhesion, while alginate utilizes polyphenol groups for its adhesion, and ionically crosslinked polysaccharide to provide cohesion. More recently, it has been emphasized that another key facet of the adhesive strategies of many marine organisms is the processes they use to form their structure and deposit adhesive components. As such, three research steps were undertaken to develop a synthetic adhesive based on these concepts, summarized in the following sections:

6.1.1 Underwater contact behaviour of catechol-conjugated alginate

In an effort to introduce mussel adhesive chemistry to alginate hydrogels, catechol functionality was covalently attached to alginate backbone utilizing carbodiimide coupling. Adhesive and mechanical testing was performed using indentation testing, where the probes were hydrogel beads formed from neat or modified alginate, each crosslinked with Ca^{2+}. Adhesion was improved to soft, organic surfaces like gelatin, including animal tissue. However, adhesion was reduced when the beads were indented on rigid inorganic surfaces, such as glass or gold. It was observed that catechol modification had a significant effect on the elastic modulus of the hydrogel, which could be responsible for the reduced adhesion on rigid surfaces. This was further supported through indentation on polyacrylamide substrates of varying stiffness. This work developed a novel technique for using hydrogel beads as a probe for indentation testing, broadening the range

of substrates for investigation of hydrogels' contact behaviour. Additionally, this work highlighted both the strengths and shortcomings of chemical modification of polymer gels, particularly in how secondary properties of the gel can be affected.

6.1.2 Algae-Mussel-Inspired Hydrogel Composite Adhesive

After incorporating mussel chemistry into algae polymer backbone, we sought to better mimic both the processes and chemistries of mussel and algae adhesion. To do so, we developed an underwater glue with structure, chemistry, and deposition process inspired by these two marine organisms. Adhesive and cohesive components were initially separate and liquid when deposited, to spread over the surface; this initial adhesive then crosslinked through ferric ions to form the final gel form of the glue. Additionally, adhesive components were deposited primarily at the surface of the adherends, mimicking mussel protein distribution and helping to ensure adhesion was present where it was needed. Using this sequential application technique resulted in a glue that demonstrated strong underwater adhesion, without requiring chemical modification of the polymer. This work highlighted the importance of looking at the processes used in adhesion in nature, and demonstrated that chemical modification is not required to utilize catechol adhesion.

6.1.3 Development of Algae-Mussel-Inspired One-Part Adhesive towards Practical Applications

After fabricating and investigating our algae-mussel-inspired glue, we sought to further improve its practicality by developing a one- or two-part adhesive that would be easy to use. One key aspect we aimed to improve upon was the stability of the system; to accomplish this, we utilized dispersion instead of dissolution for the various glue components. This required a change in both the solvent (glycerol instead of water) and the source of ferric ions (anhydrous iron (III) sulfate replacing iron (III) nitrate). Using these dispersed components, we developed two separate

formulations: a one-part glue for ease-of-use, and a two-part glue for maximizing stability and longevity. Due to the choice of solvent and other components, these glues are water-activated, further improving practicality of underwater adhesion. The resulting glues exhibited good adhesion (somewhat reduced from sequential application, but more practical in usage), even when bonding was performed underwater. Additionally, the simple application process was demonstrated, mixing between two syringes and applying to a metal weight to lift it underwater. This work highlights the importance of dispersion vs. dissolution and when one might be more desirable over the other. It also offers new insight into techniques for dispersing components that are difficult to initially mix.

6.2 Recommendations and Future Work

The research reported in this thesis has demonstrated the successful union of dual inspirations of mussel and algae adhesion into an underwater adhesive. However, some aspects of the system have yet to be fully examined. Exploring these topics would advance the usability of this adhesive system, as well as providing a deeper understanding of bioinspired adhesion and hydrogels as a whole.

(1) The algae-mussel glue is well-suited to bonding applications that occur entirely underwater. This should lend it well towards biomedical applications such as for tissue adhesives and sealants; however, to be used in these applications, the potential toxicity of the glue and its components needs to be fully understood. Studies of cell viability when exposed to the algae-mussel glue would provide an initial evaluation of the glue's toxicity. This could be accomplished through in vitro toxicity studies[158]. To further investigate the safety of the glue, these tests could be extended to include in vivo testing in mice or rabbits[159].

(2) Initial results from tensile holding tests probing viscoelastic behaviour suggested that the algae-mussel glue had some ability to regain strength under constant strain. While this is not conclusive evidence of self-healing behaviour, it is reminiscent of re-forming noncovalent bonds; this is supported by the knowledge that coordination bonds formed between catechol groups and ferric ions can lead to self-healing behaviour[160]. This potential should be further investigated, such as by cutting and attempting to rejoin the gel, or by bringing adherends back in contact after tensile adhesive testing. This could be further extended by a study of when self-healing might occur by modifying environmental conditions.

(3) It was observed under SEM that the algae-mussel glue possessed micron-scale spherical structures, with EDX analysis identifying them as composed primarily of polydopamine. However, the origin of these structures is unclear, as is their potential contribution to the mechanical and adhesive properties of the gel. Additionally, they are not present in the glycerol-dispersed algae-mussel glue, which may play a part in any differences between the systems. Structure plays an important role in the strength of adhesive systems, as evidenced by the mussel plaque and its own porous structure[67]. As such, learning more about the structure of the algae-mussel glue could provide insight into improving its strength, as well as leading to greater understanding of the effects of structure in adhesives.

(4) Finally, while glycerol has been used to disperse the components of the algae-mussel glue, it would be useful to further study its interactions with these components. This could provide fundamental insight into the properties of dispersions and the interactions of molecules like dopamine. In additional, it could provide new ideas for how to best

keep components separate within the system before delivery, extending the shelf-life and usability of the glue.

References

1. Tarakhovskaya, E. R. Mechanisms of bioadhesion of macrophytic algae. *Russ. J. Plant Physiol.* **61**, 19–25 (2014).

2. Zhao, W., Jin, X., Cong, Y., Liu, Y. & Fu, J. Degradable natural polymer hydrogels for articular cartilage tissue engineering. *J. Chem. Technol. Biotechnol.* **88**, 327–339 (2013).

3. Ahmed, E. M. Hydrogel: Preparation, characterization, and applications: A review. *J. Adv. Res.* **6**, 105–121 (2015).

4. Hoffman, A. S. Hydrogels for biomedical applications. *Adv. Drug Deliv. Rev.* **64**, 18–23 (2012).

5. Dragan, E. S. Design and applications of interpenetrating polymer network hydrogels. A review. *Chem. Eng. J.* **243**, 572–590 (2014).

6. Shen, C., Shen, Y., Wen, Y., Wang, H. & Liu, W. Fast and highly efficient removal of dyes under alkaline conditions using magnetic chitosan-Fe(III) hydrogel. *Water Res.* **45**, 5200–5210 (2011).

7. Mohammed, N., Grishkewich, N., Berry, R. M. & Tam, K. C. Cellulose nanocrystal–alginate hydrogel beads as novel adsorbents for organic dyes in aqueous solutions. *Cellulose* **22**, 3725–3738 (2015).

8. Omidian, H., Rocca, J. G. & Park, K. Advances in superporous hydrogels. *J. Control. Release* **102**, 3–12 (2005).

9. Caló, E. & Khutoryanskiy, V. V. Biomedical applications of hydrogels: A review of patents

and commercial products. *Eur. Polym. J.* **65**, 252–267 (2015).

10. Li, J. & Mooney, D. J. Designing hydrogels for controlled drug delivery. *Nat. Rev. Mater.* **1**, 16071 (2016).

11. Wang, X. *et al.* Metal–Organic Coordination-Enabled Layer-by-Layer Self-Assembly to Prepare Hybrid Microcapsules for Efficient Enzyme Immobilization. *ACS Appl. Mater. Interfaces* **4**, 3476–3483 (2012).

12. Paul, W., Paul, W. & Sharma, C. P. Chitosan and Alginate Wound Dressings : A Short Review. 17–23 (2016).

13. Balakrishnan, B., Jayakrishnan, a., Kumar, S. S. P. & Nandkumar, a. M. Anti-bacterial properties of an in situ forming hydrogel based on oxidized alginate and gelatin loaded with gentamycin. *Trends Biomater. Artif. Organs* **26**, 139–145 (2012).

14. Suzuki, Y. *et al.* Evaluation of a novel alginate gel dressing: Cytotoxicity to fibroblasts in vitro and foreign-body reaction in pig skin in vivo. *J. Biomed. Mater. Res.* **39**, 317–322 (1998).

15. Maulvi, F. A. *et al.* In vitro and in vivo evaluation of novel implantation technology in hydrogel contact lenses for controlled drug delivery. *J. Control. Release* **226**, 47–56 (2016).

16. Stapleton, F., Stretton, S., Papas, E., Skotnitsky, C. & Sweeney, D. F. Silicone Hydrogel Contact Lenses and the Ocular Surface. *Ocul. Surf.* **4**, 24–43 (2006).

17. Van Vlierberghe, S., Dubruel, P. & Schacht, E. Biopolymer-based hydrogels as scaffolds for tissue engineering applications: A review. *Biomacromolecules* **12**, 1387–1408 (2011).

18. Lee, C. *et al.* Bioinspired, calcium-free alginate hydrogels with tunable physical and

mechanical properties and improved biocompatibility. *Biomacromolecules* **14**, 2004–13 (2013).

19. Honda, M., Kataoka, K., Seki, T. & Takeoka, Y. Confined Stimuli-Responsive Polymer Gel in Inverse Opal Polymer Membrane for Colorimetric Glucose Sensor. *Langmuir* **25**, 8349–8356 (2009).

20. Gopishetty, V., Tokarev, I. & Minko, S. Biocompatible stimuli-responsive hydrogel porous membranes via phase separation of a polyvinyl alcohol and Na-alginate intermolecular complex. *J. Mater. Chem.* **22**, 19482 (2012).

21. Chan, A. W., Whitney, R. a. & Neufeld, R. J. Semisynthesis of a controlled stimuli-responsive alginate hydrogel. *Biomacromolecules* **10**, 609–616 (2009).

22. Gao, G., Du, G., Sun, Y. & Fu, J. Self-Healable, Tough, and Ultrastretchable Nanocomposite Hydrogels Based on Reversible Polyacrylamide/Montmorillonite Adsorption. *ACS Appl. Mater. Interfaces* **7**, 5029–5037 (2015).

23. Wang, W., Zhang, Y. & Liu, W. Bioinspired fabrication of high strength hydrogels from non-covalent interactions. *Prog. Polym. Sci.* **71**, 1–25 (2017).

24. Han, L. *et al.* Tough, self-healable and tissue-adhesive hydrogel with tunable multifunctionality. *NPG Asia Mater.* **9**, e372–e372 (2017).

25. Mizrahi, B. *et al.* A stiff injectable biodegradable elastomer. *Adv. Funct. Mater.* **23**, 1527–1533 (2013).

26. Mehdizadeh, M., Weng, H., Gyawali, D., Tang, L. & Yang, J. Injectable citrate-based mussel-inspired tissue bioadhesives with high wet strength for sutureless wound closure.

Biomaterials **33**, 7972–83 (2012).

27. Balakrishnan, B. & Jayakrishnan, a. Self-cross-linking biopolymers as injectable in situ forming biodegradable scaffolds. *Biomaterials* **26**, 3941–3951 (2005).

28. Ryu, J. H. *et al.* Catechol-functionalized chitosan/pluronic hydrogels for tissue adhesives and hemostatic materials. *Biomacromolecules* **12**, 2653–2659 (2011).

29. Lee, Y. *et al.* Thermo-sensitive, injectable, and tissue adhesive sol–gel transition hyaluronic acid/pluronic composite hydrogels prepared from bio-inspired catechol-thiol reaction. *Soft Matter* **6**, 977 (2010).

30. Kastrup, C. J. *et al.* Painting blood vessels and atherosclerotic plaques with an adhesive drug depot. *Proc. Natl. Acad. Sci.* **109**, 21444–21449 (2012).

31. Masuelli, M. A. & Illanes, C. O. Review of the characterization of sodium alginate by intrinsic viscosity measurements . Comparative analysis between conventional and single point methods. **1**, 1–11 (2014).

32. Sun, J.-Y. *et al.* Highly stretchable and tough hydrogels. *Nature* **489**, 133–136 (2012).

33. O, S. & G., S.-B. Alginate as immoblization matrix for cells. *Trends Biotech* **8**, 71–78 (1990).

34. Drury, J. L., Dennis, R. G. & Mooney, D. J. The tensile properties of alginate hydrogels. *Biomaterials* **25**, 3187–3199 (2004).

35. Grant, G. T., Morris, E. R., Rees, D. A., Smith, P. J. C. & Thom, D. Biological interactions between polysaccharides and divalent cations: The egg-box model. *FEBS Lett.* **32**, 195–198 (1973).

36. Stokke, B. T. *et al.* Small-Angle X-ray Scattering and Rheological Characterization of Alginate Gels. 1. Ca−Alginate Gels. *Macromolecules* **33**, 1853–1863 (2000).

37. Webber, R. E. & Shull, K. R. Strain Dependence of the Viscoelastic Properties of Alginate Hydrogels. *Macromolecules* **37**, 6153–6160 (2004).

38. Kong, H. J., Wong, E. & Mooney, D. J. Independent Control of Rigidity and Toughness of Polymeric Hydrogels. *Macromolecules* **36**, 4582–4588 (2003).

39. Jackson, G., Roberts, R. T. & Wainwright, T. MECHANISM OF BEER FOAM STABILIZATION BY PROPYLENE GLYCOL ALGINATE. *J. Inst. Brew.* **86**, 34–37 (1980).

40. Qin, Y., Jiang, J., Zhao, L., Zhang, J. & Wang, F. Applications of Alginate as a Functional Food Ingredient. in *Biopolymers for Food Design* 409–429 (Elsevier, 2018). doi:10.1016/B978-0-12-811449-0.00013-X

41. Mancini, F., Montanari, L., Peressini, D. & Fantozzi, P. Influence of Alginate Concentration and Molecular Weight on Functional Properties of Mayonnaise. *LWT - Food Sci. Technol.* **35**, 517–525 (2002).

42. Nedović, V. A. *et al.* Electrostatic generation of alginate microbeads loaded with brewing yeast. *Process Biochem.* **37**, 17–22 (2001).

43. Sultana, K. *et al.* Encapsulation of probiotic bacteria with alginate–starch and evaluation of survival in simulated gastrointestinal conditions and in yoghurt. *Int. J. Food Microbiol.* **62**, 47–55 (2000).

44. Mazutis, L., Vasiliauskas, R. & Weitz, D. A. Microfluidic Production of Alginate Hydrogel

Particles for Antibody Encapsulation and Release. *Macromol. Biosci.* **15**, 1641–1646 (2015).

45. George, M. & Abraham, T. E. Polyionic hydrocolloids for the intestinal delivery of protein drugs: Alginate and chitosan - a review. *J. Control. Release* **114**, 1–14 (2006).

46. Ågren, M. S. Four alginate dressings in the treatment of partial thickness wounds: A comparative experimental study. *Br. J. Plast. Surg.* **49**, 129–134 (1996).

47. Hanna, J. R. & Giacopelli, J. A. A review of wound healing and wound dressing products. *J. Foot Ankle Surg.* **36**, 2–14 (1997).

48. McCullagh, A., Sweet, C. & Ashley, M. Making a Good Impression (A 'How to' Paper on Dental Alginate). *Dent. Update* **32**, 169–175 (2005).

49. Al-Shamkhani, A. & Duncan, R. Radioiodination of Alginate via Covalently-Bound Tyrosinamide Allows Monitoring of its Fate In Vivo. *J. Bioact. Compat. Polym.* **10**, 4–13 (1995).

50. PARK, H. & LEE, K.-Y. Alginate hydrogels as matrices for tissue engineering. in *Natural-Based Polymers for Biomedical Applications* 515–532 (Elsevier, 2008). doi:10.1533/9781845694814.4.515

51. Augst, A. D., Kong, H. J. & Mooney, D. J. Alginate Hydrogels as Biomaterials. *Macromol. Biosci.* **6**, 623–633 (2006).

52. Lee, K. Y., Bouhadir, K. H. & Mooney, D. J. Degradation Behavior of Covalently Cross-Linked Poly(aldehyde guluronate) Hydrogels. *Macromolecules* **33**, 97–101 (2000).

53. Lansdown, A. B. & Payne, M. J. An evaluation of the local reaction and biodegradation of

calcium sodium alginate (Kaltostat) following subcutaneous implantation in the rat. *J. R. Coll. Surg. Edinb.* **39**, 284–8 (1994).

54. Rowley, J. A., Madlambayan, G. & Mooney, D. J. Alginate hydrogels as synthetic extracellular matrix materials. *Biomaterials* **20**, 45–53 (1999).

55. Ruoslahti, E. RGD AND OTHER RECOGNITION SEQUENCES FOR INTEGRINS. *Annu. Rev. Cell Dev. Biol.* **12**, 697–715 (1996).

56. Shull, K. R., Ahn, D., Chen, W.-L., Flanigan, C. M. & Crosby, A. J. Axisymmetric adhesion tests of soft materials. *Macromol. Chem. Phys.* **199**, 489–511 (1998).

57. Boesel, L. F., Greiner, C., Arzt, E. & del Campo, A. Gecko-Inspired Surfaces: A Path to Strong and Reversible Dry Adhesives. *Adv. Mater.* **22**, 2125–2137 (2010).

58. Zhou, M., Pesika, N., Zeng, H., Tian, Y. & Israelachvili, J. Recent advances in gecko adhesion and friction mechanisms and development of gecko-inspired dry adhesive surfaces. *Friction* **1**, 114–129 (2013).

59. Israelachvili, J. N. *Intermolecular and Surface Forces*. (Academic Press, 2011). doi:10.1016/C2009-0-21560-1

60. Yu, J. *et al.* Adaptive hydrophobic and hydrophilic interactions of mussel foot proteins with organic thin films. *Proc. Natl. Acad. Sci.* **110**, 15680–15685 (2013).

61. Yuk, H., Zhang, T., Lin, S., Parada, G. A. & Zhao, X. Tough bonding of hydrogels to diverse non-porous surfaces. *Nat. Mater.* **15**, 190–196 (2015).

62. Holten-Andersen, N. *et al.* pH-induced metal-ligand cross-links inspired by mussel yield self-healing polymer networks with near-covalent elastic moduli. *Proc. Natl. Acad. Sci.* **108**,

2651–2655 (2011).

63. Hu, Y. *et al.* Dual Physically Cross-Linked Hydrogels with High Stretchability, Toughness, and Good Self-Recoverability. *Macromolecules* **49**, 5660–5668 (2016).

64. Lee, H., Scherer, N. F. & Messersmith, P. B. Single-molecule mechanics of mussel adhesion. *Proc. Natl. Acad. Sci. U. S. A.* **103**, 12999–3003 (2006).

65. Saiz-Poseu, J., Mancebo-Aracil, J., Nador, F., Busqué, F. & Ruiz-Molina, D. The Chemistry behind Catechol-Based Adhesion. *Angew. Chemie Int. Ed.* **58**, 696–714 (2019).

66. Hofman, A. H., van Hees, I. A., Yang, J. & Kamperman, M. Bioinspired Underwater Adhesives by Using the Supramolecular Toolbox. *Adv. Mater.* **30**, 1704640 (2018).

67. Waite, J. H. Mussel adhesion – essential footwork. *J. Exp. Biol.* **220**, 517–530 (2017).

68. Yu, J. *et al.* Mussel protein adhesion depends on interprotein thiol-mediated redox modulation. *Nat. Chem. Biol.* **7**, 588–590 (2011).

69. Hable, W. E. & Kropf, D. L. Roles of secretion and the cytoskeleton in cell adhesion and polarity establishment in Pelvetia compressa zygotes. *Dev. Biol.* **198**, 45–56 (1998).

70. Vreeland, V., Waite, J. H. & Epstein, L. MINIREVIEW-POLYPHENOLS AND OXIDASES IN SUBSTRATUM ADHESION BY MARINE ALGAE AND MUSSELS. *J. Phycol.* **34**, 1–8 (1998).

71. Pomin, V. H. & Mourao, P. A. S. Structure, biology, evolution, and medical importance of sulfated fucans and galactans. *Glycobiology* **18**, 1016–1027 (2008).

72. Martinez Rodriguez, N. R., Das, S., Kaufman, Y., Israelachvili, J. N. & Waite, J. H. Interfacial pH during mussel adhesive plaque formation. *Biofouling* **31**, 221–227 (2015).

73. Faure, E. *et al*. Catechols as versatile platforms in polymer chemistry. *Prog. Polym. Sci.* **38**, 236–270 (2013).

74. Wise, R. a. Dopamine, learning and motivation. *Nat. Rev. Neurosci.* **5**, 483–494 (2004).

75. Waite, J. H. & Qin, X. Polyphosphoprotein from the adhesive pads of Mytilus edulis. *Biochemistry* **40**, 2887–2893 (2001).

76. Lee, H., Dellatore, S. M., Miller, W. M. & Messersmith, P. B. Mussel-Inspired Surface Chemistry for Multifunctional Coatings. *Science (80-.).* **318**, 426–430 (2007).

77. Kim, S. & Park, C. B. Dopamine-Induced Mineralization of Calcium Carbonate Vaterite Microspheres. *Langmuir* **26**, 14730–14736 (2010).

78. Pop-Georgievski, O. *et al.* Poly(ethylene oxide) Layers Grafted to Dopamine-melanin Anchoring Layer: Stability and Resistance to Protein Adsorption. *Biomacromolecules* **12**, 3232–3242 (2011).

79. Zhu, L.-P., Jiang, J.-H., Zhu, B.-K. & Xu, Y.-Y. Immobilization of bovine serum albumin onto porous polyethylene membranes using strongly attached polydopamine as a spacer. *Colloids Surfaces B Biointerfaces* **86**, 111–118 (2011).

80. Lee, B. P. Biomimetic Compounds and Synthetic Methods Therefor. (2011).

81. Lee, B. P., Huang, K., Nunalee, F. N., Shull, K. R. & Messersmith, P. B. Synthesis of 3,4-dihydroxyphenylalanine (DOPA) containing monomers and their co-polymerization with PEG-diacrylate to form hydrogels. *J. Biomater. Sci. Polym. Ed.* **15**, 449–464 (2004).

82. Lee, H., Lee, B. P. & Messersmith, P. B. A reversible wet/dry adhesive inspired by mussels and geckos. *Nature* **448**, 338–341 (2007).

83. Lee, B. P., Messersmith, P. B., Israelachvili, J. N. & Waite, J. H. Mussel-Inspired Adhesives and Coatings. *Annu. Rev. Mater. Res.* **41**, 99–132 (2011).

84. Marumo, K. & Waite, J. H. Optimization of hydroxylation of tyrosine and tyrosine-containing peptides by mushroom tyrosinase. *Biochim. Biophys. Acta* **872**, 98–103 (1986).

85. You, I., Kang, S. M., Byun, Y. & Lee, H. Enhancement of blood compatibility of poly(urethane) substrates by mussel-inspired adhesive heparin coating. *Bioconjug. Chem.* **22**, 1264–9 (2011).

86. Ma, L. *et al.* Mussel-inspired self-coating at macro-interface with improved biocompatibility and bioactivity via dopamine grafted heparin-like polymers and heparin. *J. Mater. Chem. B* **2**, 363 (2014).

87. Fischer, M. J. E. Amine Coupling Through EDC/NHS: A Practical Approach. in *Methods in molecular biology (Clifton, N.J.)* **627**, 55–73 (2010).

88. Bitton, R. & Bianco-Peled, H. Novel Biomimetic Adhesives Based on Algae Glue. *Macromol. Biosci.* **8**, 393–400 (2008).

89. McInnes, A. G., Ragan, M. A., Smith, D. G. & Walter, J. A. The high molecular weight polyphloroglucinols of the marine brown alga Fucus vesiculosus L. 1 H and 13 C nuclear magnetic resonance spectroscopy. *Can. J. Chem.* **63**, 304–313 (1985).

90. Rozen, Y. & Bianco-Peled, H. Studies of Phenol-Based Bioinspired Sealants. *J. Adhes.* **90**, 667–681 (2014).

91. Bitton, R. *et al.* The Influence of Halide-Mediated Oxidation on Algae-Born Adhesives. *Macromol. Biosci.* **7**, 1280–1289 (2007).

92. Bitton, R. *et al.* Phloroglucinol-based biomimetic adhesives for medical applications. *Acta Biomater.* **5**, 1582–1587 (2009).

93. Arunbabu, D., Shahsavan, H., Zhang, W. & Zhao, B. Poly(AAc- co -MBA) Hydrogel Films: Adhesive and Mechanical Properties in Aqueous Medium. *J. Phys. Chem. B* **117**, 441–449 (2013).

94. Jo, S. & Sohn, J. Biomimetic Adhesive Materials Containing Cyanoacryl Group for Medical Application. *Molecules* **19**, 16779–16793 (2014).

95. Zhang, W. *et al.* Surface and tribological behaviors of the bioinspired polydopamine thin films under dry and wet conditions. *Biomacromolecules* **14**, 394–405 (2013).

96. Lakhera, N. *et al.* Adhesion behavior of polymer networks with tailored mechanical properties using spherical and flat contacts. *MRS Commun.* **3**, 73–77 (2013).

97. Johnson, K. L. & Greenwood, J. A. Adhesive Contact of Elastic Bodies: The JKR Theory. in *Encyclopedia of Tribology* (eds. Wang, Q. J. & Chung, Y.-W.) 42–49 (Springer US, 2013). doi:10.1007/978-0-387-92897-5_1086

98. Johnson, K. L., Kendall, K. & Roberts, A. D. Surface Energy and the Contact of Elastic Solids. *Proc. R. Soc. A Math. Phys. Eng. Sci.* **324**, 301–313 (1971).

99. Kendall, K. The adhesion and surface energy of elastic solids. *J. Phys. D. Appl. Phys.* **4**, 320 (1971).

100. Zhang, F., Liu, S., Zhang, Y., Wei, Y. & Xu, J. Underwater bonding strength of marine mussel-inspired polymers containing DOPA-like units with amino groups. *RSC Adv.* **2**, 8919 (2012).

101. Pocius, A. V. *Adhesion and adhesives technology : an introduction*. (Hanser).

102. Goodhew, P. J., Humphreys, J. & Beanland, R. *Electron Microscopy and Analysis, Third Edition*. (Taylor & Francis, 2000).

103. Tsiper, S. *et al.* Sparsity-Based Super Resolution for SEM Images. *Nano Lett.* **17**, 5437–5445 (2017).

104. Stokes, D. J. *Principles and Practice of Variable Pressure/Environmental Scanning Electron Microscopy (VP-ESEM)*. (John Wiley & Sons, Ltd, 2008). doi:10.1002/9780470758731

105. Podor, R., Bouala, G. I. N., Ravaux, J., Lautru, J. & Clavier, N. Working with the ESEM at high temperature. *Mater. Charact.* **151**, 15–26 (2019).

106. Prutton, M. *Electronic Properties of Surfaces*. *Electronic Properties of Surfaces* (Routledge, 2018). doi:10.1201/9780203758595

107. Yang, H., Yang, S., Kong, J., Dong, A. & Yu, S. Obtaining information about protein secondary structures in aqueous solution using Fourier transform IR spectroscopy. *Nat. Protoc.* **10**, 382–396 (2015).

108. Smith, B. C. *Fundamentals of Fourier Transform Infrared Spectroscopy*. (Taylor & Francis, 1995).

109. Ferraro, J. R., Brown, C. W. & Nakamoto, K. *Introductory Raman Spectroscopy*. *Introductory Raman Spectroscopy* (Elsevier, 2016). doi:10.1016/c2009-0-21238-4

110. Williams, D. H. & Fleming, I. *Spectroscopy methods in organic chemistry*. (McGraw-Hill, 1966).

111. Wu, J. *et al.* Mussel-inspired chemistry for robust and surface-modifiable multilayer films. *Langmuir* **27**, 13684–91 (2011).

112. Wei, Q., Zhang, F., Li, J., Li, B. & Zhao, C. Oxidant-induced dopamine polymerization for multifunctional coatings. *Polym. Chem.* **1**, 1430 (2010).

113. Roberts, J. D. *Nuclear magnetic resonance. Applications to organic chemistry*. ([s.n.], 1959).

114. Cavanagh, J., Fairbrother, W. J., Palmer, A. G. I., Skelton, N. J. & Rance, M. *Protein NMR Spectroscopy: Principles and Practice*. (Academic Press, 2012).

115. Weiss, P., Fatimi, A., Guicheux, J. & Vinatier, C. *Biomedical Applications of Hydrogels Handbook. Business* **c**, (Springer New York, 2010).

116. Sweeney, I. R., Miraftab, M. & Collyer, G. A critical review of modern and emerging absorbent dressings used to treat exuding wounds. *Int. Wound J.* **9**, 601–612 (2012).

117. Alsberg, E., Anderson, K. W., Albeiruti, A., Franceschi, R. T. & Mooney, D. J. Cell-interactive Alginate Hydrogels for Bone Tissue Engineering. *J. Dent. Res.* **80**, 2025–2029 (2001).

118. Dhoot, N. O., Tobias, C. A., Fischer, I. & Wheatley, M. A. Peptide-modified alginate surfaces as a growth permissive substrate for neurite outgrowth. *J. Biomed. Mater. Res.* **71A**, 191–200 (2004).

119. Krogsgaard, M., Behrens, M. a., Pedersen, J. S. & Birkedal, H. Self-Healing Mussel-Inspired Multi-pH-Responsive Hydrogels. *Biomacromolecules* **14**, 297–301 (2013).

120. Kim, B. J. *et al.* Mussel-mimetic protein-based adhesive hydrogel. *Biomacromolecules* **15**,

1579–1585 (2014).

121. Hou, J., Li, C., Guan, Y., Zhang, Y. & Zhu, X. X. Enzymatically crosslinked alginate hydrogels with improved adhesion properties. *Polym. Chem.* **6**, 2204–2213 (2015).

122. Hong, S. H. *et al.* STAPLE: Stable Alginate Gel Prepared by Linkage Exchange from Ionic to Covalent Bonds. *Adv. Healthc. Mater.* **5**, 75–79 (2016).

123. Wang, X. *et al.* Dopamine-modified alginate beads reinforced by cross-linking via titanium coordination or self-polymerization and its application in enzyme immobilization. *Ind. Eng. Chem. Res.* **52**, 14828–14836 (2013).

124. Sudre, G., Olanier, L., Tran, Y., Hourdet, D. & Creton, C. Reversible adhesion between a hydrogel and a polymer brush. *Soft Matter* **8**, 8184–8193 (2012).

125. La Spina, R. *et al.* Controlling network-brush interactions to achieve switchable adhesion. *Angew. Chemie - Int. Ed.* **46**, 6460–6463 (2007).

126. Prüsse, U. *et al.* Comparison of different technologies for alginate beads production. *Chem. Pap.* **62**, 364–374 (2008).

127. Lee, B. P., Dalsin, J. L. & Messersmith, P. B. Synthesis and gelation of DOPA-modified poly(ethylene glycol) hydrogels. *Biomacromolecules* **3**, 1038–1047 (2002).

128. Sheppard, S. E., Sweet, S. S. & Benedict, A. J. ELASTICITY OF PURIFIED GELATIN JELLIES AS A FUNCTION OF HYDROGEN-ION CONCENTRATION. *J. Am. Chem. Soc.* **44**, 1857–1866 (1922).

129. Wang, C. X., Cowen, C., Zhang, Z. & Thomas, C. R. High-speed compression of single alginate microspheres. *Chem. Eng. Sci.* **60**, 6649–6657 (2005).

130. Hertz, H. Über die Berührung fester elastischer Körper. *J. für die reine und Angew. Math.* **92**, 156–171 (1882).

131. Shull, K. R. Contact mechanics and the adhesion of soft solids. *Mater. Sci. Eng. R Reports* **36**, 1–45 (2002).

132. Zangmeister, R. a, Morris, T. a & Tarlov, M. J. Characterization of polydopamine thin films deposited at short times by autoxidation of dopamine. *Langmuir* **29**, 8619–28 (2013).

133. Yang, J. *et al.* A clear coat from a water soluble precursor: a bioinspired paint concept. *J. Mater. Chem. A* **4**, 6868–6877 (2016).

134. Kim, S., Moon, J.-M., Choi, J. S., Cho, W. K. & Kang, S. M. Mussel-Inspired Approach to Constructing Robust Multilayered Alginate Films for Antibacterial Applications. *Adv. Funct. Mater.* **26**, 4099–4105 (2016).

135. Cholewinski, A., Yang, F. K. & Zhao, B. Underwater Contact Behavior of Alginate and Catechol-Conjugated Alginate Hydrogel Beads. *Langmuir* **33**, 8353–8361 (2017).

136. Ponzio, F. *et al.* Robust Alginate-Catechol@Polydopamine Free-Standing Membranes Obtained from the Water/Air Interface. *Langmuir* **33**, 2420–2426 (2017).

137. Tian, C. *et al.* Merging of covalent cross-linking and biomimetic mineralization into an LBL self-assembly process for the construction of robust organic–inorganic hybrid microcapsules. *J. Mater. Chem. B* **2**, 4346 (2014).

138. Li, L., Smitthipong, W. & Zeng, H. Mussel-inspired hydrogels for biomedical and environmental applications. *Polym. Chem.* **6**, 353–358 (2015).

139. Burke, S. A., Ritter-Jones, M., Lee, B. P. & Messersmith, P. B. Thermal gelation and tissue

adhesion of biomimetic hydrogels. *Biomed. Mater.* **2**, 203–210 (2007).

140. Waite, J. H. Nature's underwater adhesive specialist. *Int. J. Adhes. Adhes.* **7**, 9–14 (1987).

141. Harrington, M. J., Masic, A., Holten-Andersen, N., Waite, J. H. & Fratzl, P. Iron-Clad Fibers: A Metal-Based Biological Strategy for Hard Flexible Coatings. *Science (80-.).* **328**, 216–220 (2010).

142. Shao, H. & Stewart, R. J. Biomimetic underwater adhesives with environmentally triggered setting mechanisms. *Adv. Mater.* **22**, 729–733 (2010).

143. Lim, S., Choi, Y. S., Kang, D. G., Song, Y. H. & Cha, H. J. The adhesive properties of coacervated recombinant hybrid mussel adhesive proteins. *Biomaterials* **31**, 3715–3722 (2010).

144. Zhao, B. & Yang, F. (Kuo). Method and apparatus for adhesive bonding in an aqueous medium. (2018).

145. Sreeram, K. J., Shrivastava, H. Y. & Nair, B. U. Studies on the nature of interaction of iron(III) with alginates. *Biochim. Biophys. Acta - Gen. Subj.* **1670**, 121–125 (2004).

146. Yang, J., Cohen Stuart, M. A. & Kamperman, M. Jack of all trades: versatile catechol crosslinking mechanisms. *Chem. Soc. Rev.* **43**, 8271–8298 (2014).

147. Ceylan, H. *et al.* Mussel Inspired Dynamic Cross-Linking of Self-Healing Peptide Nanofiber Network. *Adv. Funct. Mater.* **23**, 2081–2090 (2013).

148. Michaud-Soret, I., Andersson, K. K., Que, L. & Haavik, J. Resonance Raman Studies of Catecholate and Phenolate Complexes of Recombinant Human Tyrosine Hydroxylase. *Biochemistry* **34**, 5504–5510 (1995).

149. Cholewinski, A., Yang, F. K. & Zhao, B. Algae–mussel-inspired hydrogel composite glue for underwater bonding. *Mater. Horizons* **6**, 285–293 (2019).

150. North, M. A., Del Grosso, C. A. & Wilker, J. J. High Strength Underwater Bonding with Polymer Mimics of Mussel Adhesive Proteins. *ACS Appl. Mater. Interfaces* **9**, 7866–7872 (2017).

151. Burkett, J., Wojtas, J., Cloud, J. & Wilker, J. A Method for Measuring the Adhesion Strength of Marine Mussels. *J. Adhes.* **85**, 601–615 (2009).

152. Lawrence, P. G. & Lapitsky, Y. Ionically Cross-Linked Poly(allylamine) as a Stimulus-Responsive Underwater Adhesive: Ionic Strength and pH Effects. *Langmuir* **31**, 1564–1574 (2015).

153. Pena-Francesch, A. *et al.* Pressure Sensitive Adhesion of an Elastomeric Protein Complex Extracted From Squid Ring Teeth. *Adv. Funct. Mater.* **24**, 6227–6233 (2014).

154. Wang, Z., Guo, L., Xiao, H., Cong, H. & Wang, S. A reversible underwater glue based on photo- and thermo-responsive dynamic covalent bonds. *Mater. Horizons* (2019). doi:10.1039/C9MH01148J

155. Lane, L. B. Freezing Points of Glycerol and Its Aqueous Solutions. *Ind. Eng. Chem.* **17**, 924–924 (1925).

156. Kawai, T. Freezing point depression of polymer solutions and gels. *J. Polym. Sci.* **32**, 425–444 (1958).

157. Nakamura, K., Hatakeyama, T. & Hatakeyama, H. Studies on Bound Water of Cellulose by Differential Scanning Calorimetry. *Text. Res. J.* **51**, 607–613 (1981).

158. Yang, X., Bakaic, E., Hoare, T. & Cranston, E. D. Injectable Polysaccharide Hydrogels Reinforced with Cellulose Nanocrystals: Morphology, Rheology, Degradation, and Cytotoxicity. *Biomacromolecules* **14**, 4447–4455 (2013).

159. Gan, D. *et al.* Plant-inspired adhesive and tough hydrogel based on Ag-Lignin nanoparticles-triggered dynamic redox catechol chemistry. *Nat. Commun.* **10**, 1487 (2019).

160. Krogsgaard, M., Nue, V. & Birkedal, H. Mussel-Inspired Materials: Self-Healing through Coordination Chemistry. *Chem. - A Eur. J.* **22**, 844–857 (2016).